Aqueous Poly(arylene ether ether ketone) Suspensions

by

Hong Xie

Thesis submitted to the Faculty of the Virginia Polytechnic Institute and State University

in partial fulfillment of the requirements for the degree of

MASTERS OF SCIENCE

IN

CHEMISTRY

APPROVED:

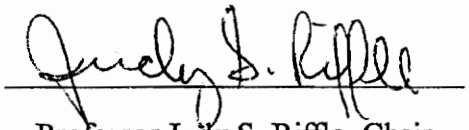

Professor Judy S. Riffle, Chair

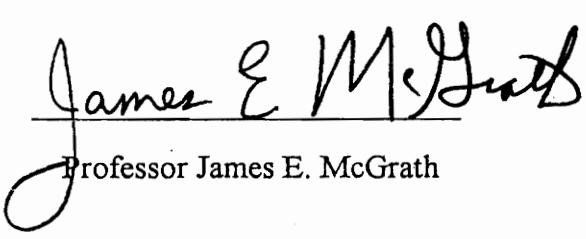

Professor James E. McGrath

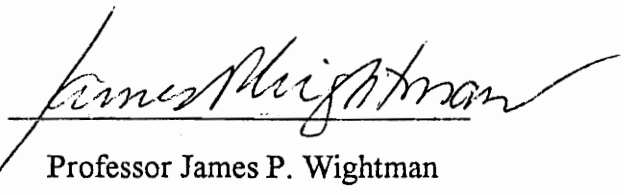

Professor James P. Wightman

March 1995

Blacksburg, Virginia

Key words: PEEK, suspension, adsorption, stabilization, composites

c.2

Aqueous Poly(arylene ether ether ketone) Suspensions

by

Hong Xie

Professor Judy S. Riffle, Chairman

Department of Chemistry

(Abstract)

Aqueous dispersion prepregging is under investigation within our laboratories for processing fiber reinforced, polymer matrix composites with environmental concern by using water instead of toxic organic solvents. This method requires that the polymers be in the form of a stable aqueous colloidal dispersion. This thesis describes the preparation of submicron diameter poly(arylene ether ether ketone) suspensions in water, and analysis of suspension stability as a function of the suspension variables. This thesis focuses on developing the procedures, and defining the parameters, for preparing stable aqueous suspensions of PEEK particles using new pyridine containing electrostatic stabilizers. Preparation of aqueous PEEK suspensions involves first adsorbing a soluble stabilizer precursor, poly(pyridine ether-co-ether ether ketimine), onto PEEK particles from a organic solvent, followed by hydrolysis of the ketimine moiety on this particle coating in conjunction with protonation of the pyridine units, forming a protonated form of poly(pyridine ether-co-ether ether ketone), which acts as an electrostatic aqueous stabilizer. Ultraviolet spectroscopy was employed to measure and compare adsorption isotherms in both THF and toluene. This high performance electrostatic stabilizer has been used successfully to stabilize aqueous suspensions of both larger particles (~ 12 micron diameter PEEK particles), as well as submicron particles. Stabilities of the

suspensions were analyzed using sedimentation experiments for the larger particle size range, and using light scattering (turbidity) for the submicron sizes. The research accomplished in this thesis is currently being used to investigate the use of these dispersions for pre-pregging both continuous carbon fiber tow and pre-woven graphite fabric.

ACKNOWLEDGMENTS

I would like to express my deepest gratitude to my advisor and committee chair, Professor Judy S. Riffle, not only for her intellectual and skillful guidance, but also for the personal support and encouragement which she unselfishly gave. I also extend my special gratitude to the other members of my research committee, Professor James E. McGrath and Professor James P. Wightman, for their time and assistance.

I take this opportunity to express my sincere thanks to the faculty, staff and students in the Department of Chemistry for their support and assistance. I also would like to take this opportunity to express my gratitude to the faculty and students I have interacted with throughout the course of this work in the Department of Chemical Engineering, Department of Materials Science and Engineering, Department of Mining Engineering and in the Department of Agriculture. I would like to acknowledge Dr. Rishey Davis (adsorption and stabilization), Dr. Chiahong Chen (adsorption), Mr. Steve McCartney (microscopy), Mr. Tom Glass (NMR), Ms. Sue Mecham (TGA, DSC), Mr. Jeff Mecham (GPC), Mr. Dave Gallo (intrinsic viscosity), Mr. Xianguo Chen (turbidity measurements), Mr. Ziqi Sun (UV) and all of my fellow graduate students in our laboratories for their friendship, guidance and assistance.

I would like to express my deepest thanks to my undergraduate advisor, Professor Xi Sheng in Beijing University of Aeronautics and Astronautics, and my graduate advisor, Professor Shaojun Huang in Southern China University of Technology, for their encouragement and friendship throughout the years. I am especially indebted to my family members for all of their faith and encouragement.

Thanks go out to my childhood friends, high school friends and college friends and friends in Blacksburg for their encouragement and the beautiful memories together.

Table of Contents

List of Figures

Chapter 1. Literature Review

1.1 Introduction

The research described in this thesis covers several topics including synthesis and properties of poly(ether ether ketone)s, and polymer adsorption and dispersion stability. This literature review is intended to present a general background of these topics for the experimental and results sections that follow.

1.2 Introduction to Poly(arylene ether ketone)s

In recent years, poly(arylene ether ketone)s have become important engineering thermoplastics and matrix resins for high performance fiber reinforced composites because of their excellent chemical, physical and mechanical properties.[1-3] Ketone functionality in the polymers capable of permitting semi-crystallinity in rigid biphenol based poly(arylene ether ketone)s. Therefore, the semi-crystalline polymers have very good solvent resistance in contrast to amorphous engineering thermoplastics, such as bisphenol-A polysulfones. The only known room temperature solvent for PEEK or PEKK is concentrated sulfuric acid.

The crystallinity of poly(arylene ether ketone)s, coupled with the fact that their melting points are generally above 300°C, leads to synthetic difficulties since the polymers precipitate out of most solvents at normal synthetic temperatures. In order to keep the polymers in solution and thus to obtain high molecular weight polymers, either strong acidic media in which the carbonyl groups are protonated (the Friedel-Crafts acylation

process) or very high temperatures (the nucleophilic process) are applied. Effort has also been devoted to alternative techniques for synthesizing poly(arylene ether ketone)s, which circumvent these problems. A review of synthetic methods follows with emphasis on nucleophilic aromatic substitution.

1.3 Synthetic Methods

1.3.1 Nucleophilic Aromatic Substitution

The mechanisms for nucleophilic aromatic substitution differ from direct substitution mechanisms, S_N1 and S_N2. The S_N2 route, which requires back-side approach of the nucleophile, is impossible due to the geometry of the substituted benzene ring; and the S_N1 route would involve the extremely unstable phenyl cation. However, nucleophilic aromatic substitutions do occur via either the addition-elimination (S_NAr) or elimination-addition (benzyne) mechanisms.[4] Almost all of the poly(arylene ether ketone)s prepared by nucleophilic processes are via the addition-elimination mechanism. Therefore, the discussion will only focus on the polymerization via the addition-elimination mechanism.

In the addition-elimination mechanism (Figure 1.1)[4], the nucleophile first attacks an electron-deficient π^* orbital on the ring. The second step involves the loss of the leaving group, thus the net substitution is obtained. The addition intermediate, called a Meisenheimer complex, is greatly stabilized by an electron withdrawing group, such as nitro, cyano, sulfone or carbonyl groups, ortho or para to the point of substitution.

A good combination of leaving group, electron withdrawing group and nucleophile can make the S_NAr reaction possible to be carried out to essentially 100% conversion. Therefore it is possible to use this mechanism to synthesize high molecular weight, step-growth linear polymers.[5-7] The polymerization process by nucleophilic aromatic substitution, originally developed for the production of polysulfones,[5] has been successfully adapted to the synthesis of poly(arylene ether ketone)s. An example of the nucleophilic process is the synthesis of poly(ether ether ketone), which is produced by the chemistry shown in Figure 1.2.[8] This reaction involves the use of activated aromatic difluorides in which a carbonyl group serves as the electron-withdrawing group, and the nucleophile is a phenolate anion. The nature of the leaving group, electron-withdrawing group, the metal cation and the solvent all have a marked influence on the course and rate of polymerization. In the S_NAr reaction, the leaving group, often a halide, has the order of reactivity, F>>Cl>Br>I, which is the opposite of S_N2 reactions where I>Br>Cl>F. The reason for this difference is that the rate-determining step in the S_N2 mechanism is breaking of the carbon-halide bond, while in the S_NAr reaction, the rate-determining step is attack of the nucleophile. The more electronegative leaving group makes the aromatic ring more electron deficient, thus, the rate-determining step is faster. The reactivity of the S_NAr reaction increases with electron withdrawing groups in the order of $N=N<C=O<SO_2\sim NO_2$. The electron withdrawing group stabilizes the addition intermediate, i.e., Meisenheimer complex. The reaction order is Cs>K>Na>Li for the alkali metal cation. The choice of solvent is complicated and depends on the specific case. The solvent not only has to solvate the nucleophile but also must solvate the polymer. Generally dipolar aprotic solvents, such as NMP, DMAc and DMSO, are good since their dipolar functions can interact with the ketone on the polymer backbone and thus increase

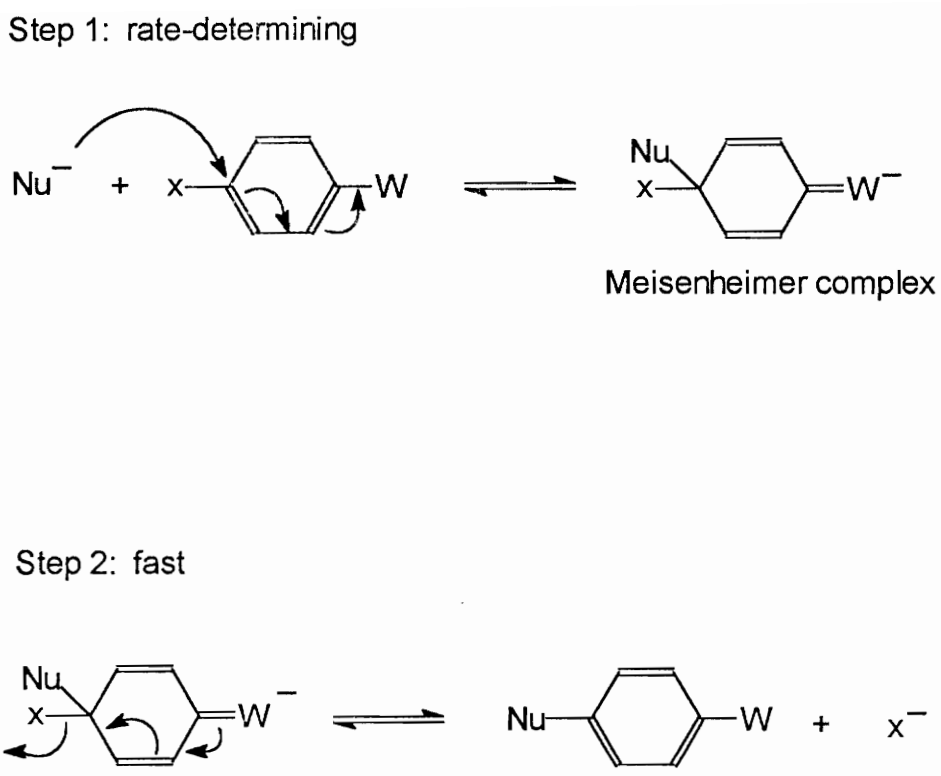

Figure 1.1 Addition-elimination (S_NAr) mechanism[4]

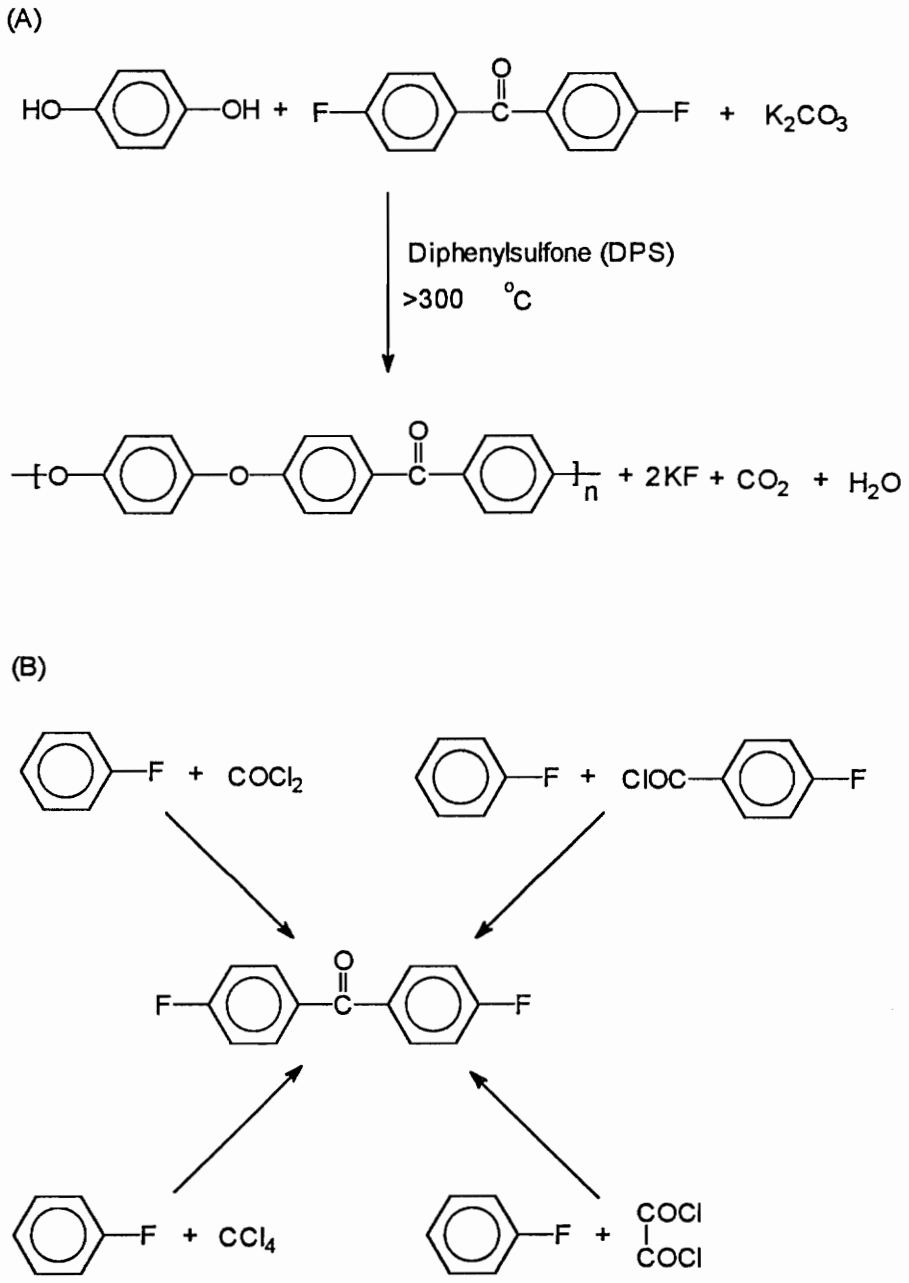

Figure 1.2 (A) Synthesis of PEEK by nucleophilic aromatic substitution; (B) syntheses of 4,4'-difluorobenzophenone (monomer)[8]

the solubility. More importantly, they serve to solvate the positive counterions which increases reactivity of the phenolate ion and they stabilize the polar reaction intermediates.

The crystalline poly(ether ketone)s are generally not soluble in non-acidic organic solvents at low temperatures. Therefore they require a high boiling solvent which can withstand high temperatures (e.g. >325°C) without decomposition. Solvents such as diphenylsulfone (DPS) are used to accommodate these temperatures. Under such high temperatures, side reactions like ether exchange and cleavage become important.[8,9] Another side reaction has also been suggested. Since the hydrogen atom ortho to halogens is relatively acidic, especially with the presence of an electron-withdrawing ketone group, the basic phenolate might abstract the proton ortho to a halogen at high temperature (Figure 1.3).[3] The resulting carbanion can either attack the carbonyl group or displace a halide, leading to branching or even gel formation, although the extent of this kind of side reaction is very minimal.

The effect of crystallinity on solubility is still a concern during nucleophilic aromatic substitution syntheses of poly(arylene ether ketone)s. For this reason, three alternative approaches have been developed, all of which utilize amorphous soluble precursor polymers that are initially formed, then chemically transformed to the final polymer. In one approach, a ketal derivative of 4,4'-dihydroxybenzophenone was synthesized and used as a monomer (Figure 1.4).[10] It was then reacted with 4,4'-difluorobenzophenone under mild reaction conditions by nucleophilic aromatic substitution to produce an amorphous polyketal (Figure 1.5).[10] This soluble precursor was quantitatively converted to high molecular weight, crystalline, poly(ether ketone) by acid hydrolysis of the acetal function. In the second approach, bulky groups such as t-butyl

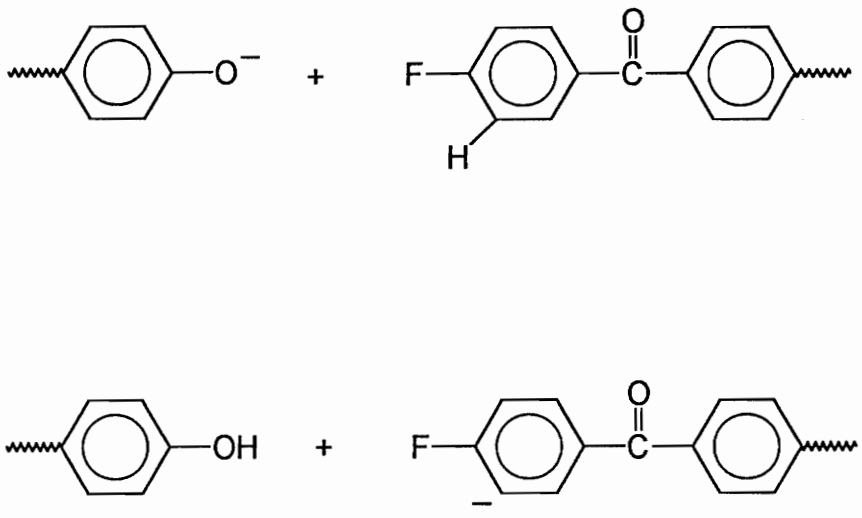

Figure 1.3 Possible side reaction leading to branching at high temperature[3]

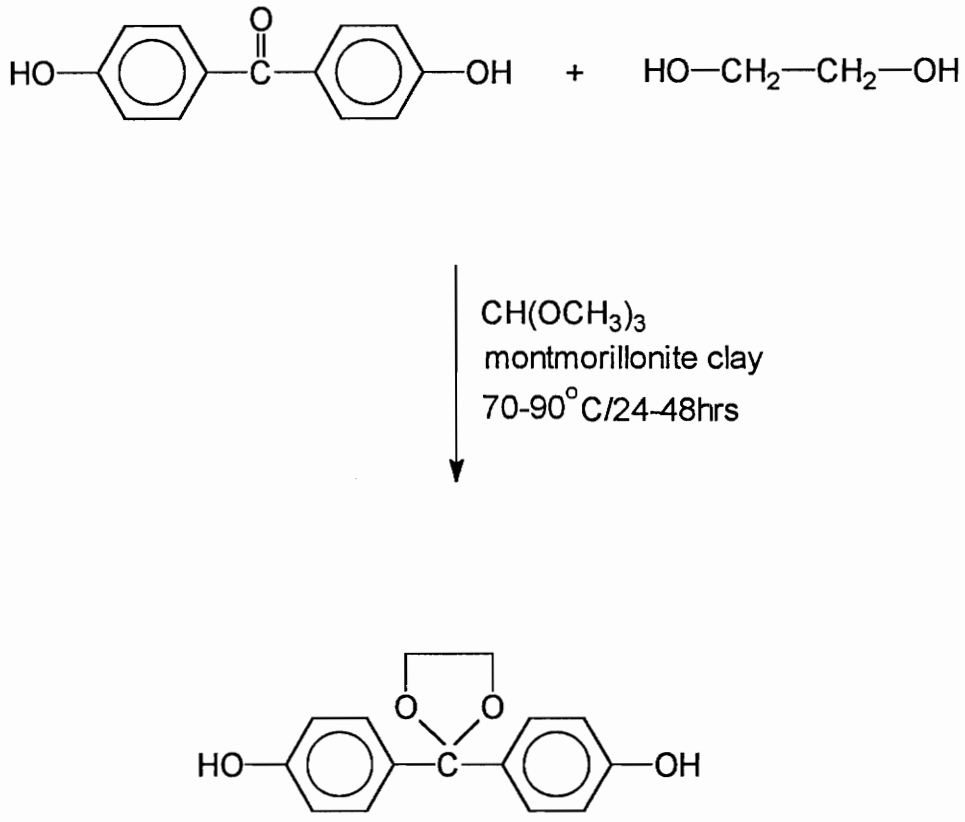

Figure 1.4 Synthesis of ketal monomer[10]

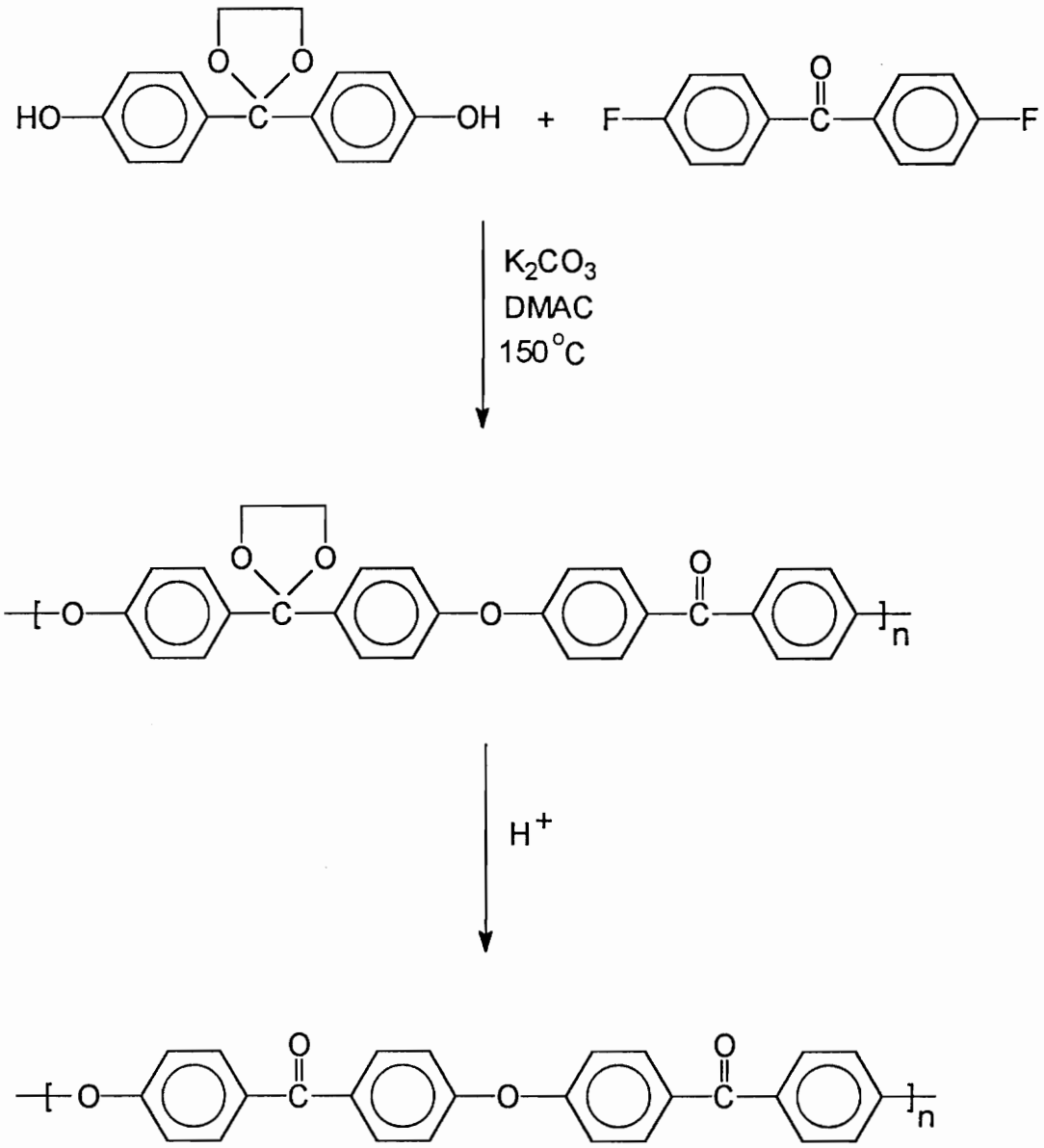

Figure 1.5 Synthesis of poly(ether ketone) via ketal monomer[10]

were substituted onto hydroquinone, which was then reacted with 4,4'-difluorobenzophenone to form an amorphous t-butylated poly(ether ketone).[11] The removal of these bulky groups was achieved using Lewis or Bronstead acid catalyzed cleavage of the t-butyl substituent (retro Friedel-Crafts alkylation). In the third approach, a ketimine derivative of 4,4'-difluorobenzophenone was synthesized (Figure 1.6).[12-14] The electron-withdrawing ability of the ketimine is sufficient to enable nucleophilic aromatic substitution, and thus to form an amorphous ketimine precursor polymer (Figure 1.7).[12] Upon acid hydrolysis, the soluble precursor was transformed into a high molecular weight, crystalline poly(arylene ether ketone). If hydroquinone is used as the bisphenol, as shown in Figure 1.7, the polymer formed after hydrolysis is exactly poly(ether ether ketone) (PEEK) (Figure 1.8).[12] A very important discovery made by McGrath et al. was that upon hydrolysis of the ketimine precursor polymer, PEEK precipitated from solution in the form of very small particles. This thesis will focus on this issue by describing the preparation of aqueous PEEK suspensions for prepregging high performance continuous graphite fiber composites.

1.3.2 Friedel-Crafts Acylation

Wholly aromatic poly(ether ketone)s were synthesized via Friedel-Crafts acylation using aluminum chloride in solvents such as dichloromethane and nitrobenzene (Figure 1.9).[15,16,17] Due to the crystallinity of the poly(arylene ether ketone)s, premature precipitation of the polymers results in low molecular weights and the polymers are of no practical use. This problem was solved by Marks et al. (du Pont) by using a mixed HF/BF_3 (solvent/catalyst combination).[18] The premature precipitation was prevented through complexation of the Lewis acid with the polyketone's carbonyl groups.

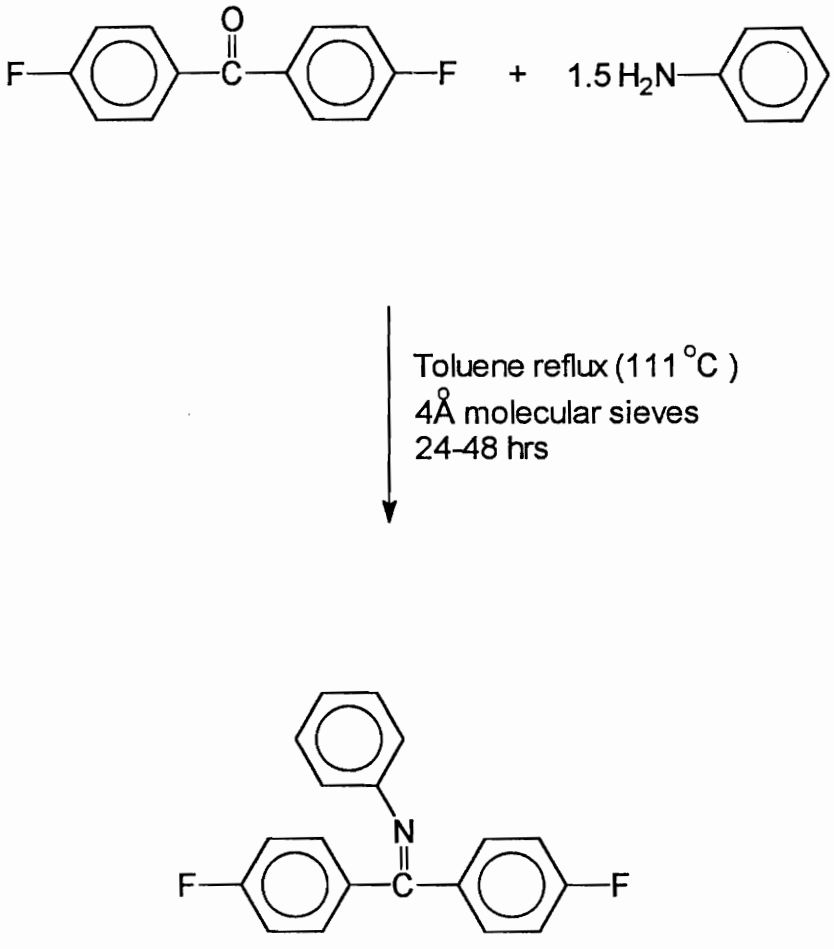

Figure 1.6 Synthesis of ketimine momomer[12-14]

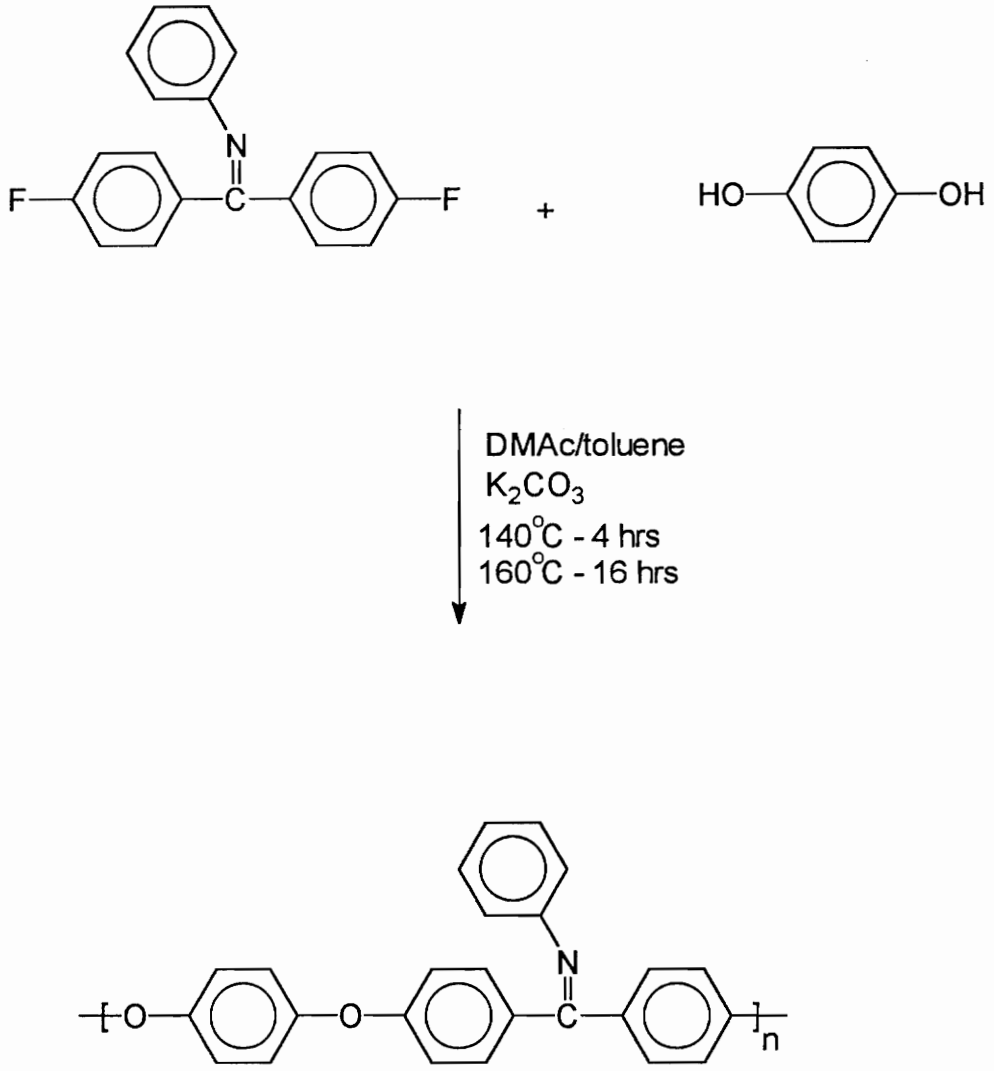

Figure 1.7 Synthesis of poly(ether ether ketimine) (PEEKt) from ketimine monomer[12]

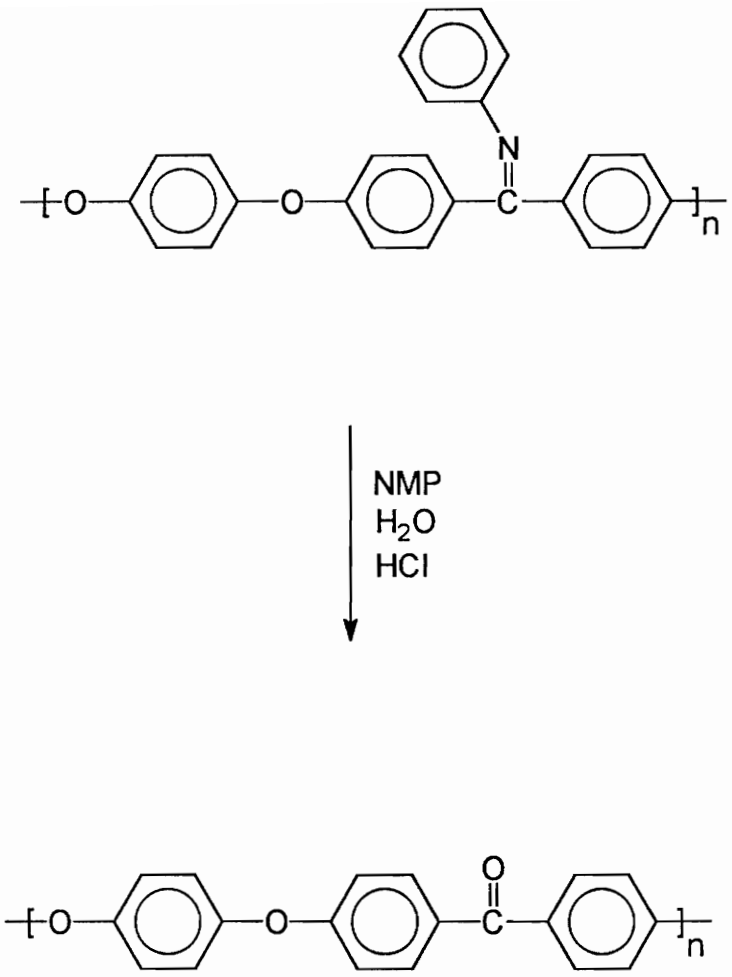

Figure 1.8 Hydrolysis of PEEKt to PEEK[12]

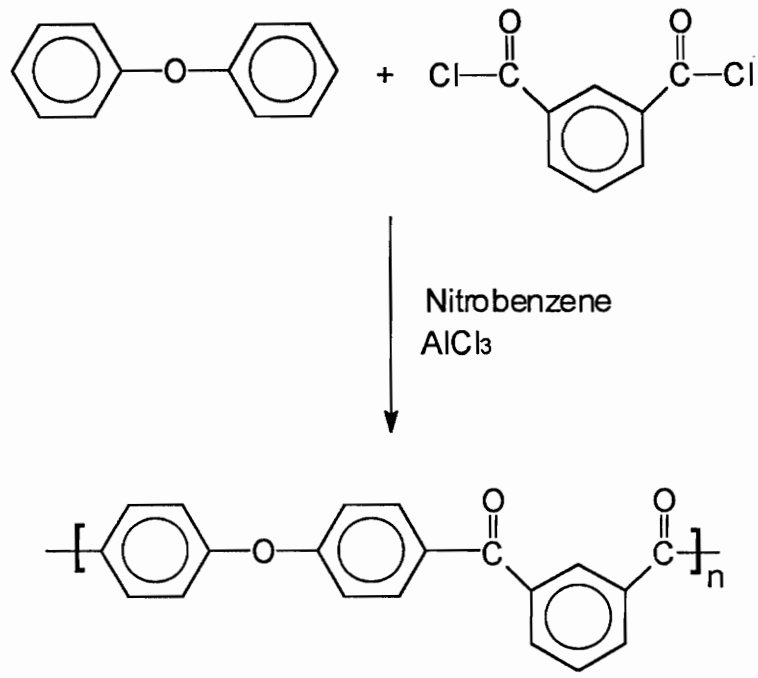

Figure 1.9 Poly(arylene ether ketone) by Friedel-Crafts Acylation[15,16]

Poly(arylene ether ketone)s produced by this route is high molecular weight and has good mechanical properties. A limitation of Friedel-Crafts chemistry for making polymers is that the substrate must be activated for electrophilic aromatic substitution by an electron donating substituent, such as an ether or an alkyl moiety. Alkyl substituents can lead to thermooxidative instability.[8]

1.3.3 Coupling of Aromatic Dichlorides

Recently, the synthesis of poly(arylene ether ketone)s using the nickel-catalyzed coupling of aromatic dichlorides containing ether and ketone structures in the presence of zinc, triphenylphosphine and bipyridine, has been reported.[19,20] However only low to medium molecular weights were obtained because of premature precipitation. To increase the molecular weight of the resulting polymers, tert-butyl groups were incorporated on the aromatic dichlorides, resulting in amorphous poly(arylene ether ketone)s (Figure 1.10).[21] These polymers are soluble in common organic solvents, such as THF, dichloromethane and chloroform. Reasonably clean de-tert-butylation was reported by treating the amorphous polymers with trifluoromethanesulfonic acid in the presence of toluene. Crystalline poly(arylene ether ketone)s were produced, as shown in Figure 1.11.[21] However, long reaction times are required for de-tert-butylation (>20 hours).

1.4 Properties of Poly(arylene ether ketone)s

The crystalline poly(arylene ether ketone)s exhibit high temperature performance, with T_g values ranging from 100°C to over 200°C and T_m values from about 300°C to well over 400°C. They also exhibit good solvent and radiation resistance partly as a result

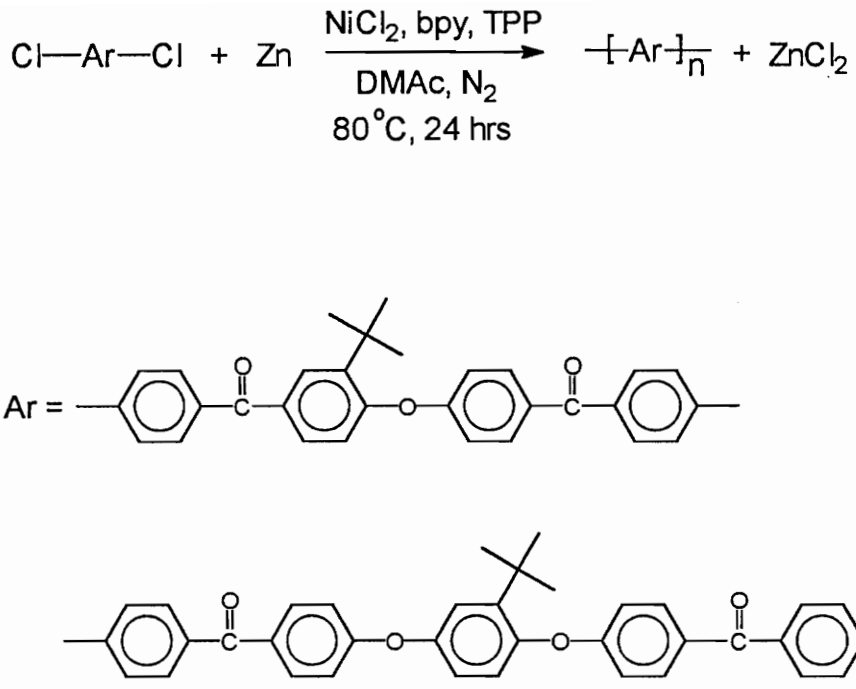

Figure 1.10 Synthesis of tert-butyl-substituted poly(ether ketone)s by nickel-catalyzed coupling polymerization of aromatic dichloride[21]

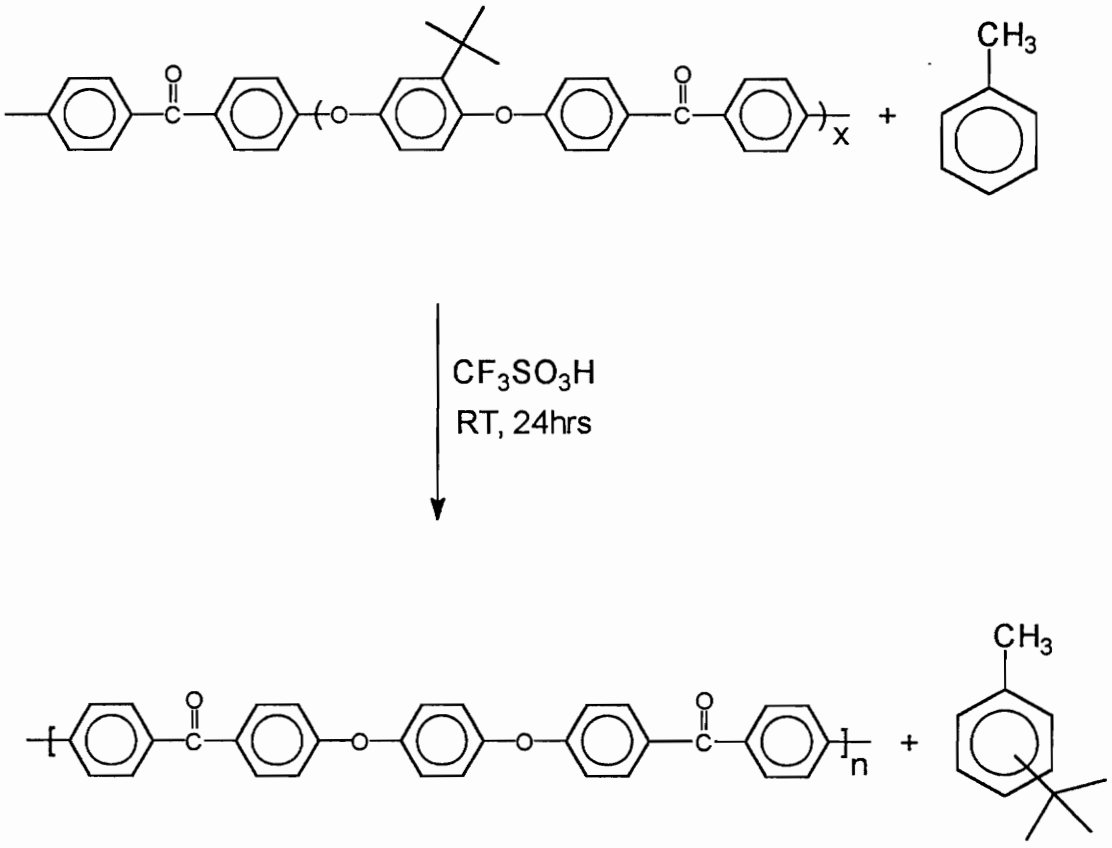

Figure 1.11 Trans-tert-butylation by trifluoromethanesulfonic acid[21]

of their semi-crystalline morphology. They have low flammability, and yield relatively low levels of smoke and toxic gas upon burning. As a general class, the poly(arylene ether ketone)s are strong, tough materials with good wear and abrasion resistance.[8]

Among the poly(arylene ether ketone)s, a very important polymer is poly(ether ether ketone). PEEK is a high performance engineering thermoplastic with many commercial uses including matrices for graphite fiber reinforced composites. PEEK has a T_g of ≈ 143°C and T_m ≈ 334°C. The crystallinity of PEEK ranges from 0 to 48%[8] depending on its thermal history.[22] Thermophysical properties of PEEK are important because of its use in advanced engineering applications. Pressure-volume-temperature properties such as the pressure dependence of T_g and T_m were determined experimentally. The increments of T_g and T_m with pressure is about 0.57 - 0.59°C/MPa and 0.483°C/MPa respectively.[23] It is reported that the thermodynamic melting point of the PEEK crystal is 384°C and the surface free energy of the PEEK crystal is 39 erg/cm^2. The heat of fusion of the PEEK crystal (39.5 cal/g) has been determined from a linear relationship between the heat of fusion and the density.[24]

Since PEEK is relatively insoluble, characterization of its solution properties is quite challenging. Several acidic solvents have been explored for PEEK including H_2SO_4, HSO_3Cl, HF and mixtures of p-chlorophenol/o-dichlorobenzene, etc.. Solubility is induced since these strong acids protonate the carbonyl oxygen. Sulfuric acid also sulfonates the PEEK backbone selectively and quantitatively on the activated aromatic ring (Figure1.12).[25] Intrinsic viscosities of PEEK in sulfuric acid and phenol-1,2,4-trichlorobenzene (phenol-TCB) (50/50 by weight) were measured, and the Mark-Houwink

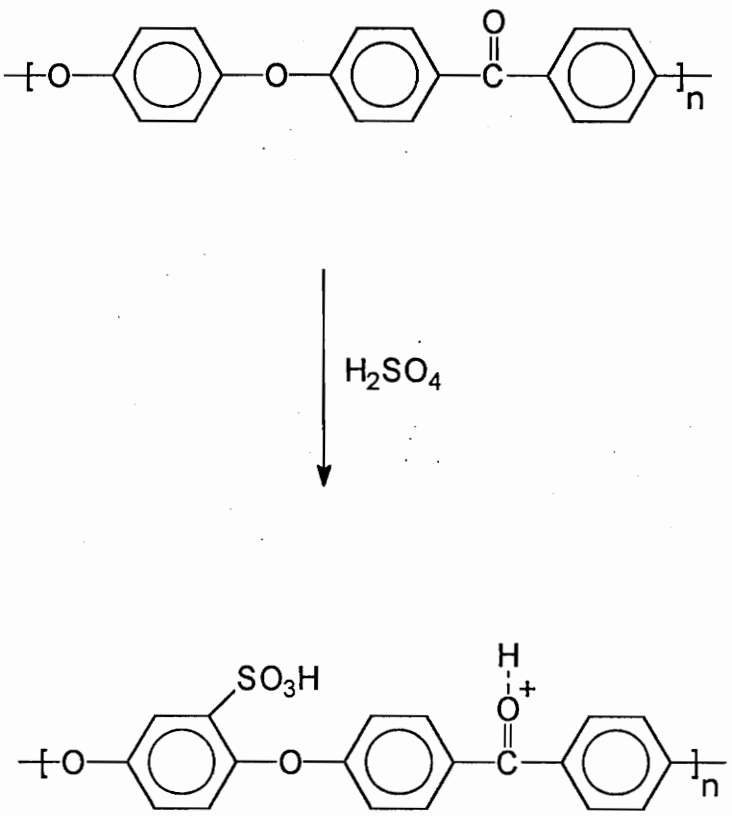

Figure 1.12 Sulfonation of PEEK[25]

expressions for PEEK in sulfuric acid (Eq. 1.1) and (phenol-TCB) (Eq. 1.2) were determined.[25]

$$[\eta]^{H_2SO_4}_{25°C} = 3.849x10^{-5}(\bar{M}_w)^{0.94} \text{ (dl/g)} \qquad \text{Eq. 1.1}$$

$$[\eta]^{phenol\text{-}TCB}_{115°C} = 7.588x10^{-4}(\bar{M}_w)^{0.67} \text{ (dl/g)} \qquad \text{Eq. 1.2}$$

in which, $[\eta]$ is the intrinsic viscosity of PEEK, and M_w is weight-average molecular weight of the polymer. Using the Mark-Houwink equation, the molecular weight of a PEEK polymer can be calculated by measuring its intrinsic viscosity.

1.5 Composite Materials

1.5.1 Introduction

A composite can be broadly defined as the material created when two or more distinct components are combined and oriented in order to achieve superior properties. By this definition, many materials fall into this scope. For example, wood is a natural composite because it consists of an oriented hard phase for strength and stiffness and a softer phase for toughness. Important examples of structural composites are the materials formed by aligning extremely strong and stiff continuous fibers in a polymer resin matrix or binder. The fibers primarily used in these composites include glass fibers, graphite fibers and aromatic polyamides (Kevlar). These fibers are of low density (1.44-2.7 g/cm^3) and extremely high strengths (3-4.5 GPa) and moduli (80-550 GPa).[26] When combined with a resin, these fibers, which make up about 55-70 weight or volume %, provide

mechanical properties exceeding those of most metals. Although the polymer matrix has a relatively low strength and low modulus, it plays an important role. It maintains the fiber at desired orientations and spacing; transmits shear loads between fiber layers so that the resistance to bending and compression is increased; it protects the fiber from surface damage; it also tends to keep cracks isolated and blunted, which dissipates energy; and the matrix gives the composite toughness.

Therefore, the combination of high-modulus fibers and high temperature toughened resins provides a material which is light and has high stiffness and strength. A partial list of advantages of polymer matrix composites relative to metals follows:[27]

1. Lower density
2. Potential increased design flexibility
3. Better damage tolerance
   - increased impact resistance
   - increased fracture toughness
   - greater scuff resistance
4. Better corrosion resistance
5. High specific strength and stiffness
6. Low thermal coefficient of expansion
7. Better fatigue resistance

1.5.2 Composite Processing

Solution prepregging is one method for applying the polymer to the fibers. Here, the fibers (or cloth) are impregnated with the resin solution to make prepregs, then the

solvent is removed by evaporation. Another method for processing composites is melt prepregging, in which high temperature is applied to impregnate the fibers (or cloth) with melted resins or resin presursors.

Thermoplastic resins have many potential advantages over thermosets.[28] A shorter production cycle is required since thermoplastics do not have to chemically react during processing. Thermoplastics also have an infinite shelf life and there is no solvent or refrigeration involved in storage. Thermoplastics are also tougher than unmodified thermosets.

With all these potential advantages of thermoplastics, however, large-scale solution prepregging using thermoplastics is impractical since high performance thermoplastics are typically insoluble or soluble only in expensive, high-boiling solvents such as m-cresol or possibly 1-methyl-2-pyrrolidinone (NMP). Also, environmental concerns will almost certainly result in legislation against the use of such solvents in the near future. Melt prepregging with thermoplastics is also difficult because the melt viscosities of the resins are too high to achieve complete impregnation. Recently, two new techniques to prepare thermoplastic prepregs, electrostatic prepregging and aqueous suspension prepregging, have been developed to circumvent these problems.[29-33] In aqueous dispersion prepregging, the carbon fiber tow is passed through a concentrated suspension of the matrix resin where it picks up the small resin particles. Water is used as the medium instead of toxic organic solvents (Figure 1.13).[33] This technique requires that the resin be in the form of small particles and that it be dispersed in the water to form a stable aqueous suspension. If the particle size is less than $\approx$ 1 micron in diameter, this method may have potential for directly prepregging woven cloth.[34]

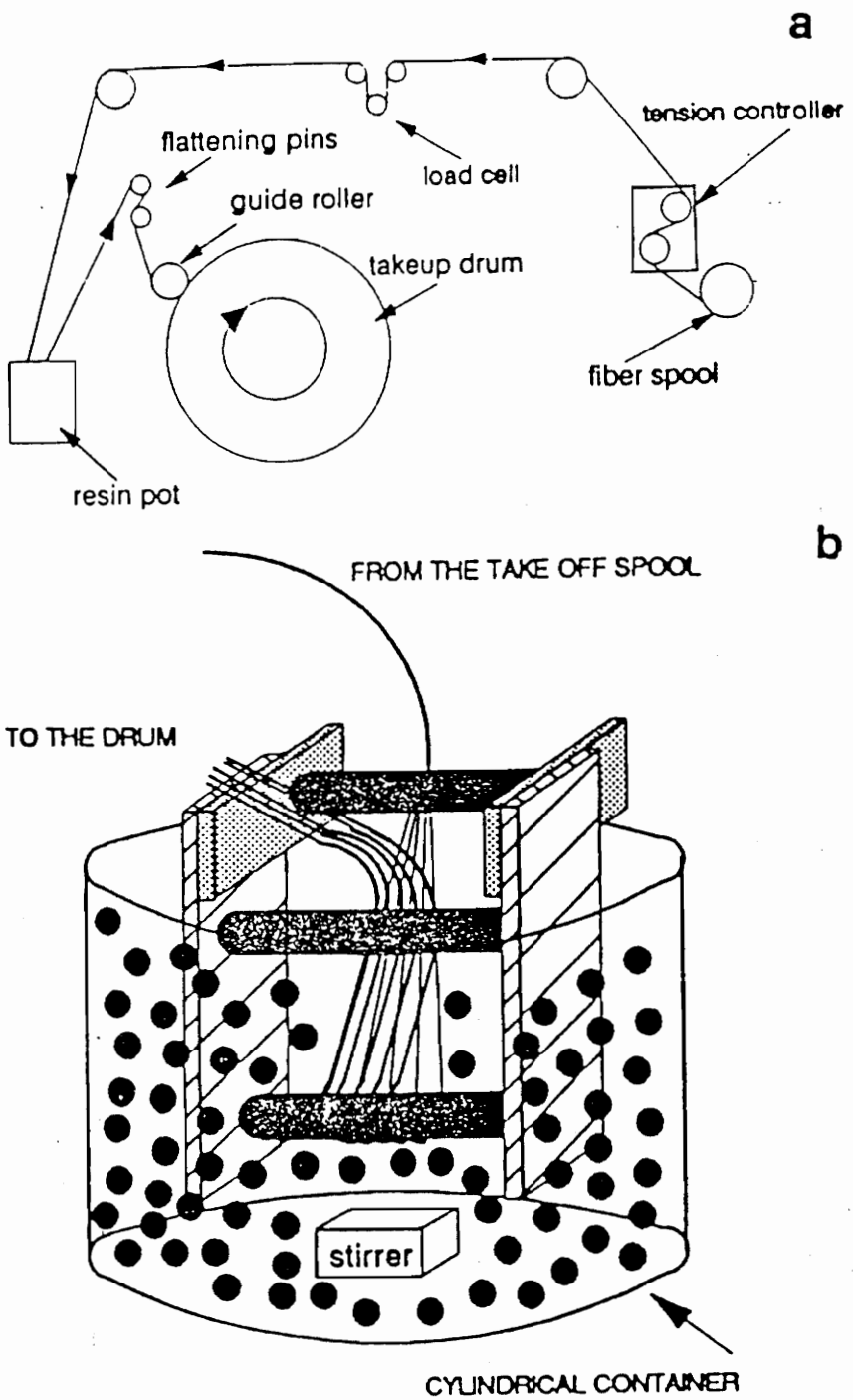

Figure 1.13 Aqueous dispersion prepregging: (a) Drumwinder; (b) resin pot[33]

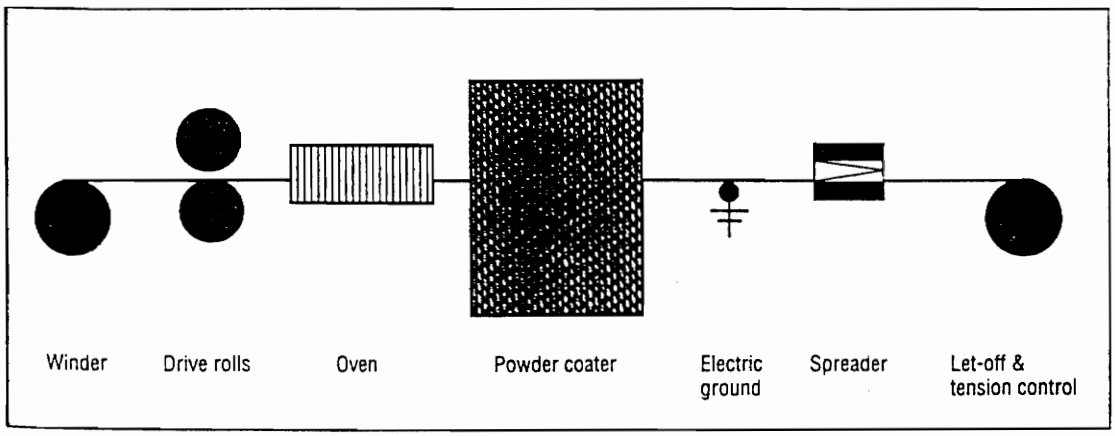

Figure 1.14 Process diagram for electrostatic prepregging of composites[28]

In electrostatic preprergging, the matrix resin is coated onto the continous carbon fibers as a dry powder by an electrostatic attraction. This is introduced by putting an electrical current across the fibers (Figure 1.14).[28] This method is solvent free, and does not require high temperatures to make low viscosity melts. This technique, however, requires the resin be in the form of small, dry particles with an optimal particle size between ≈ 50-80 microns in diameter. With smaller sizes, the particles agglomerate, resulting in uneven coatings; with larger sizes, the particles would not adhere to the filaments because they are too heavy to be attracted by the electrostatic force.

1.6 Polymer Adsorption and Stabilization

1.6.1 Polymer Adsorption

Polymer adsorption is energetically driven. It occurs when the affinity of the polymer for the adsorbent overcomes the unfavorable entropic forces in which the number of conformations a polymer chain can assume is reduced upon adsorption. The source of free energy gain is due to contacts between polymer segments and the adsorbent. Polymers usually have high affinities for adsorbents since large numbers of segments are present in a polymer chain.[35]

Important theories for describing polymer adsorption include the Scheutjens-Fleer (S-F) mean field theory (Lattice theory)[36,37] and scaling theory.[38] The theory proposed by de Gennes is based on scaling relations for semi-dilute polymer solutions. It relates the amount of adsorbed polymer, distribution of segments and the hydrodynamic layer thickness to its molecular weight, polymer concentration and solubility. For block

copolymers, the effect on layer thickness of the block length ratio between anchor and tail blocks has also been modelled and studied. In the S-F mean field theory, a lattice between two parallel plates is used in order to make the number of possible conformations of the various molecules finite. The lattice is divided into equidistant layers parallel to the surfaces. It is assumed that each lattice site is occupied by a segment or a solvent molecule. Using the self consistent field (SCF) theories for polymer solutions as a starting point, the lattice theory modeled the partition function and the structure for a mixture of polymer chains and solvent molecules near an interface. The segment-solvent interaction is taken into account by use of the Flory-Huggins parameter χ, and it is associated with desolvation of the segments upon adsorption. The molecular interactions, both solvent and polymer segments, at the interface are described in terms of the segmental adsorption energy parameter χ_s . χ_s KT is defined by Silberberg as the energy change associated with the transfer of a polymer segment in pure polymer from a bulk site to a surface site, minus the corresponding energy change for a solvent molecule in pure solvent.[39] Adsorption occurs only when the adsorption energy exceeds a given value, the so-called critical adsorption energy, denoted by χ_{sc} KT. One of the terms contained in χ_{sc} is the loss of chain conformations upon adsorption. Adsorption of a polymer segment includes first breaking contacts of the segment with solvent molecules followed by displacing solvent molecules from the surface, and then adsorbing of the segment onto the surface. Only when the total free energy involved in the whole process is negative can the adsorption occur. According to the Scheutjens-Fleer mean field theory, the amount of adsorbed polymer is generally affected by molecular weight (MWt), volume fraction of polymer in the solution at equilibrium adsorption (ϕ^*), polymer segment-solvent interaction (χ) and polymer segment-interface interaction (χ_s).

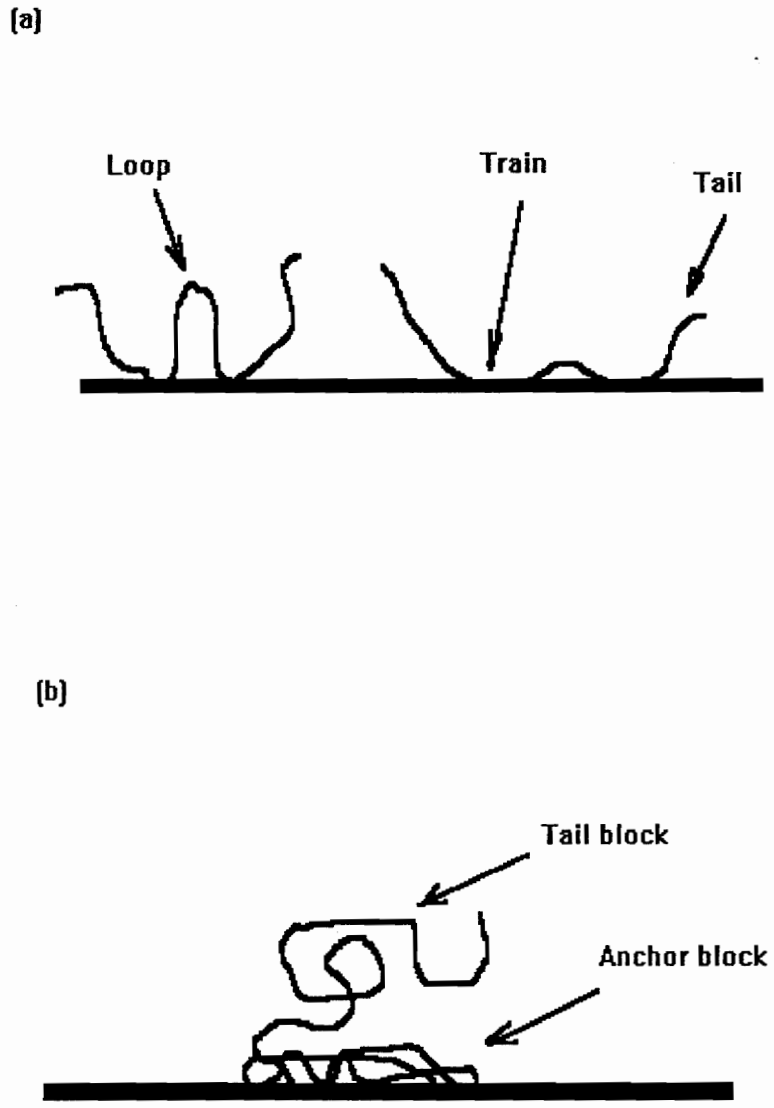

Figure 1.15 Schematic representation of polymer adsorption conformations on solid surfaces. (a) Homopolymer/random copolymer; (b) Diblock copolymer

An adsorbed polymer molecule generally has segments arranged in loops, trains, tails and bridges, as shown in Figure 1.15. "Loops" are defined as the stretches of segments in the solution, and both ends of the stretches are on the surface; "trains" are flat sequences in contact with the surface; "tails" are free ends of the molecules extending into solution; and "bridges" are segments where the ends are adsorbed on different surfaces. For block copolymers, the anchor block tends to form loop-train conformations while the other block assumes tail conformations (Figure 1.15).

1.6.2 Difference Between Polymer Adsorption and Small Molecule Adsorption

Polymer adsorption differs greatly from the adsorption of small molecules and low molecular weight surfactants. The differences are: 1) Since a polymer chain contains many segments, it has much more adsorption sites than the small molecules. As a result, the adsorption energy of the polymer chain is much higher than that of the small molecules. The adsorption of polymer is of the high-affinity type. The isotherms can not be predicted by Langmuir adsorption theory, which has been proven to work well with low molecular weight species; 2) The conformations of the polymer are changed upon adsorption, owing to the complex interactions among the absorbent surfaces, polymer chains and solvents. There is no such change during the adsorption of low molecular weight species. Also, the conformations of the polymers are dependent on the polymer concentration and molecular weight; 3) The entropy loss upon adsorption is more significant than that of small molecules.

1.6.3 Fundamental Features of Polymer Adsorption

1. Effect of the Solvent on Adsorption

A polymeric chain assumes a coiled conformation in dilute solution. The size and shape of this coil are determined by the polymer-solvent interaction (χ parameter) and the intra-molecular interactions. There is a well-defined correlation between the χ parameter and the chain size. This correlation is based on the concept of osmotic action of the solvent over the polymer chain.[40] The osmotic action of the solvent makes the coil swell and inflate, assuming less probable conformations. Equilibrium is reached when the osmotic forces are equal to the elastic forces which hinder such expansion. Following is the expression for equilibrium osmotic pressure of polymer solutions:

$$\pi/c = RT/M + A_2c + A_3c^2 + \cdots \qquad \text{Eq.1.3}$$

in which π is the osmotic pressure; c is the concentration of polymer in the solution; M is the molecular weight of the polymer; and A_2 and A_3 are virial coefficients. A_2 (the second virial coefficient) is a function of the Flory-Huggins coefficient χ and characterizes the interaction energy between solvent molecules and polymer. The solvent is better at higher A_2 values. Increasing A_2 leads to an increasing osmotic pressure and hence larger sizes of the molecules in the solution. This in turn leads to a higher viscosity of the solution. Experiments[41,42] demonstrated that the intrinsic viscosity changes correspondingly with the second virial coefficient and thus it can be used as a measure of the power of the solvent. In a poor solvent, more macromolecules are adsorbed because: 1) The polymer chains are more coiled as if their sizes are smaller; and 2) The weaker interaction of polymer with solvent promotes the adsorption. The solvent-surface interaction also affects polymer adsorption. A high affinity of the solvent for the

adsorbent surface may prevent the polymer from adsorbing. Thus the amount of adsorption will be lower.

2. Effect of Temperature on Adsorption

Many parameters which control polymer adsorption onto a surface change with temperature. Examples include the mobility of macromolecules, the solvent power, the adsorbent-solvent interaction and the adsorption of solvent which is competing with the adsorption of the polymer. All of these factors must be taken into account when considering the sign of the temperature coefficient of adsorption. Thus the temperature effect on polymer adsorption is complex and may lead to either increased or decreased adsorption depending on the properties of the system.

3. Effect of Molecular Weight on Adsorption

An increase in molecular weight corresponds to an increased number of segments per chain. In other words, more adsorption sites are presented in a longer polymer chain, which, in turn, has higher adsorption energy than small molecules. Therefore the initial part of the adsorption isotherm typically shows a steeper progression as molecular weight is increased, i.e., the isotherm is more of the high-affinity type with higher molecular weight.

4. Effect of Molecular Weight Distribution on Adsorption

The adsorption rate of short chain molecules is higher than that of long chain molecules due to their higher diffusion coefficients. Therefore, short chain molecules are adsorbed from the polymer solution during the initial stages of adsorption and occupy the surface sites of the adsorbent. Since long chain molecules have higher affinities and thus adsorb preferentially, they are able to displace the pre-adsorbed short chain molecules until thermodynamic equilibrium is established.[43,44] This phenonmenoun is the so-called competitive adsorption.[43,44] Because of this competitive adsorption of smaller vs. larger macromolecules, the adsorption of highly polydispersed polymers requires longer times to reach equilibrium relative to monodisperse polymers. The initial portion of the adsorption isotherms for these widely polydisperse systems is more rounded in shape as opposed to those for the monodisperse systems.

1.6.4 Polymer Stabilization of Colloidal Dispersions

Adsorbed polymer can lead either to stabilization or flocculation depending on the free energy change upon the approach of two particles. For a polymeric stabilizer, the following requirements must be met. The segmental adsorption energy must be larger than the critical adsorption energy. As discussed in section 1.6.1, the critical adsorption energy is the energy required to overcome the unfavorable entropic forces due to the loss of chain conformations upon adsorption. If the segmental adsorption energy is less than the critical adsorption energy, the polymer will stay in solution rather than adsorbing onto the adsorbent. The particles must be completely covered to avoid additional adsorption of segments. For example, if a particle is not completely covered, these bared surface sites might adsorb segments of polymer which is already adsorbed onto another particle. In the

case of steric stabilization, the tails should be soluble and thus provide a repulsive steric force between particles.[35]

Stabilization methods include electrostatic stabilization and steric stabilization or a combination of both (Figure 1.16). In order to prevent particles from coagulating, significant repulsive forces are required which operate over at least the distance where van der Waals attractive forces are significant (e.g., 5-10 nm).[45] For electrostatic stabilization of colloidal dispersions, a charged particle is surrounded by counterions in the liquid phase. This gives rise to an electrical double layer. The mutual repulsion of these double layers imparts stability to the suspension. For steric stabilization, suspension stability is imparted by the spatial extensions of polymer molecules. The r.m.s. end-to-end distance of linear carbon backbone polymers is given roughly by $\langle r^2 \rangle^{0.5}(nm) \sim 0.06M^{0.5}$ (θ condition), where M is the molecular weight of polymers. Therefore for terminally adsorbed polymers with modest molecular weight, their spatial extensions are greater than the range of the attraction forces between the colloidal particles.

Many theories have been developed to monitor the interaction forces between colloidal particles.[45-47] An important theory, the modified Deryagain-Landau-Verwey-Overbeek (DLVO) theory, takes into account the electrostatic repulsion force, van der Waals attraction force and the steric repulsion force and gives the final expression for the total pair potential interaction energy between particles:[45-48]

$$V_T(h) = V_A(h) + V_E(h) + V_S(h) \qquad \text{Eq. 1.4}$$

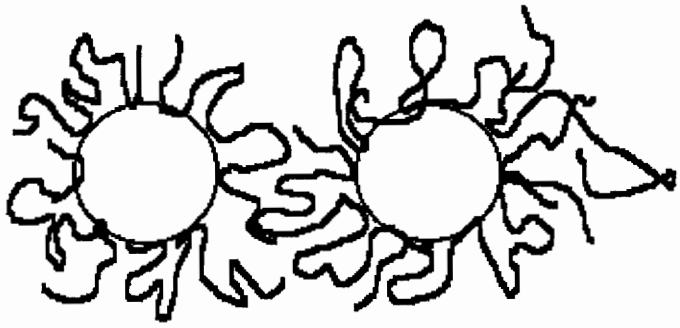

a

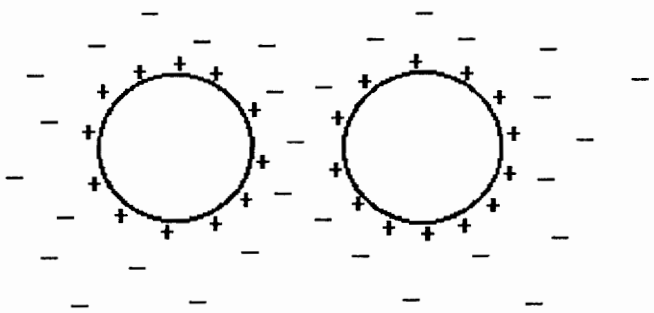

b

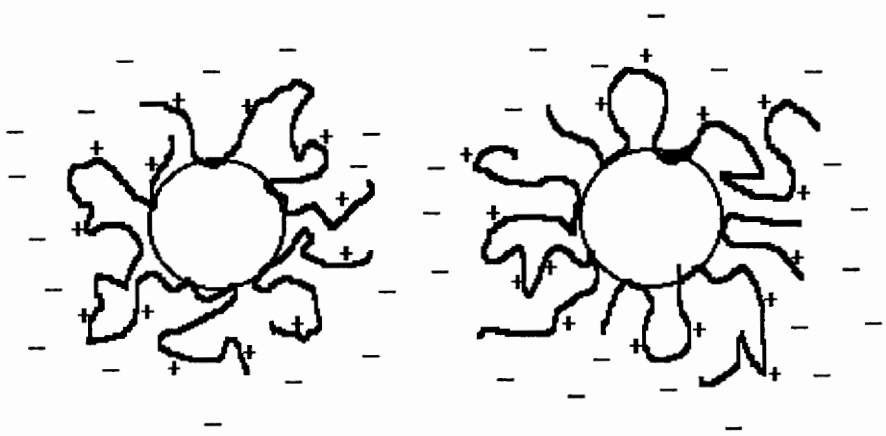

c

Figure 1.16 Polymeric stabilization: a) Steric stabilization; b) Electrostatic stabilization; c) Combination of steric and electrostatic stabilization

in which, V_T, V_A, V_E, V_S = total pair interaction potential, van der Waals attraction, electrostatic repulsion and steric repulsive potentials respectively;

h = minimum distance between particle surfaces;

The van der Waals attraction energy decays approximately with the sixth power of the distance between particles, therefore it is significant only over very short distance (5-10 nm)[45]. The potential energy of attraction between two spherical particles of material 1 in a liquid phase of material 2 is given by the following form:[49]

$$V_A = -A/12 \{(x^2 + 2x)^{-1} + (x^2 + 2x + 1)^{-1} + 2\ln[(x^2 + 2x)(x^2 + 2x + 1)^{-1}]\} \quad \text{Eq. 1.5}$$

For short distances, $h/a < 1$, this equation can be approximated by:[50]

$$V_A \cong - (aA)/(12h) \quad \text{Eq. 1.6}$$

where, $x = h/2a$, and h = shortest intersurface distance between particles, a = radius of the particles; A = the composite Hamaker constant. A is given by:

$$A = (A_{11}^{1/2} - A_{22}^{1/2})^2 \quad \text{Eq. 1.7}$$

in which, A_{11} and A_{22} are the Hamaker constants of the particles and the medium respectively. The Hamaker constant of a material is related to the nature of the material, and it increases with the refractive index n. As shown in equation 1.7, when the Hamaker constants of the particles and the liquid medium are closer, the composite Hamaker constant is smaller, and in turn, the van der Waals attraction forces between the particles are smaller (equation 1.6). Typical values for the Hamaker constant for particles in water

are 0.3 ~ $1x10^{-20}$ J for hydrocarbon particles, 0.5 ~ $5x10^{-20}$ J for oxides and halides, and 5 ~ $30x10^{-20}$ J for metal particles.[50] Therefore, it is easier for hydrocarbon particles to be dispersed in water than oxides, halides and metal particles in terms of the van der Waals attraction forces.

When two colloidal particles of the same charge approach each other, electrostatic repulsion forces are generated between their electrostatic double-layers. The range of these repulsion forces depend on the thickness of the double-layer (κ^{-1}) (Figure1.17)[47]:

$$\kappa^{-1} = [(\varepsilon kT)/(2e^2I)]^{1/2} \qquad \text{Eq. 1.8}$$

where ε is the dielectric constant of solution; k is the Boltzmann's constant; T is the temperature; e is the electronic charge. I is the ionic strength, $I = 1/2 \cdot \sum n_i(z_i)^2$, where n_i is the molarity of ionic species in solution, z_i is the valence of ionic species in solution and the summation is over all the low molecular weight ionic species in solution. The electrostatic interaction between two particles decays approximately exponentially with the surface-surface distance h, and it can be expressed as follows:[49]

$$V_E(h) = 2\pi\theta_r\theta_o\psi_s^2 a \ln[1 + \exp(-\kappa h)] \quad \kappa a > 10 \qquad \text{Eq. 1.9}$$

$$V_E(h) = 4\pi\theta_r\theta_o\psi_s^2 \exp(-\kappa h)/(h + 2a) \quad \kappa a < 3 \qquad \text{Eq. 1.10}$$

For κa values between 3 and 10, V_E can be obtained by interpolation. ψ_s is the diffuse layer potential; θ_r and θ_o are the relative permittivity of the solution phase and that of free

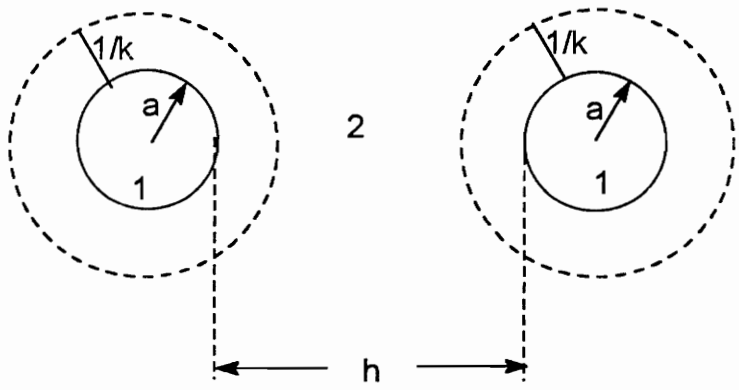

Figure 1.17 Interaction between two spherical particles, radius a, of material 1 in a liquid medium 2.[47]

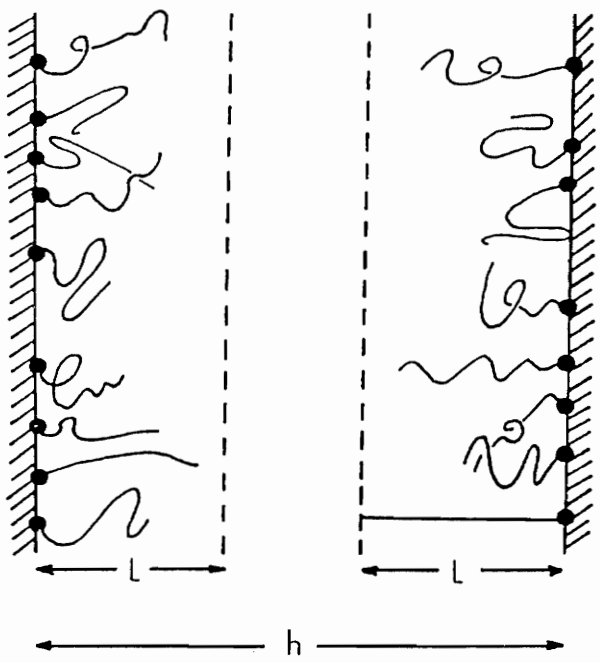

Figure 1.18 Schematic representation of two interacting surfaces bearing terminally attached polymer chains[47]

space. V_E is small when the ionic strength of the medium is high or the dielectric constant of the medium is low such that it will not support ionization.

Another important factor for stabilization can be a steric contribution, V_S. Various mean-field theories of polymer solutions have been applied to estimate the free energy of overlap of two layers of solvated chain molecules. Figure 1.18 is a schematic illustration of two interacting surfaces of distance h covered with terminally anchored polymer chains of contour length L. When $h<2L$, the two layers interact (interpenetrate or indent, or both) and the segment density in the interaction zone increases. The associated free energy change in the mixing of chain segments with solvent within a small volume δV can be estimated using the theory of Flory and Krigbaum:[51]

$$\delta(\Delta G_m) \cong (kT/V_1)[(\chi-1)\phi_2 + (0.5 - \chi)\phi_2^2] \qquad \text{Eq. 1.11}$$

in which, V_1 is the volume of a solvent molecule, ϕ_2 is the volume fraction of segments within δV, and χ is the segment-solvent interaction parameter. χ is a function of termperature, pressure and segment concentration. For polymer-solvent systems where dipole-dipole interactions and H-bonding are not significant, χ is dominated by van der Waals interactions, which is always attractive between chemically identical segments. Therefore χ is positive in most cases. The mixing energy can be either positive or negative based on different values of χ and ϕ_2 (Eq. 1.11). When the mixing energy is positive, its contribution to the steric interaction is repulsion; When the mixing energy is negative, its contribution to the steric interaction is attractive. In addition to the mixing contribution, there is an elastic contribution to steric stabilization. For example, at very small separations, such as $h < L$, the interpenetration or indentation between the adsorbed

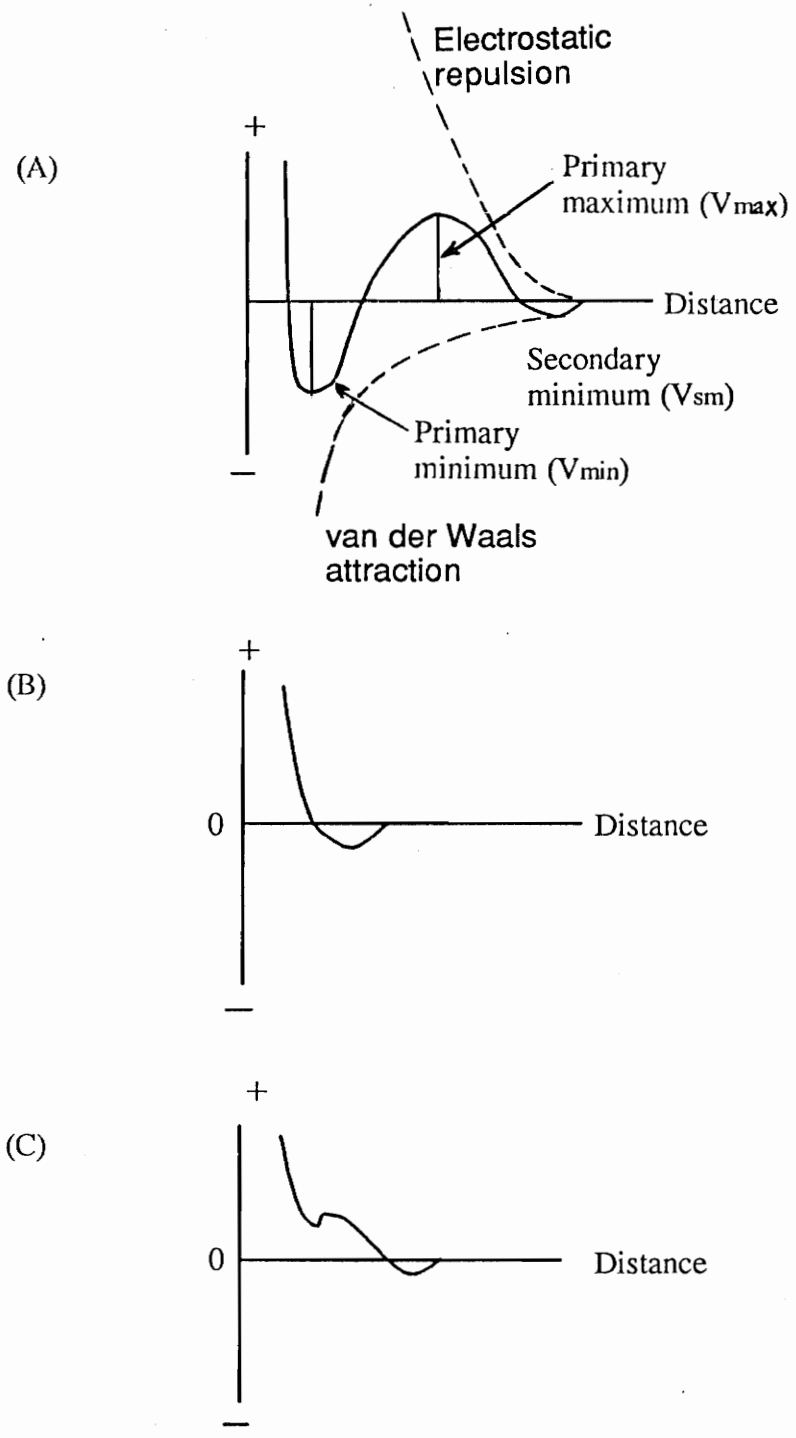

Figure 1.19 Particles interaction energy as a function of distance; (A) Electrostatic stabilization; (B) Steric stabilization; (C) Electrostatic and steric stabilization combination.[45,48]

layers results in loss of configurational freedom experienced by the anchored chains.[47] Thus, an additional entropic or elastic effect is contributable to steric stabilization and it is purely repulsive. Therefore, the steric interaction consists of two compontents: one is a repulsive elastic (entropic) contribution and one is a mixing contribution which can be either repulsion or attraction.

Figure 1.19[45,48] shows the interaction energy between two particles as a function of the distance between particle surfaces.[45,48] For a suspension stabilized by electrostatic forces (Figure 1.19a), a primary and a secondary energy minimum exist. At the primary minimum (Vmin), particles have strong van der Waals attractions and will coagulate. At the secondary minimum (Vsm), loose, and often reversible, flocculation occurs. The primary maximum (Vmax) serves as a barrier to coagulation. An effective electrostatic stabilizer must provide a high energy barrier to prevent particles from approaching the separation distance corresponding to the primary minimum. For example, if the energy barrier is sufficiently large ($\geq$ 25 kT),[45] the rate of coagulation will be so slow that a kinetically stable suspension may be obtained.

1.6.5 Characterization of Aqueous Suspensions

1. Sedimentation Experiments

Sedimentation of a suspension occurs due to a greater density of the particles relative to that of the liquid phase. However, small particles, e.g., diameter < 1 micron, will never completely settle because the gravitational force is low and counterbalanced by the Brownian motion of the particles. Density of PEEK is about 1.3 g/mL depending on different degrees of crystallinity and thermal histories. When a stabilized suspension

settles, the repulsive forces necessary to ensure stability enable the particles to move past each other and form closely packed sediments. On the other hand, less stable suspensions tend to flocculate and form network structures. The settling of these network structures forms loosely packed sediment and have higher sedimentation volume.[52] To illustrate this point, polystyrene suspensions stabilized by polyvinylalcohol (PVA) fractions of different molecular weights were centrifuged gently and the sediments were freeze-dried and examined by scanning electron microscope. Figure 1.20 shows the scanning electron micrographs of these sediments.[52] Stable suspensions (C and L), which were stabilized by higher molecular weight PVA, formed a close-packed sediment. The weakly flocculated suspension (O), stabilized by lower molecular weight PVA, formed a open-structured sediment. Therefore, sediment volume of the suspensions can be used to determine the relative stabilities of suspensions.

2. Turbidity Measurement

In the thermodynamic sense, lyophobic dispersions are not stable. The word "stable" is used to describe a dispersion in which the flocculation rate is slow. Therefore the kinetics of flocculation can be used for characterizing the stabilities of dispersions.[46,53-55] The rate of coagulation depends on the collision frequency of particles and the probability that their thermal energies are sufficient to overcome the repulsion forces upon collisions. In experimental test, the kinetic measurements can be monitored with a turbidimeter using moderately dilute suspensions. The turbidity is measured as a function of time. The time it takes to reach a certain degree of coagulation can be used as a criterion for determining the relative stabilities of suspensions. The faster the suspension coagulates, the less stable the suspension.

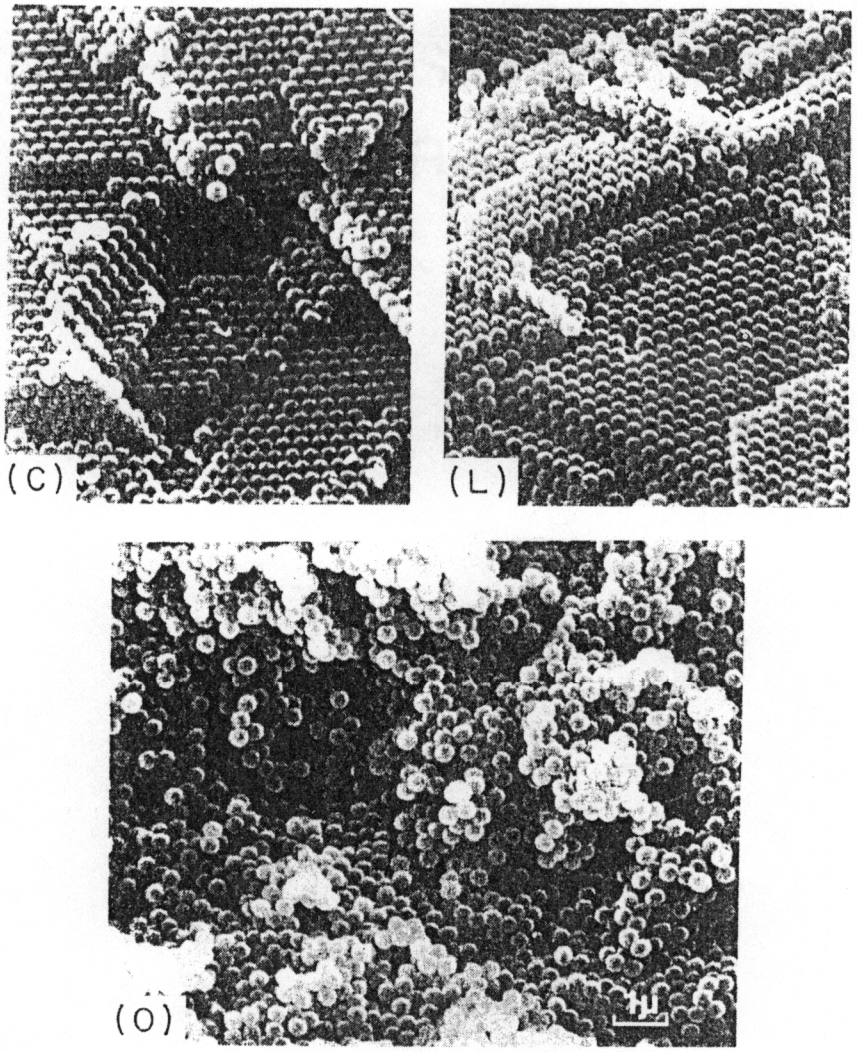

Figure 1.20 Scanning electron micrographs of polystyrene sediments stabilized by PVA fractions: (C) MWt = 43,000; (L) MWt = 28,000; (O) MWt = 8,000.[52]

Chapter 2. Experimental

2.1 Solvents and Purification

2.1.1 Tetrahydrofuran (THF): HPLC grade tetrahydrofuran was obtained from Mallinckrodt and used as received. (b.p. 67°C)

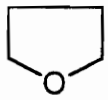

2.1.2 Toluene: Toluene, purchased from EM Science, was purified by washing 800 mL with 60 mL concentrated sulfuric acid twice. The residual sulfuric acid was removed by washing twice with water (100 mL each) followed by a saturated sodium bicarbonate solution until basic (3x50 mL). 100 mL water was used for the final washing. The toluene was stirred over magnesium sulfate in an Erlenmeyer flask (2-4 hours) then decanted into another flask and stirred with phosphorous pentoxide for an additional 8 hours. The dried toluene was distilled from sodium and benzophenone under a nitrogen purge. (b.p. 111°C/760 mm Hg)

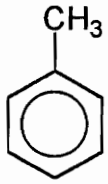

2.1.3 N-Methyl Pyrrolidone (NMP): NMP was purchased from Fisher and used as received. (b.p. 205°C/ 760 mm Hg)

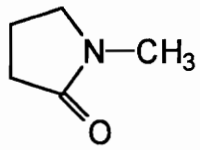

2.1.4 Water (H_2O): Water was purified by using a Barnstead NANOPURE II deionizer until the measured resistance was greater than 17 ohms. This was particularly critical for the electrostatic stabilization experiments.

2.1.5 Deuterated Chloroform ($CDCl_3$): $CDCl_3$, purchased from Cambridge Isotope Laboratories, was used as received. It was used as an NMR solvent, often with 0.05% TMS as an internal reference.

2.1.6 N,N-Dimethylacetamide (DMAc): DMAc, obtained from Fisher, was stirred with calcium hydride for 8 hours followed by distillation under reduced pressure (about 200 millitorr). (b.p. 164.5 -166°C)

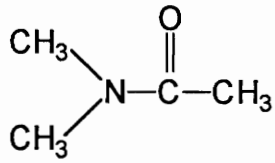

2.1.7 Hexane (C_6H_{14}): Hexane, purchased from EM Science, was used as received. It was used as a cosolvent for developing TLC plates. (b.p. 68-69°C)

2.1.8 Ethyl Acetate ($CH_3COOC_2H_5$): Ethyl acetate, obtained from Fisher, was used as received. It was used as a cosolvent for developing TLC plates. (b.p. 77.2°C)

2.2 Reagents and Purification

2.2.1 Hydrochloric Acid (HCl): 12.1 N hydrochloric acid was obtained from EM Science and used as received.

2.2.2 Aniline: Aniline, purchased from Aldrich, was dried over calcium hydride and tin(II) chloride for 8 hours and then distilled under reduced pressure (about 200 millitorr). (b.p. 184°C)

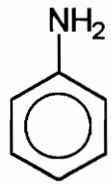

2.2.3 Molecular Sieves: 4Å molecular sieves, purchased from Fisher, were dried for at least 8 hours at 180°C under vacuum prior to use in monomer synthesis.

2.2.4 Potassium Carbonate (K_2CO_3): Fisher brand K_2CO_3, used in poly(arylene ether) syntheses, was dried under vacuum at 180°C for 8 hours prior to use.

2.2.5 Glacial Acetic Acid (CH_3COOH): Glacial acetic acid, obtained from Fisher, was used as received. (b.p. 116-118°C)

2.2.6 Poly(ether ether ketone) Particles: PEEK particles with a diameter of 12 microns, provided by ICI Americas Inc., were used after extensive extraction with THF followed by drying under vacuum at room temperature until constant weight (about 24 hours).

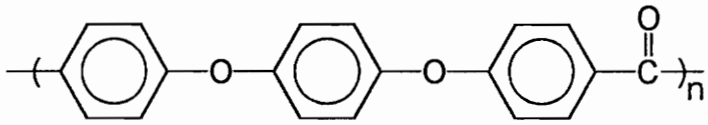

2.2.7 Triton X-100: Triton X-100, obtained from Aldrich, was used as an aqueous suspension stabilizer for PEEK particles.

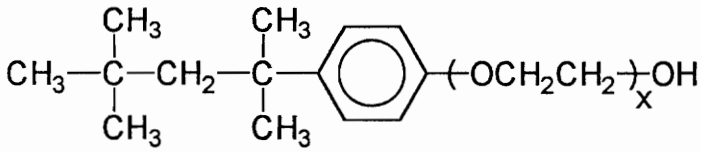

x = 10 (average)

2.3 Monomer Purification

2.3.1 4,4'-Difluorobenzophenone (DFBP): DFBP was kindly provided by ICI and purified by recrystallization from ethanol followed by drying in a vacuum oven at about 90°C overnight. (FW = 218.20 amu; m.p. 102-105°C)

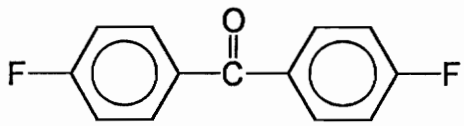

2.3.2 Hydroquinone (HQ): Gold Label hydroquinone (>99.9% purity) was purchased from Aldrich and used as received. (FW = 110.11 amu; m.p. 174.4-176.6°C)

2.3.3 2,6-Dichloropyridine: 2,6-Dichloropyridine was obtained from Aldrich, recrystallized from ethanol, and vacuum dried at 50°C prior to use. (FW = 147.99 amu; m.p. 87-88°C)

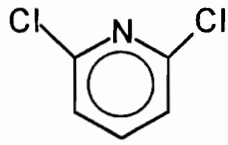

2.4 Synthesis of Monomer and Polymer

2.4.1 Synthesis of 4,4'-Difluoro(N-benzohydroxylidene aniline) (ketimine monomer): Synthesis of 4,4'-difluoro(N-benzohydroxylidene aniline) follows the procedure developed by A. Brink in Prof. Riffle's laboratories.[56] 120 g (0.55 moles) of 4,4'-difluorobenzophenone and 80 mL (0.88 moles) of aniline were added into a 1000 mL four-necked round-bottomed flask equipped with a nitrogen inlet, overhead stirrer, Dean Stark trap and a condenser. Then 500 mL of toluene and 300 g of 4Å molecular sieves were added. Then this reaction mixture was stirred at toluene refluxing temperature until 100% conversion to the ketimine had occurred (about 24 hours) as determined by ^{1}H NMR and Thin Layer Chromatography (TLC) using a developing solvent of ethyl acetate and hexane (1:5 by vol.). After reaction was complete, molecular sieves were removed by

filtration. The solvent was removed by rotary evaporation. The excess aniline was removed by recrystallization. The reaction product was recrystallized twice from toluene and dried at 90°C under vacuum to provide a pure yellow crystalline material with melting point of 114-115°C at a yield of 70%.

2.4.2 Synthesis of Poly(ether ether ketimine) (PEEKt): Synthesis of poly(ether ether ketimine) follows the procedure developed by A. Brink in our laboratories.[56] It was conducted via nucleophilic aromatic substitution in a polar solvent. The molecular weight was controlled to 20,000 g/mol by offsetting the stoichiometry using the Carother's equation to provide a hydroquinone terminated polymer.

First, 3.3 g (0.03 moles) of hydroquinone, 8.63 g (0.0295 moles) of 4,4'-difluoro(N-benzohydroxylidene aniline) and 6.22 g (0.045 moles) of potassium carbonate were dissolved in 60 mL of NMP in a 250 mL four-necked round-bottomed flask equipped with a condenser, Dean Stark trap, overhead stirrer and nitrogen inlet. Then 40 mL of toluene were added as an azeotroping agent. The reaction mixture was heated to toluene refluxing temperature and held for three hours to dehydrate the system, and then the temperature was raised to 170°C to react for 12 hours. After reaction was complete, the reaction was cooled, the solution was diluted with tetrahydrofuran (about 40 mL) and neutralized with 2.5 mL of glacial acetic acid. Finally, this solution was precipitated into a mixture of methanol and water (80:20 by vol.), soxhlet extracted with methanol, and dried under vacuum at 60°C for 8 hours followed by 140°C overnight.

2.4.3 Synthesis of Poly(pyridine ether-co-ether ether ketimine): The procedure of synthesizing poly(pyridine ether-co-ether ether ketimine) was first developed by A. Brink

in our laboratories.[56] The following is a exemplary procedure for the synthesis of poly(pyridine ether-co-ether ether ketimine) via nucleophilic aromatic substitution in a polar aprotic solvent. This copolymer contains 80 mole percent 4,4'-difluoro(N-benzohydroxylidene aniline) and 20 mole percent 2,6-dichloropyridine with uncontrolled molecular weight using a 1:1 stoichiometry of the monomers. Controlled molecular weight copolymers were also made in a similar way using tert-butylphenol as the endcapping reagent.

5.5056 g Hydroquinone (0.0500 moles), 11.7326 g 4,4'-difluoro(N-benzohydroxylidene aniline) (0.0400 moles) and 10.3650 g potassium carbonate (0.0750 moles) were dissolved in 90 mL of DMAc in a four-necked round-bottomed flask equipped with a Dean Stark trap, condenser, nitrogen inlet, overhead stirrer and thermometer. 50 mL toluene was added as an azeotroping agent. The system was dehydrated at 140°C for three hours followed by raising the temperature to 160°C. Once the temperature was equilibrated, 1.4799 g of 2.6-dichloropyridine (0.0100 moles) and 30 mL of DMAc were added. The reaction mixture was allowed to react for 35 hours at 160 °C, then precipitated into methanol/water (80:20) and dried at 60°C under vacuum for 8 hours followed by 120°C overnight.

2.4.4 Hydrolysis of Poly(ether ether ketimine) to Poly(ether ether ketone): The following is a procedure of acid hydrolysis for the imine functionality to the ketone, as developed by A. Brink as a part of his Ph.D. research.[56] The conditions of the acid hydrolysis are such that the pyridine moiety in the backbone is also protonated during this procedure.

2 g of poly(pyridine ether-co-ether ether ketimine), 38 mL of NMP and 1.6 mL of H_2O were added into a flask, followed by increasing the temperature to 80°C. Once the mixture was homogeneous, 3 mL of an HCl/NMP solution (1 part of 12.1 N aqueous HCl in 4 parts of NMP) was added into the polymer solution while stirring continuously. The polymer precipitated immediately. The precipitated particles were then washed with water and centrifuged. After the solvent and acid were totally removed, the washed particles were resuspended in water using an aqueous suspension stabilizer, Triton X-100. The suspension was then sonicated for 3 minutes at 75 watts to break up any aggregates, followed by particle size measurement using a centrifugal particle size analyzer as described in the characterization section.

2.5 Adsorption Experiments

2.5.1 Time-dependent Studies: The following example is a procedure for adsorption of the electrostatic stabilizer precursor, poly(pyridine ether-co-ether ether ketimine) onto 12 micron diameter PEEK particles. It is designed to define the time period necessary to reach adsorption equilibrium. The stabilizer used in the adsorption studies was a poly(pyridine ether-co-ether ether ketimine) copolymer with a molar ratio of pyridine to ketimine of 30/70 and a targeted molecular weight of 25,000 g/mole.

8 mL of the stabilizer solution of toluene containing a constant weight of 0.0120 g stabilizer and 0.6 g 12 micron PEEK particles were charged to a vial. The mixture was sonicated for 3 minutes at 75 watts followed by stirring for a certain amount of time at room temperature. Then the particles were separated from the solution by centrifugation and the supernatant was collected for the UV/VIS measurements.

Aliquots of the supernatant and original stabilizer solutions were transferred to vials and the toluene was evaporated on a hot plate. The poly(pyridine ether-co-ether ether ketimine) stabilizer remaining in the vials was redissolved in HPLC grade THF (UV cut-off 220 nm). Percent adsorption of the stabilizer onto the PEEK particles was calculated using the following equation:

$$\% \text{ Adsorption} = [1 - \frac{\text{absorbance of supernatant}}{\text{absorbance of stabilizer solution}}] \times 100$$

The amount of adsorbed stabilizer in grams was calculated as follows:

Amount of Adsorption = (% Adsorption)(initial weight [g] of stabilizer)

2.5.2 Adsorption onto 12 Micron Diameter PEEK Particles: Adsorption isotherms of poly(pyridine ether-co-ether ether ketimine) onto PEEK particles were measured. Stabilizer solutions were prepared by dissolving 1 to 20 weight percent of stabilizer relative to particles in toluene. To study the isothermal adsorption of the stabilizer onto 12 micron PEEK particles, 5 mL of the stabilizer solution were charged to a vial containing 0.6 g PEEK particles. The mixture was sonicated for 3 minutes. After sonication the stabilizer/PEEK mixture was stirred for 70 hours at room temperature until adsorption equilibrium was achieved. The particles were separated from the solution by centrifugation and the supernatant was collected for the UV/VIS measurements. The amount of adsorbed stabilizer was determined in the same manner as described previously.

2.5.3 Adsorption onto Submicron PEEK Particles: A different procedure was applied to the submicron particles since they tend to aggregate. 10 mL of stabilizer solution were

added into a vial with 1.00 g "wet" (in toluene) submicron particles (about 0.07 g after drying). The samples were sonicated and centrifuged. After removing 2 mL of the supernatant as the "original stabilizer solution", the sample was sonicated extensively to break up the aggregates before adsorption at room temperature. The samples were allowed to reach equilibrium over the course of three days and subsequently centrifuged and the supernatants collected for analysis by UV/VIS.

2.5.4 Hydrolysis of Poly(pyridine ether-co-ether ether ketimine) After Adsorption onto the Particles: After adsorption, the sample was centrifuged and the supernatant was removed. The sediment was stirred at room temperature in 10 mL of a mixture of NMP, H_2O and HCl with a 10:1 volume ratio of NMP to H_2O, and a 1.3:1 mole ratio of HCl to imine functionality in the poly(pyridine ether-co-ether ether ketimine). After adding this solvent mixture, an intense yellow color was observed. Approximately 20 minutes are required for the color to disappear. This color change may indicate that the ketimine-pyridine copolymer coated on the particles was hydrolyzed. Then the sample was centrifuged and the supernatant was removed. The particles were rinsed with ethanol to remove traces of toluene and other soluble chemicals, and to render their surfaces wettable with water. Finally water was introduced to prepare aqueous dispersions of PEEK particles.

2.6 Characterization of Aqueous PEEK Suspensions

2.6.1 Sedimentation Experiments: Sedimentation experiments were used for characterizing the stabilities of 12 micron diameter PEEK suspensions. After hydrolysis of the poly(pyridine ether-co-ether ether ketimine), the coated particles were dispersed in

calculated volumes of water (adjusted to pH = 2 or 4 with hydrochloric acid) in graduated cylinders. The volume of the sediment was recorded after the suspension was allowed to settle for designated times.

2.6.2 Turbidity Measurements: Turbidity measurements were designed to characterize the stabilities of submicron PEEK suspensions. 15 mL water (adjusted to pH = 2 or 4 using hydrochloric acid) was charged to a sample tube containing 0.1 g "wet" (~7 mg after drying) coated submicron PEEK particles. After the sample was sonicated for 3 minutes, the turbidities of the suspension were measured with a Turbidimeter at ambient temperature as a function of time.

2.7 Instrumentation

2.7.1 Nuclear Magnetic Resonance (NMR) Spectroscopy: Proton NMR (^{1}H NMR) was utilized to determine reaction conversion, monomer purity, as well as the reaction products. The ^{1}H NMR studies were conducted on a Varian Unity NMR spectrometer operating at 400 MHz. Sample concentrations were typically in the range of 1% to 10% solids using deuterated solvents such as $CDCl_3$.

2.7.2 Thin Layer Chromatography (TLC): TLC plates (silica gel on glass, mean pore diameter, 60Å; mean particles size, 2-25 micron) were used to determine reaction conversion and monomer purity. The developing solvents were usually a mixture of solvents, such as hexane, ethyl acetate, methanol, chloroform, dichloromethane, in various designated proportions.

2.7.3 Thermogravimetric Analysis (TGA): TGA was used to determine the thermal stability, thermo-oxidative stability and to detect any possible solvent contamination in the polymers. It was conducted on a Perkin-Elmer Series 7 thermal analyzer, with an air purge at a heating rate of 10°C per minute. The weight loss of the sample was measured as a function of temperature. The temperature corresponding to 5% weight loss was recorded and used as a criterion to determine the upper temperature limit of the sample for a DSC experiment.

2.7.4 Differential Scanning Calorimetry (DSC): By measuring the intensity difference of the electric current (heating flow) between sample and reference as a function of temperature, DSC was used to determine the glass transition temperature and melting temperature of polymers. DSC experiments were performed on a Perkin-Elmer Series 7 thermal analyzer, usually under a nitrogen purge at a heating rate of 10°C per minute.

2.7.5 Scanning Electron Microscopy (SEM): SEM measurements were conducted using a Philips 420T scanning transmission electron microscope (STEM) with a secondary electron detector, operating at 60 kV in the SEM mode. The sample preparation was as follows: the sample was placed on a copper strip as a dilute suspension, dried in a vacuum oven at room temperature, and then gold coated with a high resolution sputter coater at 630 volts, 32 mA for 3 minutes. SEM was used to examine the size and distribution of the submicron PEEK particles prepared in our laboratories.

2.7.6 Intrinsic Viscosity Measurement: Intrinsic Viscosity Measurements were used to characterize the interaction between solvent and polymer chains. The viscosity of the polymer solution was recorded using a B204 Ubbelhode Viscometer at 25°C. The

intrinsic viscosity calculation was done using the Macintosh computer and program INT*2.

2.7.7 Particle Size Analysis: The particle size (median diameter) and particle size distribution were measured on a Centrifugal Particle Size Analyzer by Shimadzu. This instrument detects the turbidity of the settling suspensions and correlates the sedimentation rate to particle size by using Stokes law. Several parameters were required for the calculation. Density and viscosity of the solvent (water) are 0.998 g/mL and 0.938 cP; Density of the particles was approximated by that of bulk poly(ether ether ketone), 1.3 g/mL.

2.7.8 Sonication: Suspension samples were sonicated to break up aggregates and flocculates using a Sonic Disruptor by TeKmar at 20 watts or a Ultrasonic Cleaner at 117 volts, 0.7 amps and 50-60 Hz.

2.7.9 Turbidity Experiments: A light scattering apparatus (Patio/XR Turbidimeter, Hach company) measures at ambient temperature the turbidity of a settling suspension, thus giving information on the stability of the suspension.

2.7.10 UV-VIS: A Perkin-Elmer, Lambda 4B, UV-VIS Spectrophotometer was used to measure the concentrations of Poly(pyridine ether-co-ether ether ketimine) solutions.

Chapter 3. Results and Discussion

3.1 Preparation of Materials

3.1.1 Introduction

The objective of this research was to prepare aqueous poly(ether ether ketone) suspensions suitable for processing composites by aqueous dispersion prepregging. This thesis includes several areas: 1) Preparation of fine PEEK particles; 2) Preparing the high performance aqueous electrostatic stabilizer; 3) Adsorption of the stabilizer onto the particles; 4) Preparing aqueous suspensions of the coated particles and analyzing the stabilities of the suspensions. This section is a brief discussion of the material preparation, including synthesis of PEEK particles and the stabilizer essentially following the procedures developed by A. Brink in our laboratories.[56] Preparation of fine PEEK particles first involves the synthesis of a soluble, amorphous precursor, poly(ether ether ketimine) (PEEKt), followed by acid hydrolysis of PEEKt to PEEK in the form of fine particles. Preparation of the electrostatic stabilizer involves synthesis of a soluble stabilizer precursor, which is a random copolymer of ketimine and pyridine moieties, followed by acid hydrolysis of the stabilizer precursor to form the actual electrostatic stabilizer.

3.1.2 Synthesis of 4,4'-Difluoro(N-benzohydroxylidene aniline)

Condensation of 4,4'-difluorobenzophenone and aniline to form 4,4'-difluoro(N-benzohydroxylidene aniline) (ketimine monomer) is well established,[19,21,56] as shown in

Figure 3.1. The reaction can be monitored by TLC and ^{1}H NMR. An excess amount of aniline was used to ensure complete reaction of 4,4'-difluorobenzophenone. The reaction was completed when the stoichiometrically limiting reagent, 4,4'-difluorobenzophenone was totally consumed as monitored by TLC and ^{1}H NMR. In the TLC experiment, a mixed solvent, 1 part ethyl acetate and 5 parts hexane, was used as the developing solvent. At the beginning of the reaction, the TLC results showed intense spots of aniline and 4,4'-difluorobenzophenone. As the reaction proceeded, the product, 4,4'-difluoro(N-benzohydroxylidene aniline) appeared and increased in intensity. Finally, the spot corresponding to 4,4'-difluorobenzophenone almost could not be detected, and the reaction was considered complete. An NMR technique was also used to determine the extent of reaction. The peak corresponding to the four identical protons in 4,4'-difluorobenzophenone (7.82 ppm) (Figure 3.2) disappeared as the reaction proceeded, while other peaks including the protons ortho and trans to the phenyl group on the nitrogen (imine phenyl) (7.75 ppm) (Figure 3.3)[56] increased in intensity.

Interpretation of the NMR spectrum of 4,4'-difluoro(N-benzohydroxylidene aniline), the ketimine monomer, is complicated. In the ketimine monomer, the bulky ketimine prevents both of the fluorine containing aromatic rings from being in the same plane with the imine double bond. Computer modeling of the ketimine structure (Figure 3.4)[56] shows that the fluorine containing ring cis to the imine phenyl is not coplanar to the imine double bond. Therefore it can't completely feel the electron-withdrawing nature of the double bond. As a result, both ortho and meta protons cis to the imine phenyl move upfield, i.e., 7.14 ppm for the ortho protons (originally at 7.82 ppm, see Figure 3.2) and 6.96 ppm for the meta protons (originally at 7.17 ppm, see Figure 3.2), during the conversion to ketimine, as shown in ^{1}H NMR (Figure 3.5) and 2-D ^{1}H NMR (Figure

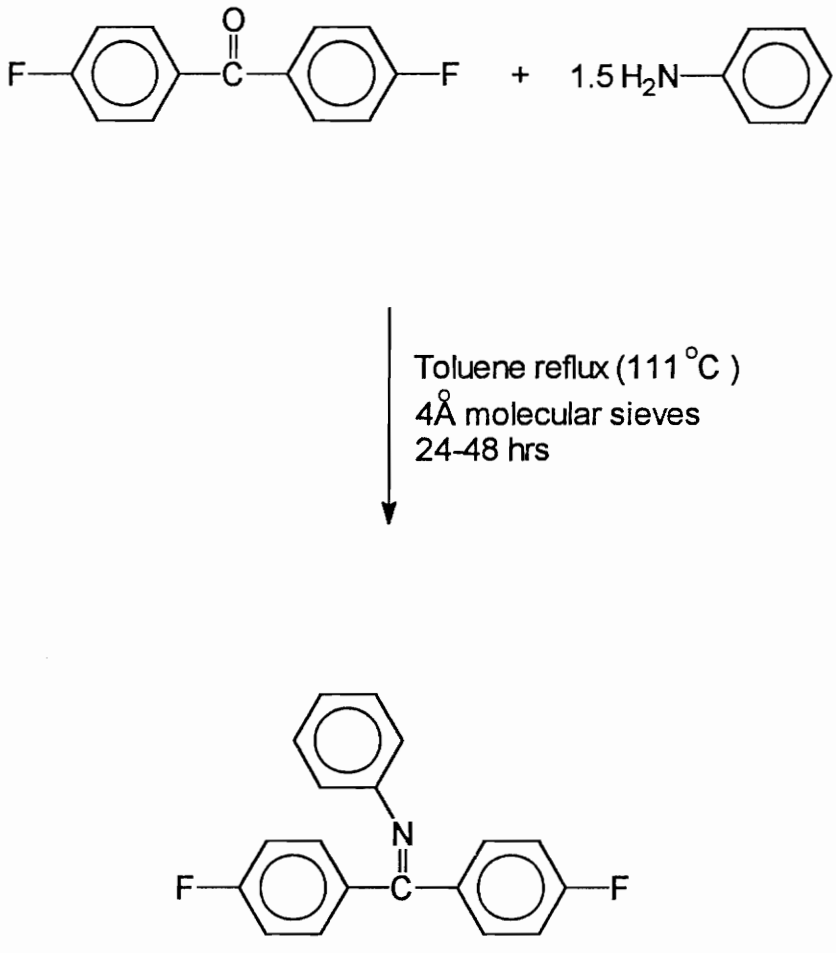

Figure 3.1 Synthesis of 4,4'-difluoro (N-benzohydroxylidene aniline)[56]

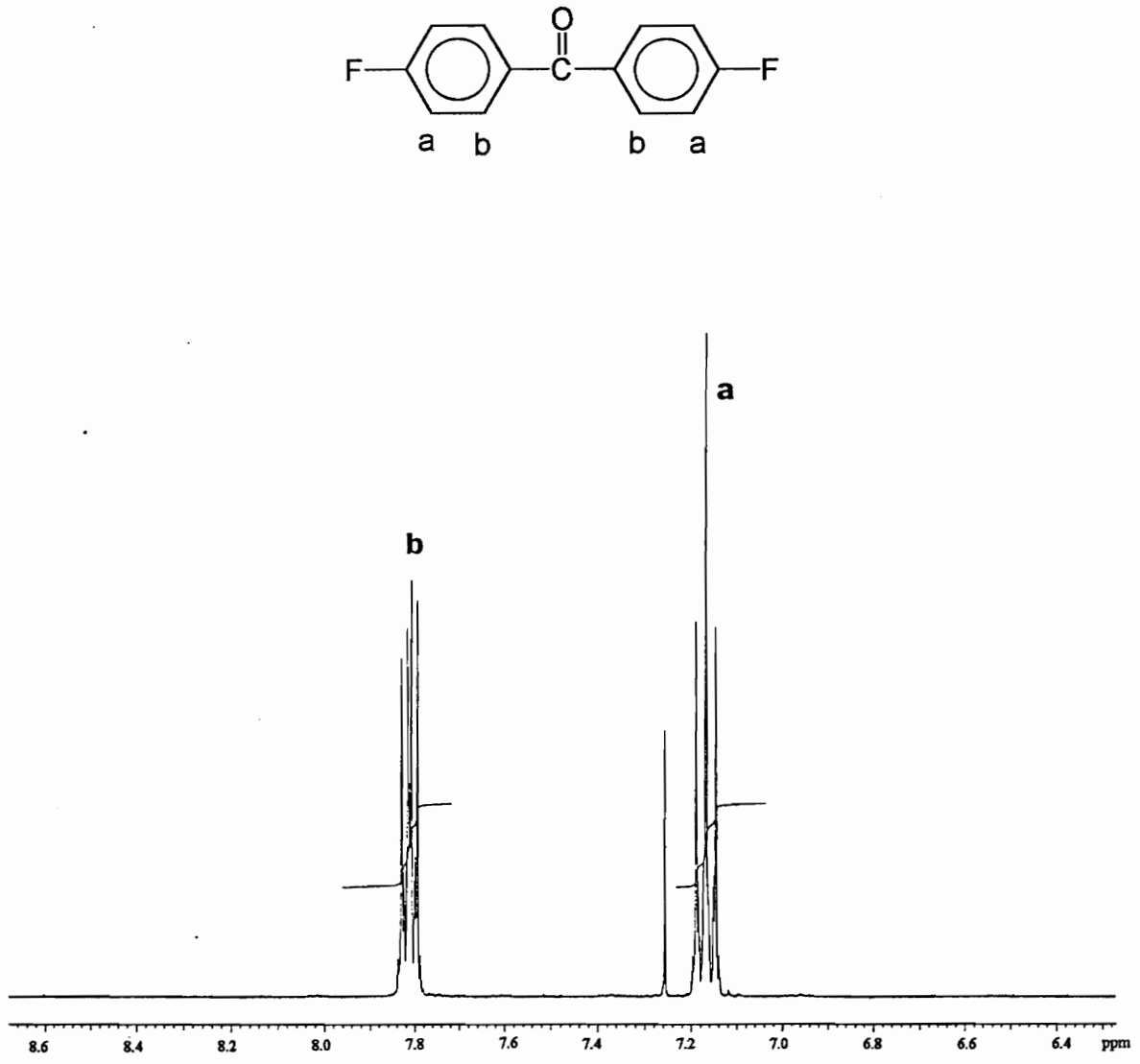

Figure 3.2 ^{1}H NMR of 4,4'-difluorobenzophenone

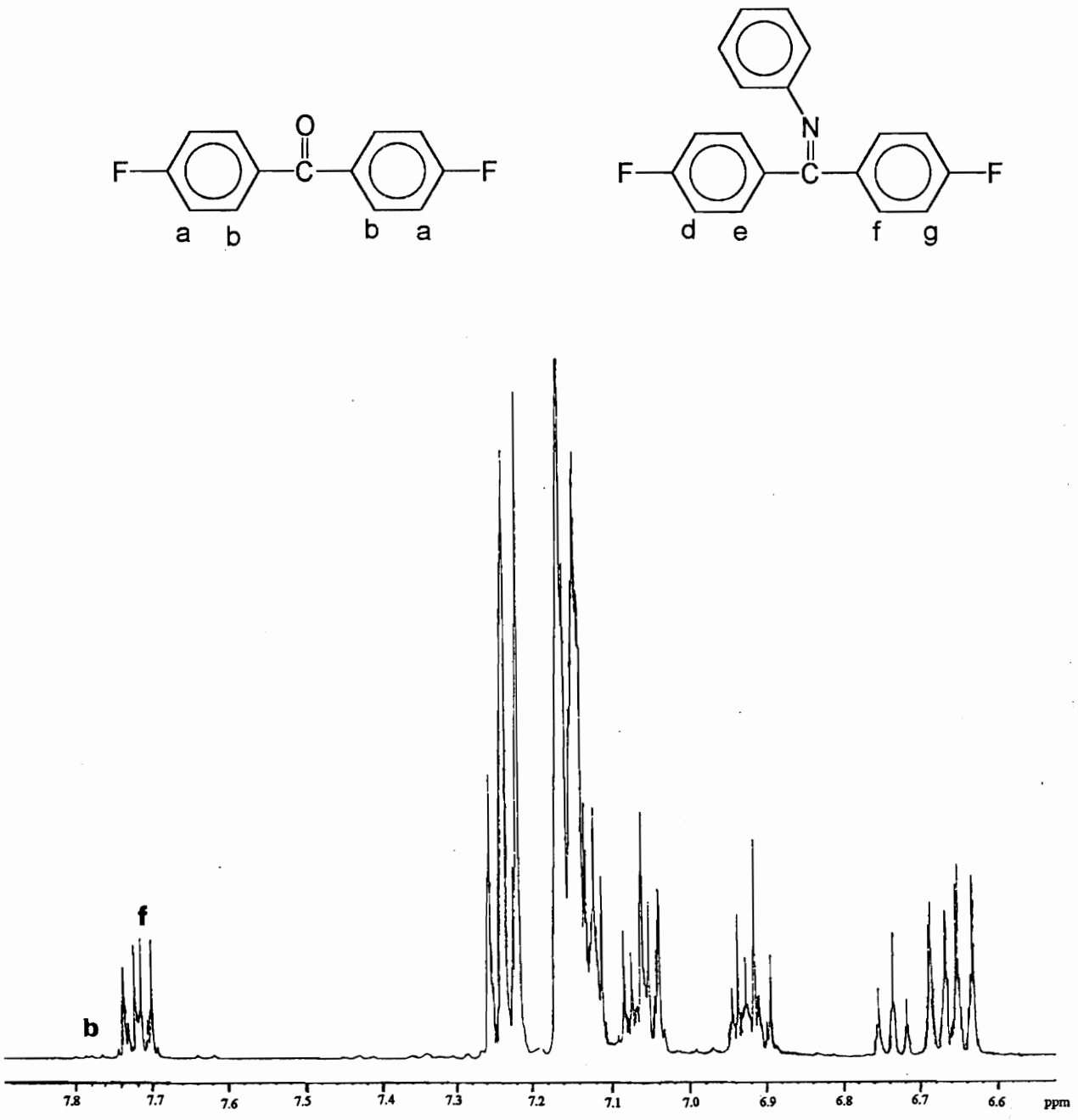

Figure 3.3 ^{1}H NMR of 4,4'-difluoro (N-benzohydroxylidene aniline)[56]

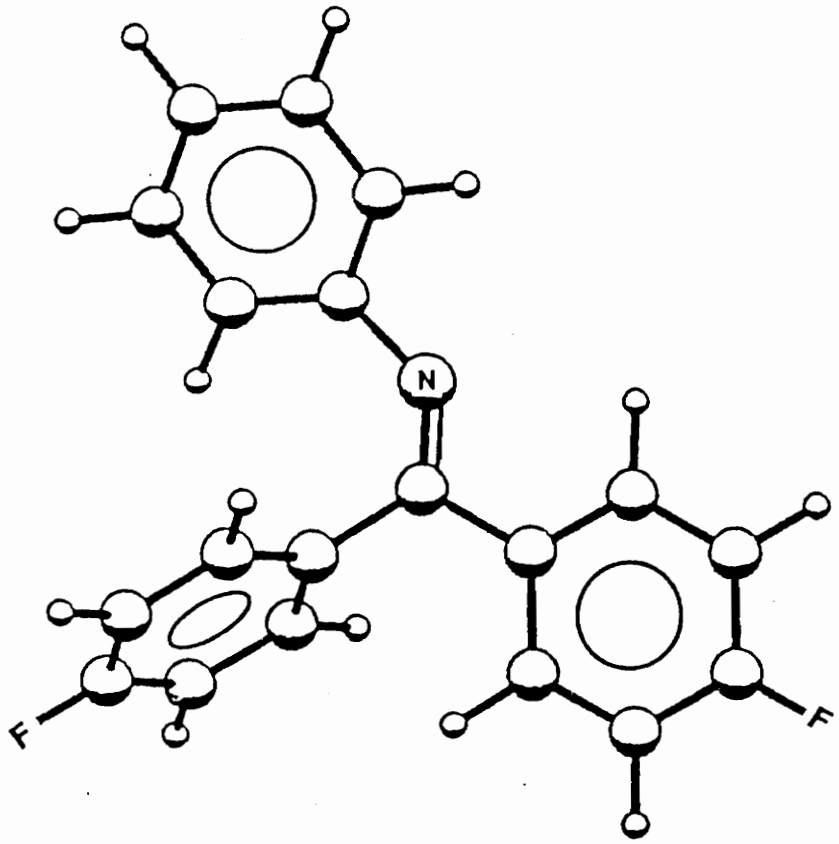

Figure 3.4 3-D Configuration of 4,4'-difluoro (N-benzohydroxylidene aniline) (PC Model)[56]

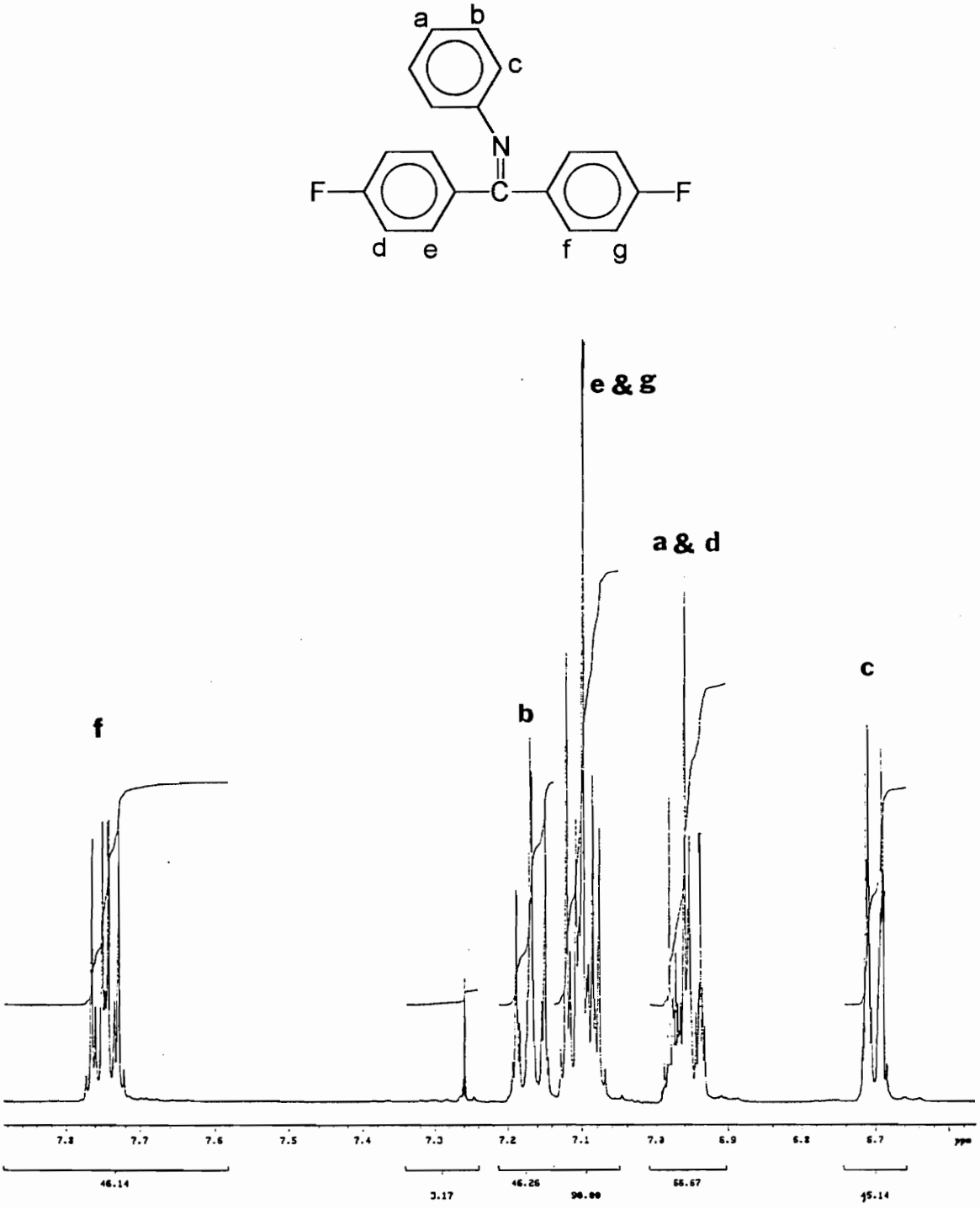

Figure 3.5 ^{1}H NMR of 4,4'-difluoro (N-benzohydroxylidene aniline) (ketimine monomer)

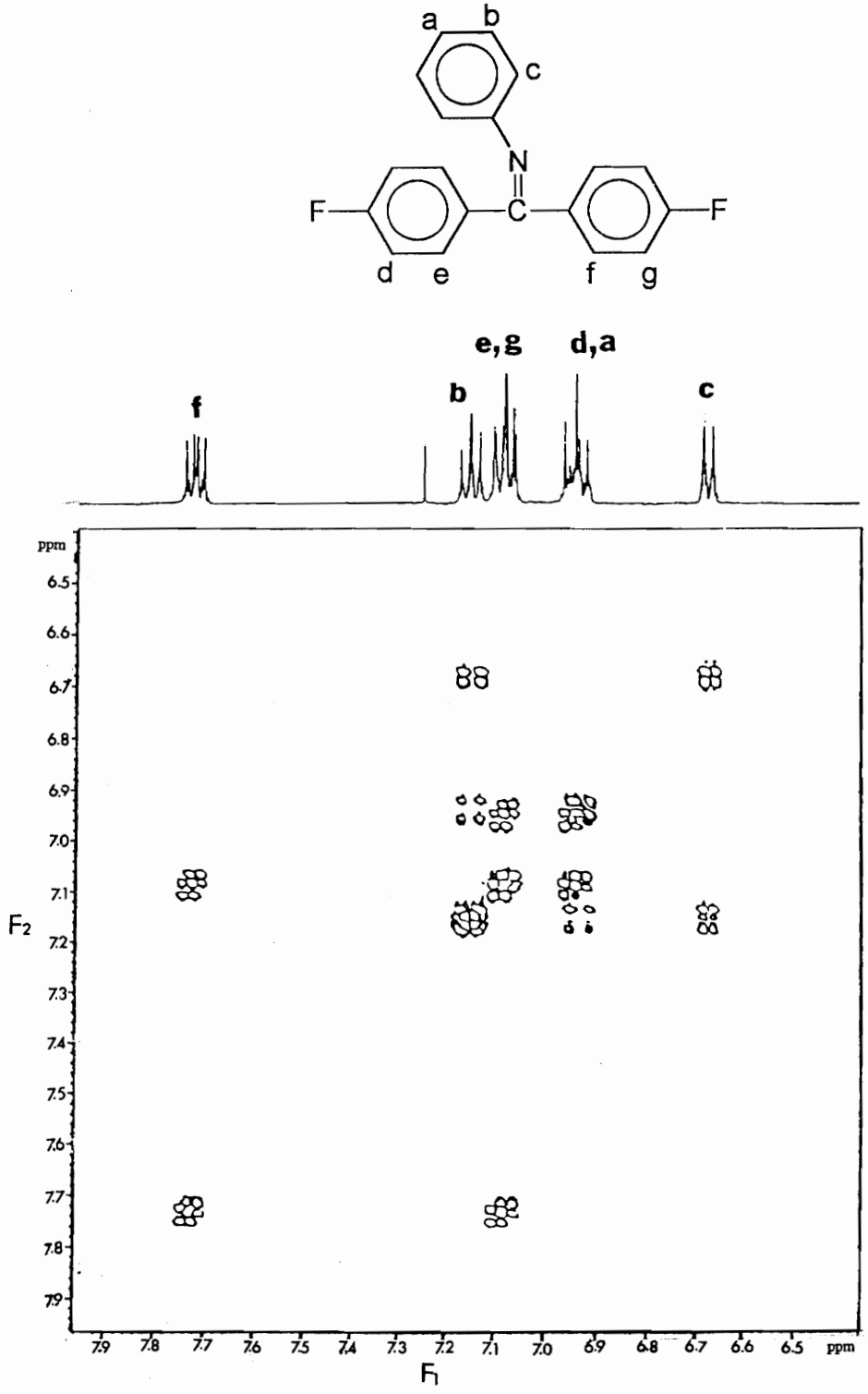

Figure 3.6 2-D ^{1}H NMR of 4,4'-difluoro (N-benzohydroxylidene aniline)[56]

3.6)[56] of the ketimine monomer. Since the ortho and meta protons trans to the imine phenyl are on the ring which is coplanar to the imine double bond, they feel the electron-withdrawing nature of the double bond. However, the electron-withdrawing ability of imine is weaker than that of ketone. Thus, their chemical shifts also move slightly upfield (7.75 ppm for the ortho protons and 7.10 ppm for the meta protons).

The ketimine monomer can be purified by recrystallization two times from toluene followed by drying at 90°C under vacuum. It is a pure yellow crystalline material with a melting point of 114-115°C.

3.1.3 Synthesis of Poly(ether ether ketimine) (PEEKt)

Synthesis of poly(ether ether ketimine) from 4,4'-difluoro(N-benzohydroxylidene aniline) and hydroquinone is well established (Figure 3.7).[19,21,56] Poly(ether ether ketimine) is an amorphous, soluble precursor polymer of poly(ether ether ketone). It is soluble in solvents such as NMP, toluene, THF, DMAc and chloroform. Its glass transition temperature is 164°C as determined by DSC.[56] The ^{1}H NMR spectrum of PEEKt in $CDCl_3$ is shown in Figure 3.8.

3.1.4 Hydrolysis of Poly(ether ether ketimine) to Poly(ether ether ketone)

Acid hydrolysis of poly(ether ether ketimine) readily converts the imine functionalities to ketone (Figure 3.9). Since poly(ether ether ketone) is semi-crystalline and insoluble, it crystallizes from solution in the form of small particles.[56] The thermal

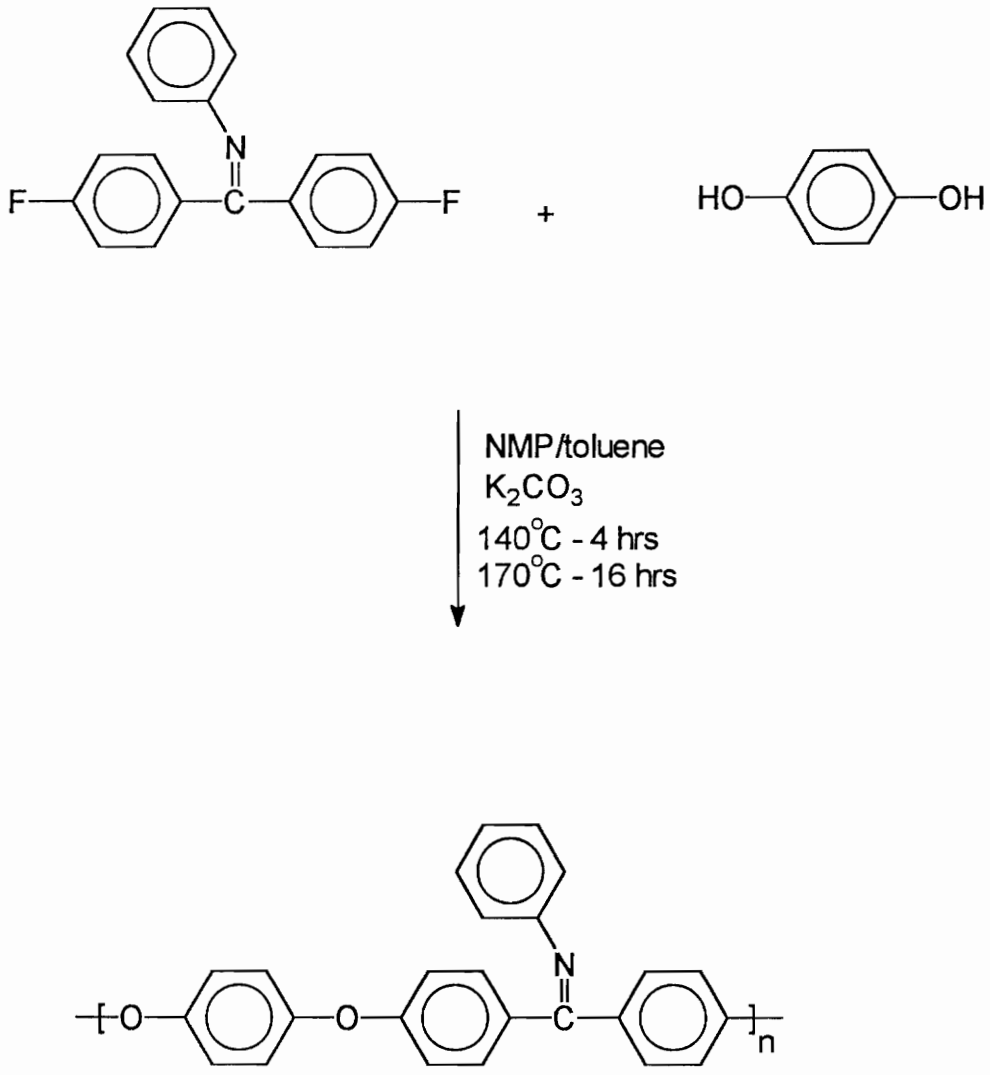

Figure 3.7 Synthesis of poly(ether ether ketimine) (PEEKt)

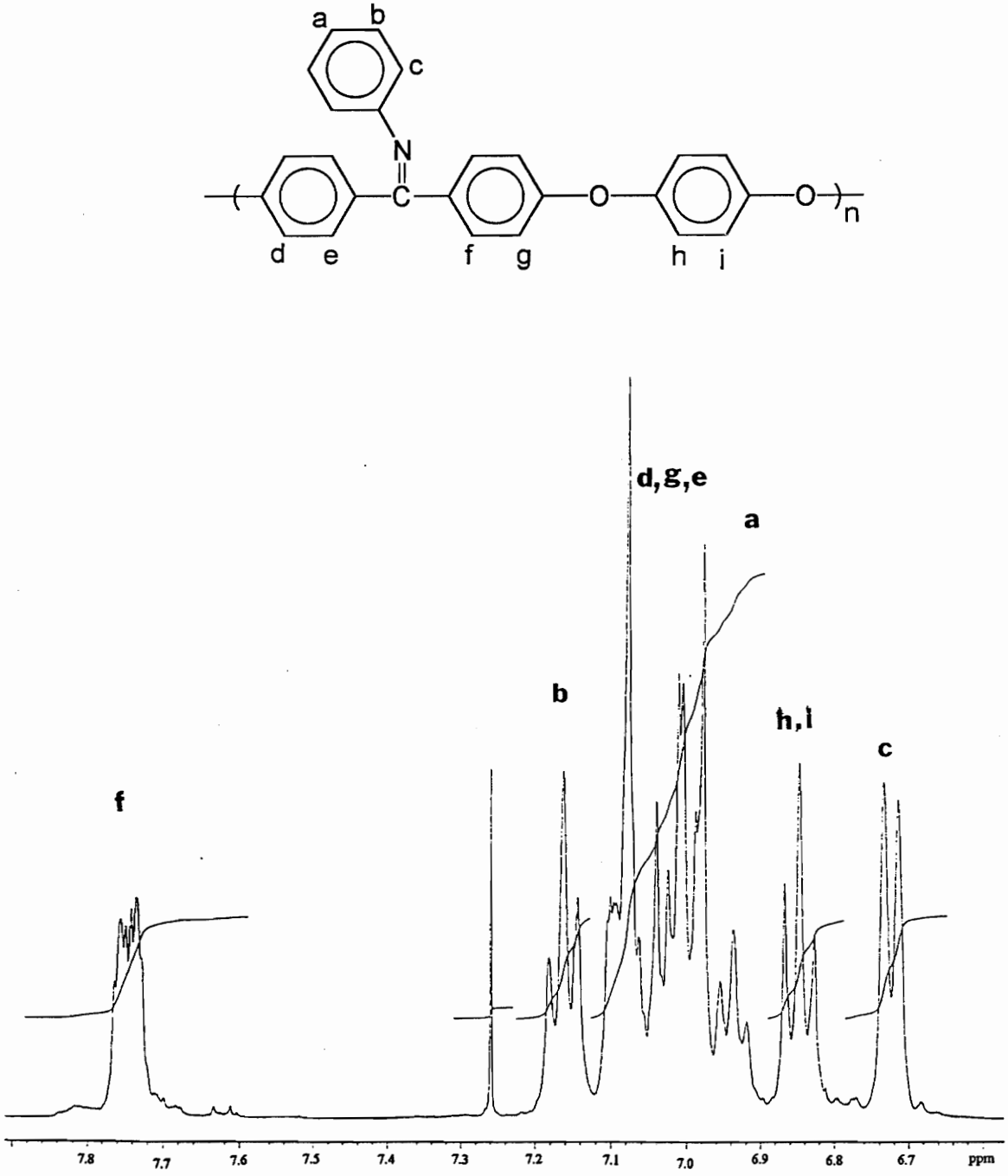

Figure 3.8 ^{1}H NMR of poly(ether ether ketimine) (PEEKt)

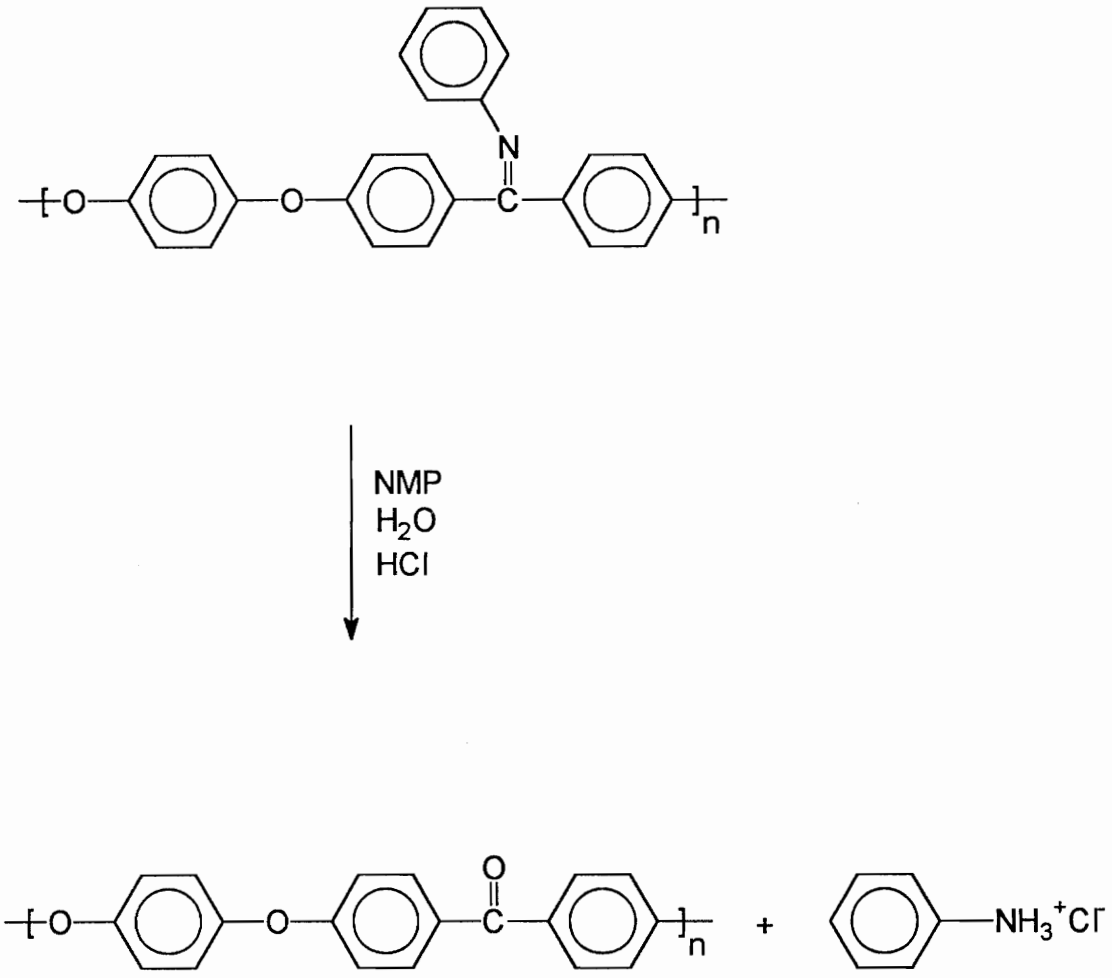

Figure 3.9 Hydrolysis of poly(ether ether ketimine) to poly(ether ether ketone)

stability and transition temperatures such as T_g and T_m of thus prepared PEEK is essentially identical to that of commercial PEEK as determined by TGA and DSC.[56]

The PEEK particles were dispersed in water using Triton X-100 (an aqueous surfactant) as the stabilizing agent. The particle size was measured using a Particle Size Analyzer (PSA) by the sedimentation method based on Stokes' law. Sedimentation from an initially uniform suspension is employed. A light scattering apparatus detects the change in concentration of the suspension since the intensity of transmitted light increases as the particle concentration decreased. The Particle Size Analyzer gives the particle size (Stokes diameter) and size distribution (the quantity of particles corresponding to specific particle diameters). An example of data calculated using these measurements is illustrated in Figure 3.10. The median diameter is the particle size at which the accumulation of the particles (from the smallest size) is half of the total amount of particles. Another kind of PEEK particles, supplied by ICI, has a median diameter of 12 microns as measured by PSA (Figure 3.10). These particles are made by ball milling, and the PSA results show a large distribution of the particle sizes. One batch of the smallest submicron particles were also analyzed by Scanning Electron Microscopy (SEM) (Figure 3.11) since the lower detection limit with the Particle Size Analyzer is ~ 0.1 micron diameters. The first (A) was taken at a magnification of 25,000 times with a scale bar of 0.5 microns. The second (B) was taken at a magnification of 100,000 times with a scale bar of 0.5 microns. These photomicrographs show that these particular submicron particles are rice-shaped with a length of $\approx$ 0.1 microns and width $\approx$ 0.05 microns. The particle size distribution is relatively uniform. The particle size results from SEM and the Particle Size Analyzer are relatively close with the provision that the samples were well-dispersed using Triton X-100. The size of the particles from hydrolysis of poly(ether ether ketimine)s can be

Submicron PEEK Particles

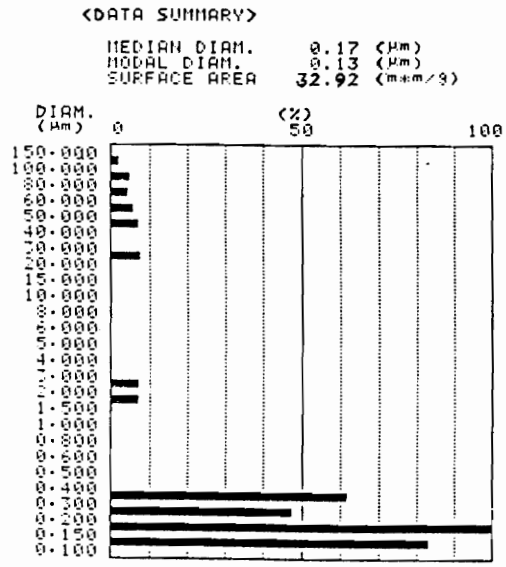

Median Diam. = 0.17 micron

12 Micron PEEK Particles

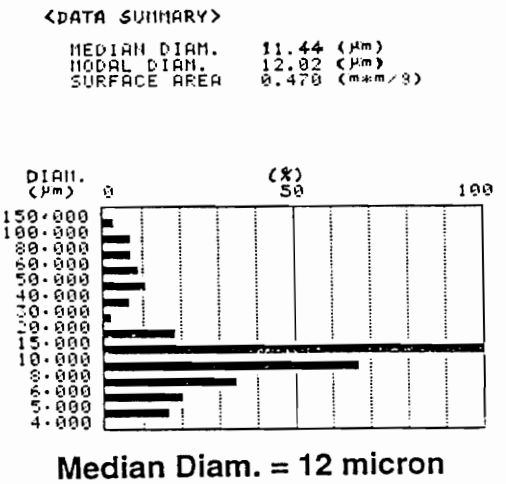

Median Diam. = 12 micron

Figure 3.10 Particle Size Analysis of a: the submicron PEEK particles; b: the 12 micron PEEK particles

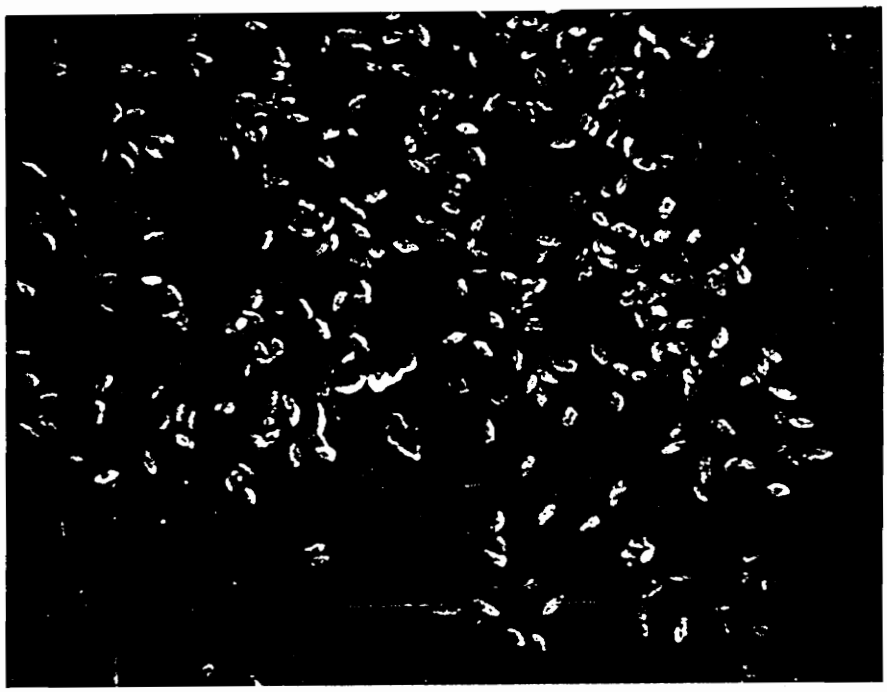

(a)

(b)

Figure 3.11 Scanning Electron Micrographs (SEM) of the submicron PEEK particles

controlled within a certain range by the temperature, acid concentration, water concentration and solvent concentration.[56]

3.1.5 Synthesis of Poly(pyridine ether-co-ether ether ketimine) (Stabilizer Precursor) and Poly(pyridine ether-co-ether ether ketone) (Stabilizer)

Poly(pyridine ether-co-ether ether ketimine) was synthesized by copolymerization of 2,6-dichloropyridine and 4,4'-difluoro(N-benzohydroxylidene aniline) with hydroquinone according to the scheme outlined in Figure 3.12. Poly(pyridine ether-co-ether ether ketimine) is an amorphous, soluble stabilizer precursor. It can be transformed into poly(pyridine ether-co-ether ether ketone) by acid hydrolysis (Figure 3.13). Upon hydrolysis, this polymeric stabilizer crystallizes from solution and presumably lies rather tightly against the PEEK particle surfaces. Simultaneously, hydrolysis results in protonation of the pyridine, which enables the polymer to function as a electrostatic stabilizer. Its temperature at 5% weight loss is 523°C in air by TGA.[56] Therefore it should withstand composite consolidation conditions of approximately 400°C without degradation or burn-out.

Another requirement for the stabilizer is that it must be miscible with the polymer matrix, PEEK. The miscibility study was conducted using DSC by V. Velikove in Prof. Marand's group. The 50:50 blend of the stabilizer (with 30 mole % pyridine) and PEEK shows only one glass transition temperature (Figure 3.14),[56] indicating that the stabilizer is miscible with PEEK and will not lead to phase separation in the composite material. Also, the pyridine units might offer specific interactions with the carbon fiber and thus provide a good interface between the matrix and the fiber.[57]

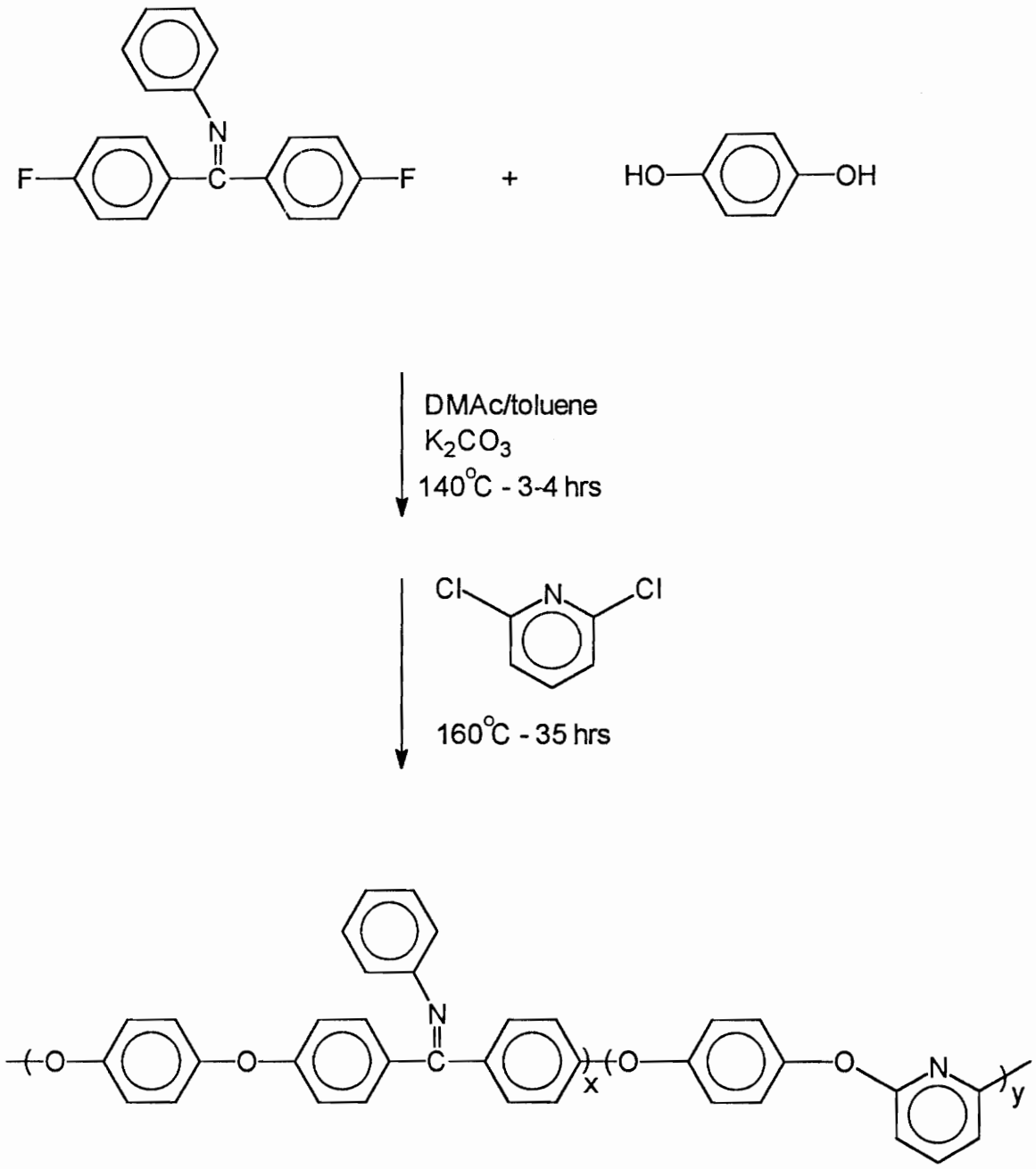

Figure 3.12 Synthesis of poly(pyridine ether-co-ether ether ketimine) (stabilizer precursor)[56]

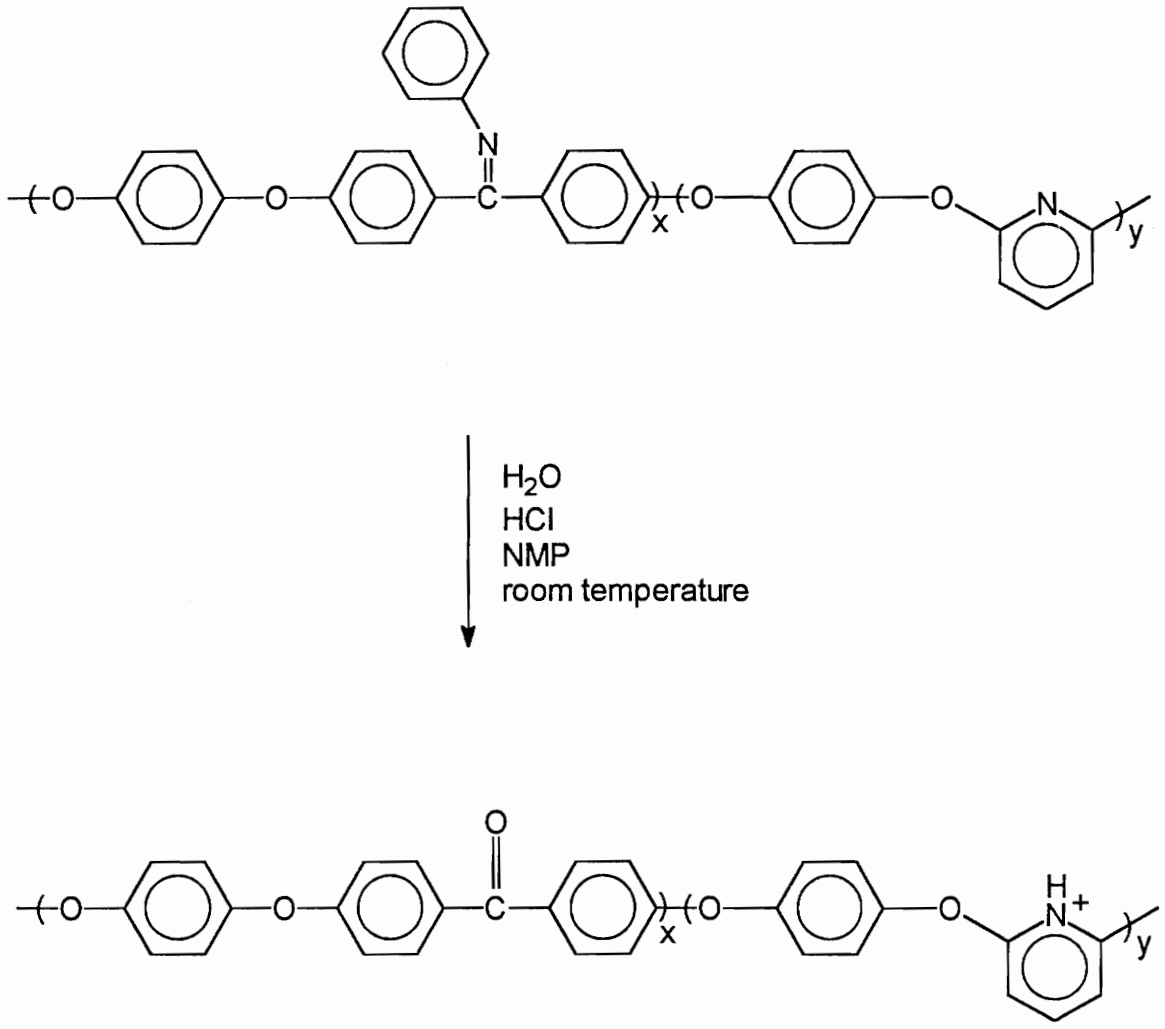

Figure 3.13 Acid hydrolysis of poly(pyridine ether-co-ether ether ketimine) (stabilizer precursor) to poly(pyridine ether-co-ether ether ketone) (electrostatic stabilizer)[56]

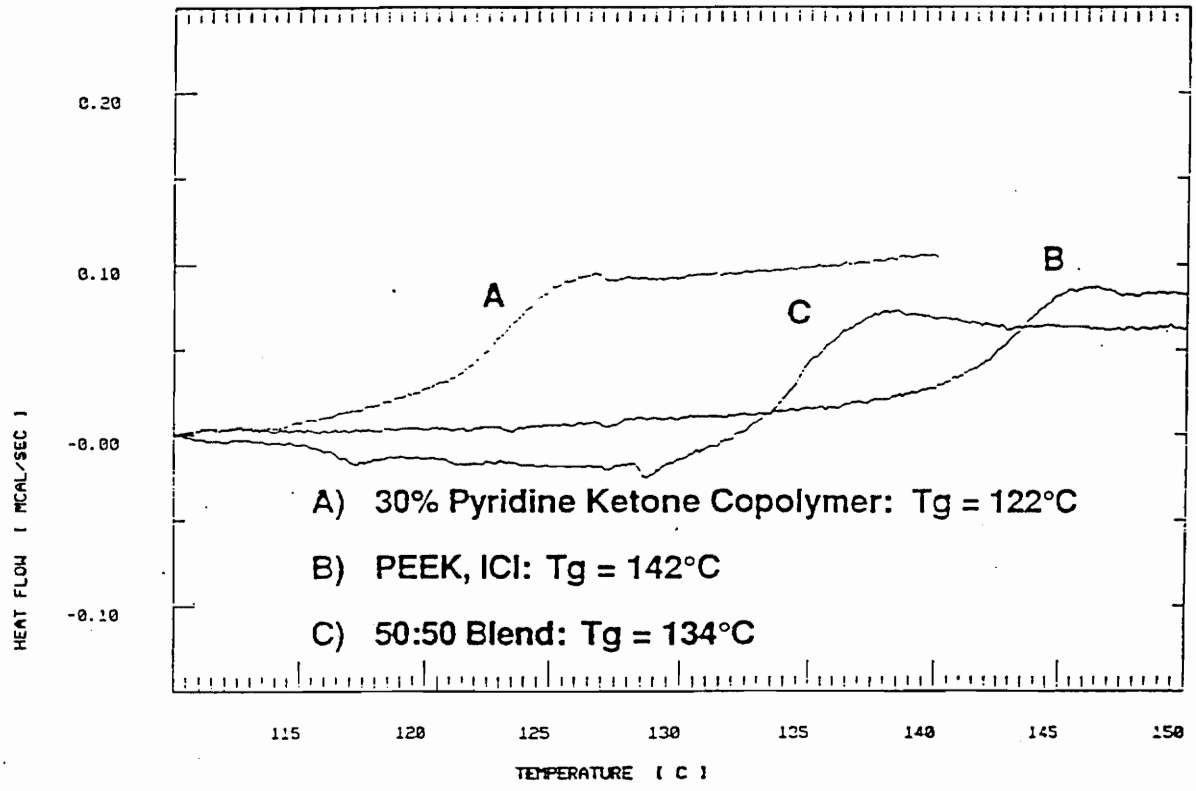

Figure 3.14 DSC demonstration of the miscibility of PEEK and poly(pyridine ether-co-ether ether ketone) (stabilizer)[56]

3.2 Adsorption Studies of the Stabilizer Precursor onto PEEK Particles

3.2.1 Introduction

In recent years, poly(ether ether ketone)s, e.g. PEEK, have become one of the most important thermoplastic matrix resins for high performance fiber reinforced composites because of their excellent thermal, chemical and mechanical properties. However, both large-scale solution prepregging and melt prepregging with PEEK are impractical because solution prepregging involves the use of toxic organic solvents and melt prepregging involves impregnating the fibers with a high viscosity melt. Aqueous dispersion prepregging is a relatively new technique for processing fiber reinforced, polymer matrix composites in an "environmentally friendly" manner. However, this technique requires that the resin must be in the form of particles and be dispersed in water to form a stable aqueous suspension. Since PEEK is hydrophobic, PEEK particles alone can't be dispersed in water. Therefore, an aqueous dispersion stabilizer is required for preparing aqueous dispersions of PEEK particles. This stabilizer should also have good thermal stability to withstand the high processing temperatures for composites. In the previous section, the preparation of submicron PEEK particles and a high performance electrostatic stabilizer are discussed. This section focuses on developing procedures and defining parameters for preparing and characterizing aqueous suspensions of PEEK particles using the materials prepared previously, i.e., the PEEK particles and stabilizers. As shown in Figure 3.15, the preparation of aqueous PEEK suspensions from the particles and stabilizer involves first adsorbing the soluble stabilizer precursor, poly(pyridine ether-co-ether ether ketimine), onto PEEK particles from an organic solvent, followed by hydrolysis of the ketimine moiety on this particle coating in conjunction with

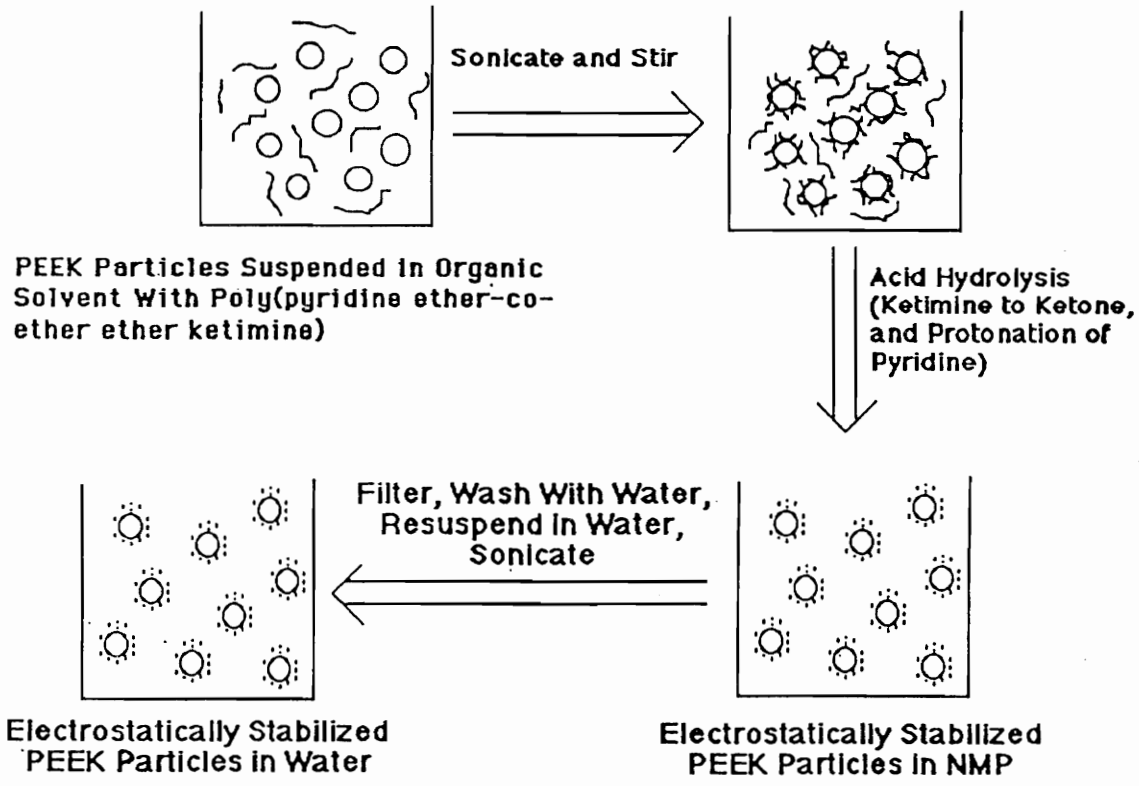

Figure 3.15 Preparation of aqueous PEEK suspensions

protonation of the pyridine units. These electrostatically stabilized PEEK particles are then rinsed and dispersed in water and stabilities of the suspensions are analyzed.

There are two sizes of particles used in this research. One of them was provided as a gift by the ICI Company. These particles have a median diameter of 12 microns as measured by the Particle Size Analyzer. These PEEK particles will be referred to as 12 micron PEEK particles in this thesis. Submicron PEEK particles with median diameter 0.35 micron were prepared by rapidly acid hydrolysis of a soluble precursor, poly(ether ether ketimine).

Since the 12 micron PEEK particles and the submicron particles have greatly different size ranges, the techniques used for analyzing the stabilities of suspensions of these two kinds of particles were different. To analyze the stabilities of 12 micron PEEK particle suspensions, sedimentation experiments were employed. For the submicron particle suspensions, the force of gravity (proportional to the mass of the particle) which causes the particles to settle is counterbalanced by the Brownian motion of the particles. Thus, these particles never completely settle. Therefore, sedimentation techniques can't be used to analyze the stability of submicron particle suspensions. Instead, a light scattering apparatus, a turbidimeter, was used to analyze the stability of the submicron suspensions. Unfortunately, this technique is limited to fairly dilute suspensions because at higher concentration, the intensity of transmitted light is too low for the detector to make an accurate measurement. Since different techniques were used for analyzing the stabilities of suspensions of the 12 micron PEEK particles and the submicron particles, isothermal adsorption studies were also conducted for both of these particles.

3.2.2 Measuring the Amount of Stabilizer Adsorbed

In order to establish the adsorption isotherms for adsorption of polymer onto particles, the amount of the polymer adsorbed was measured. Adsorption analyses must be quite sensitive because the concentrations involved are usually very low. Two basic techniques for measuring the adsorption isotherms are: 1. Measuring the concentration change upon adsorption by using spectroscopic methods; 2. Directly observing the adsorbed amount by gravimetric analysis.[52] Practical difficulties are also presented such as separating the equilibrium solution after adsorption is completed.

A relatively small amount of particles were used for the adsorption of the stabilizer precursor, poly(pyridine ether-co-ether ether ketimine), onto PEEK particles. Correspondingly, the concentrations of the stabilizer were very low. For example, in the isothermal adsorption experiment with 0.6 g of 12 micron PEEK particles, 0.006 - 0.072 g of the stabilizer precursor (1 - 12 wt. % relative to particles) were dissolved in 10 mL solvent; in the isothermal adsorption experiment with 0.025 g of submicron particles, 0.00125 - 0.005 g of the stabilizer precursor (5 - 20 wt. % relative to particles) were dissolved in 10 mL solvent. To work with such a small quantity, directly measuring the adsorbed amount is not recommended. Since UV spectroscopy is a relatively sensitive technique to measure the concentration of dilute solutions, it was used to measure the change in solution concentrations upon adsorption. Following is a exemplary procedure for adsorption of the stabilizer precursor onto PEEK particles and for measurement of the adsorbed amount.

In the adsorption studies, a designated amount of stabilizer precursor was dissolved in the solvent. This solution was then stirred with PEEK particles for a certain period of time to allow the stabilizer precursor to adsorb onto the particles. After adsorption, the coated particles were separated from the solution by centrifugation. The supernatant was carefully withdrawn and measured by a Perkin-Elmer, Lambda 4B UV/Vis spectrophotometer in the range 200 - 300 nm, where absorption occurs because of the aromatic double bond. The adsorbed amount of stabilizer precursor, $W_{a.s}$ (mg), can be calculated as follows:

$$W_{a.s} = W_{t.s} (1 - I_s/I_o) \qquad \text{Eq. 3.1}$$

where, $W_{t.s}$ (mg) = the total amount of the stabilizer precursor in the solution;

I_o = absorbency of the original stabilizer precursor solution;

I_s = absorbency of the supernatant at the same wavelength (the original stabilizer precursor solution).

Solvents for the stabilizer precursor include THF, toluene and NMP. Isothermal adsorption measurements were conducted in toluene since good adsorption was obtained. To measure the UV absorbency, small amounts of the original stabilizer precursor solution in toluene were removed using a micropipette (accuracy to 0.01 mL) and then diluted with toluene. At first, toluene was considered as the solvent for the UV experiments. The stabilizer precursor exhibits an absorbency peak maximum at $\lambda \approx 280$ nm. However, toluene has a maximum absorption at $\lambda \approx 260$ nm. Using toluene as the solvent for the UV measurements introduced systematic error although double beam UV spectroscopy was used. In double beam UV spectroscopy, UV absorption of the solvent is subtracted

from the sample since pure solvent is used as reference. However, the absorbency of the toluene is so strong that the intensity of transmitted light is considerably reduced and accurate measurements cannot be made. Therefore toluene was not appropriate as the solvent for the UV samples. The isothermal adsorption experiments were conducted in toluene since this was a poor solvent for the stabilizer, and, hence, a good solvent for adsorption. THF has a UV cut-off at $\approx$ 220 nm, and it is a good solvent for the stabilizer precursor. Therefore it was used as solvent for the UV measurements. A procedure was developed to convert the UV samples of the stabilizer solutions from toluene to THF. First, a small sample of stabilizer solution in toluene was charged to a 20 mL vial by using a micropipette. Toluene was evaporated by gently heating the sample on a hot plate until the total weight of the vial and the dried stabilizer was constant. Then HPLC grade THF was added to the vial to make a solution with a concentration suitable for UV spectroscopy.

To ensure the validity of this procedure, a calibration experiment was carried out. A stabilizer precursor solution in toluene of known concentration was prepared. Then different amounts of this solution were added to several vials using a micropipette. These samples were heated gently on a hot plate to evaporate the solvent (toluene), and then dissolved in HPLC grade THF to make known concentrations of stabilizer precursor solutions in THF for UV measurements. A typical UV absorbency plot of the stabilizer precursor, poly(pyridine ether-co-ether ether ketimine) (30 mole % pyridine) in THF is shown in Figure 3.16. The peak height at λ = 279.8 nm was used to determine the absorbency of the stabilizer solution. UV absorption was plotted as a function of stabilizer precursor concentrations in THF (Figure 3.17). These concentrations were obtained

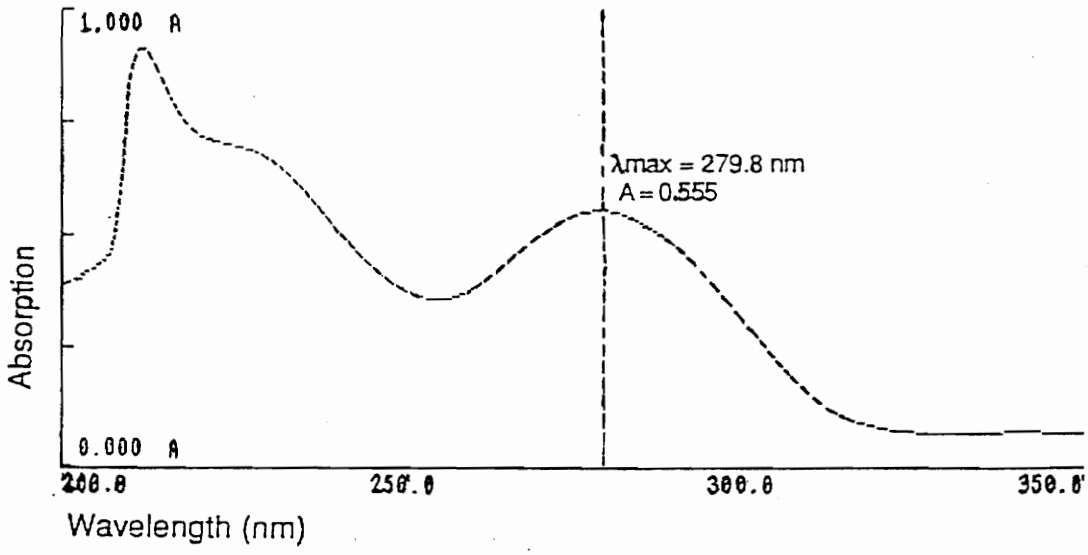

Figure 3.16 UV spectrum of poly(pyridine ether-co-ether ether ketimine) (stabilizer precursor) (THF)

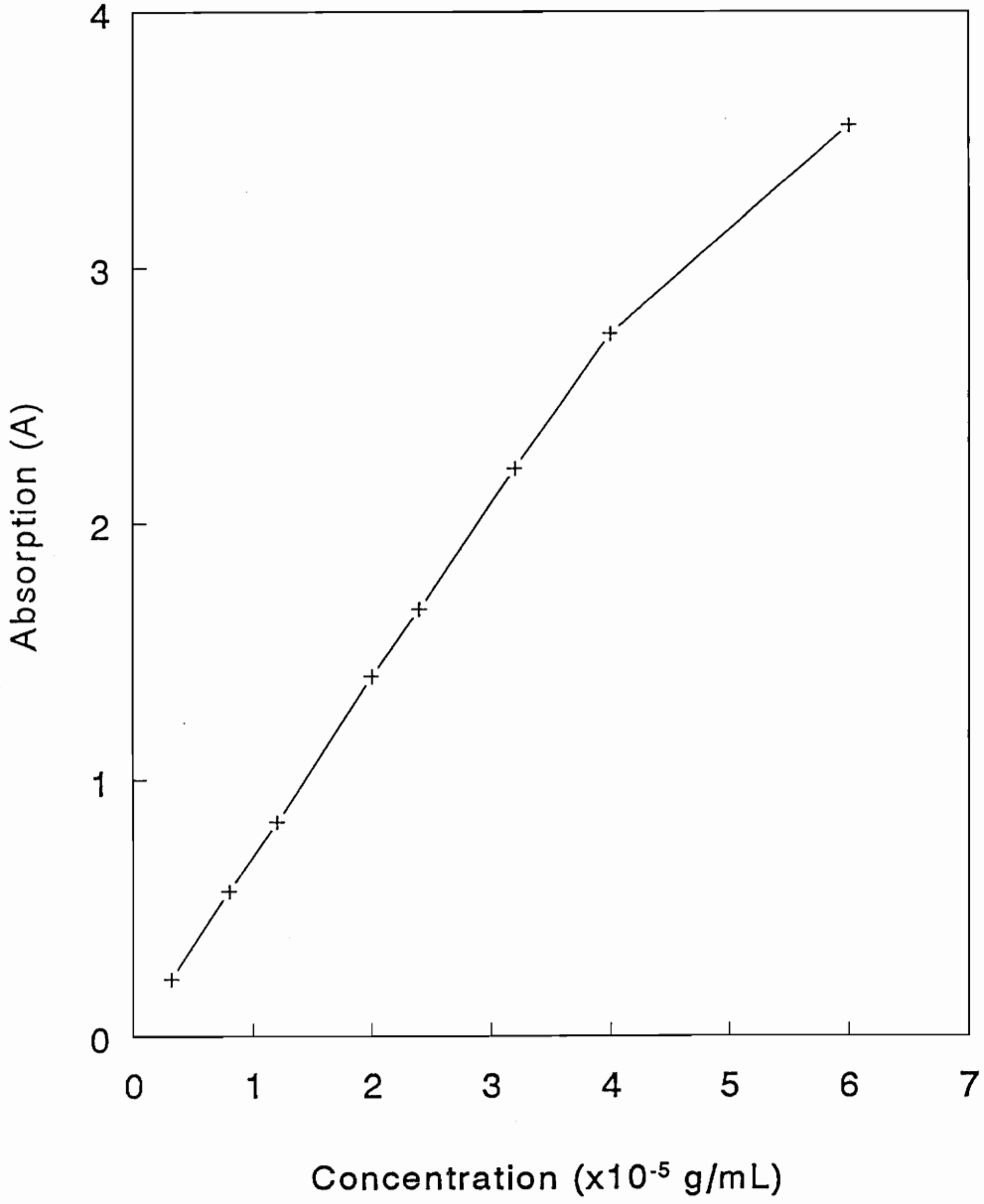

Figure 3.17 Calibration curve: UV absorptions of stabilizer precursor in THF versus concentration

based on the original concentration of the toluene solution, their masses for each of the individual samples and the volumes of THF used to dissolve the dried stabilizer precursor. The actual UV absorptions should be linearly proportional to the calculated concentrations. As shown in Figure 3.17, the absorptions at 279.8 nm were linear with concentration, except at high concentration, where Beer's law was not valid. The following conclusions were drawn from these experiments: 1. This procedure could be used to correctly measure the stabilizer concentrations in toluene solution. 2. The samples for UV measurement should be diluted to a concentration range of $\approx 3x10^{-6}$ - $4x10^{-5}$ g/mL. Within this range, the UV absorbencies were proportional to the concentrations, i.e., Beer's Law was valid. At higher concentrations, Beer's Law was no longer valid and errors were produced in UV measurements. If either of these two conclusions couldn't be established, the calibration curve would not be linear. The amount of stabilizer precursor absorbed was calculated using equation 3.1.

3.2.3 Time-dependent Studies

Time-dependent studies were conducted to determine the time required for equilibrium adsorption of the poly(pyridine ether-co-ether ether ketimine) onto the PEEK particles from toluene at room temperature. The time period for equilibrium to be reached is related to the rate at which polymers diffuse to, and relax into, their equilibrium configuration at an interface. In general, all time-dependent parameters can be used to determine the rate of adsorption. For example, if the adsorbent has a flat surface, ellipsometry can be used to measure the thickness of the adsorbed layer with time; when the adsorbent is in the form of small particles, the amount of adsorbed polymer can be measured with time. The adsorption process for a macromolecule involves three stages:

1. The macromolecule diffuses to a particle surface; 2. The macromolecule undergoes configurational changes and relaxes towards its equilibrium conformation; 3. Other macromolecules which have higher adsorption energies may displace the segments or molecules initially adsorbed.

It is important that the amount of stabilizer adsorbed is constant to establish that equilibrium adsorption has been reached. This equilibrium state allows for isothermal adsorption measurements to be reproducible. To determine the time for adsorption to reach equilibrium, the adsorption percentages (= $(1-I_s/I_0)x100\%$, I_0 was the UV absorbence at 289.8 nm of polymer in the original solution, and I_s that of the supernatant after adsorption) were measured as a function of time (Figure 3.18). The stabilizer precursor, poly(pyridine ether-co-ether ether ketimine), used was 25,000 g/mole Mn (20 mole % pyridine) as determined by GPC.[56] The weight of the pyridine-ketimine copolymer used for these experiments was 1.25% relative to particles. The amount of particles used was 0.6 g (12 micron PEEK particles). Toluene was used as the solvent and adsorption was conducted at room temperature.

As shown in Figure 3.18, before reaching adsorption equilibrium, the percent adsorption increased with time. At adsorption equilibrium, the particle surfaces were completely covered by the polymer molecules which had relaxed to their equilibrium conformations, and no more molecules could adsorb. The amount of adsorption at equilibrium was calculated by comparing the stabilizer precursor concentration of the original solution to that of the supernatant after reaching equilibrium adsorption. About 70 hours were required to reach adsorption equilibrium at room temperature in toluene.

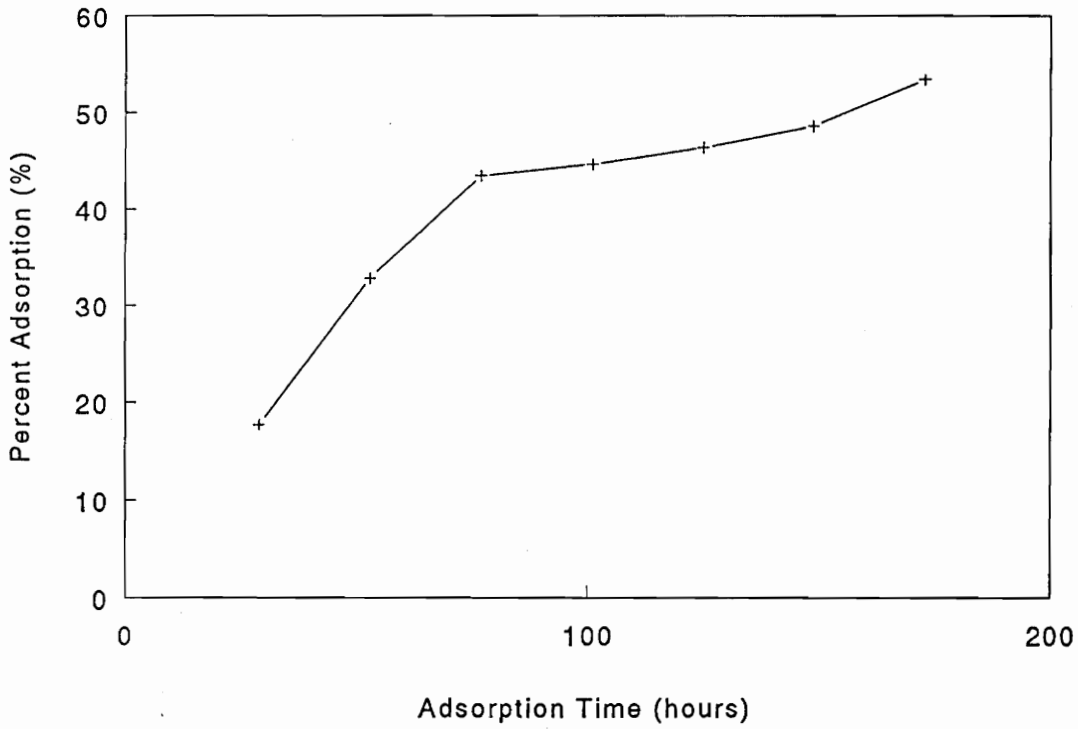

Figure 3.18 Percent adsorption versus adsorption time for adsorption of poly(pyridine ether-co-ether ether ketimine) (stabilizer precursor) onto the 12 micron PEEK particles at room temperature using toluene as solvent

This rather long adsorption time is probably related to the stabilizer's polydispersity of 2.0 which results from the mechanism of condensation polymerization by which it was prepared. Since short chain molecules have a higher diffusion coefficient, they have a higher rate of adsorption. Therefore, at the initial stage, the particle surfaces may have been occupied by the short chain molecules. However, short chain molecules have less segments and, hence, less adsorption sites than long chain molecules. Therefore long chain molecules have higher adsorption energies and are, thus, thermodynamically favored for adsorption. They are able to displace the pre-adsorbed short chain molecules until thermodynamic equilibrium is established. This is an example of so-called "competitive adsorption". This displacement takes various times depending on the nature of the adsorbent surface, solvent and polymer molecules. Thus, relatively polydisperse stabilizers often require long times for adsorption equilibrium to be reached.[35,58]

The rate of adsorption also depends greatly on the nature of adsorbent. Adsorption of a polymer onto a planar surface or nonporous particles may reach adsorption equilibrium within a few hours, while it may take much longer when the solid surface is porous; especially when the pore size is sufficiently small.[59] The 12 micron PEEK particles were ballmilled down to that size at ICI. Figure 3.19 shows scanning electron micrographs of the 12 micron PEEK particles at a magnification of 25,000 with a 0.5 micron scale bar. It shows that the particle surface is rather porous and irregular. It may contribute to the rather long time for adsorption equilibrium to be reached.

In adsorption studies of poly(2-ethyl-2-oxazoline) (PEOX) onto silica,[48] the time for adsorption to reach equilibrium was $\approx$ 6 hours. In that system, the polymer PEOX had

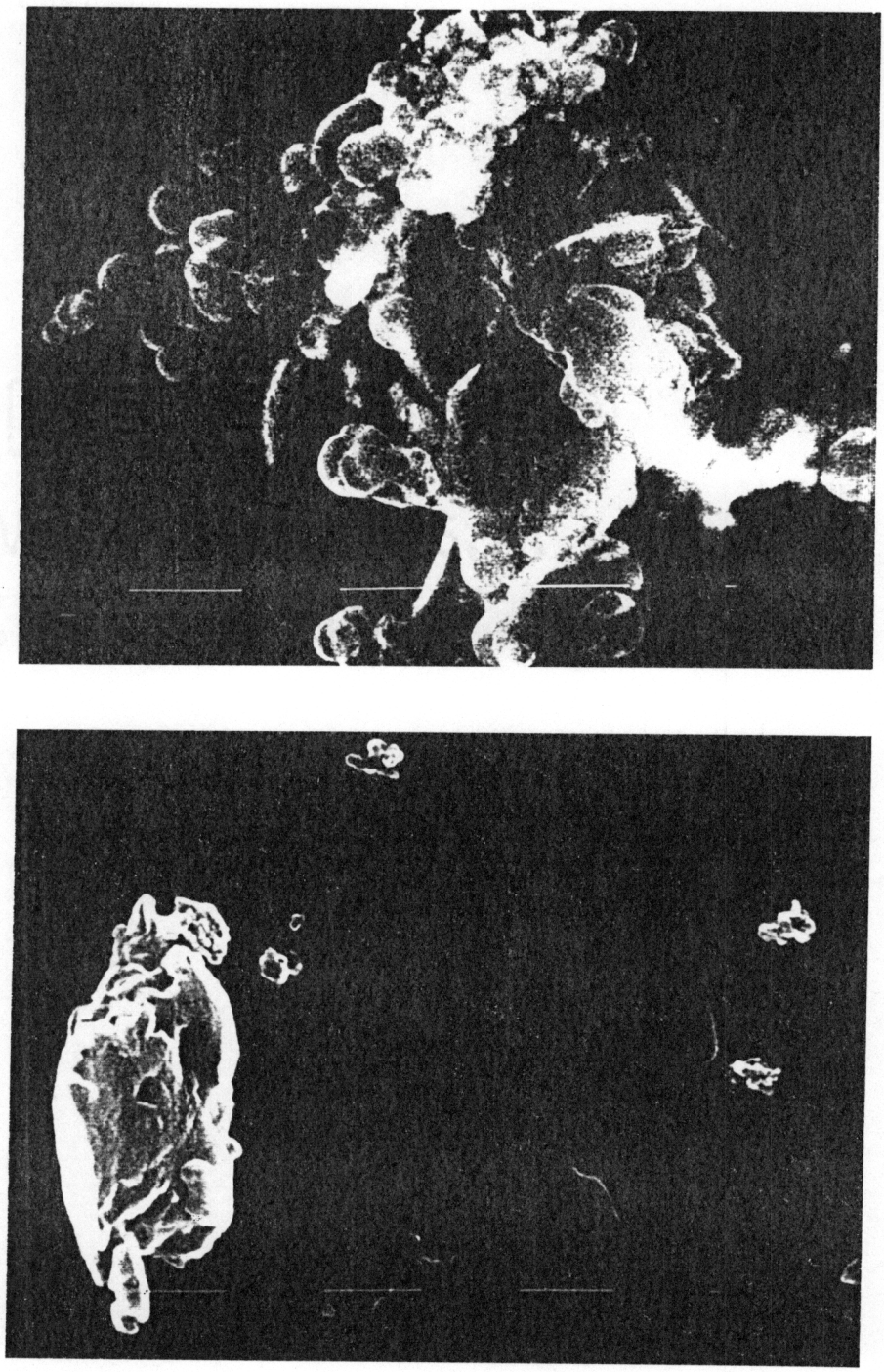

Figure 3.19 Scanning Electron Micrographs of 12 micron PEEK particles at magnification of 25,000 with a 0.5 micron bar

a relatively narrow molecular weight distribution of 1.54 and the silica particles were uniform spheres. Therefore adsorption of PEOX onto the silica particles takes much less time to reach equilibrium. By comparison, one can see the great effects of the polydispersity and the nature of the solid surface on the rate of adsorption. These conclusions qualitatively agree with the theory.[44,58]

On the basis of these results, it is determined that ≈ 70 hours were required to reach adsorption equilibrium. The submicron PEEK particles have a more regular shape instead of a porous surface, as shown in Figure 3.11. Therefore it should take less time for adsorption to reach equilibrium in that system. However, 70 hours was chosen as the standard for all the adsorption experiments in order to ensure that equilibrium adsorption had been reached.

3.2.4 Solvent Effects on Adsorption

Solvent effects were observed for adsorption of the stabilizer precursor, poly(pyridine ether-co-ether ether ketimine) (25,000 g/mole Mn, 30 mole % pyridine) onto both the 12 micron particles and the submicron particles. Adsorption results indicated essentially no adsorption from THF but good adsorption from toluene (>50% adsorption at 1 wt.% stabilizer precursor relative to particles) at room temperature. In order to investigate this phenomenon, the intrinsic viscosity of the stabilizer precursor was measured using a Ubbelhode Viscometer at 25°C. The intrinsic viscosity of the stabilizer precursor was 0.23 dL/g in THF and 0.16 dL/g in toluene at 25°C, indicating that THF has a stronger interaction with the stabilizer precursor relative to toluene. According to the Scheutjens-Fleer mean field theory, the amount of adsorbed polymer is generally

affected by molecular weight (MWt), the volume fraction of polymer in the solution at equilibrium adsorption (ϕ^*), polymer segment-solvent interactions (χ) and polymer segment-interface interactions (χ_S). Adsorption occurs only when the segmental adsorption energy parameter, χ_S exceeds a given value, the so-called critical adsorption energy, denoted by χ_{sc}.

In the S-F mean field theory, the structure of an interface is described in terms of the volume fraction of segments in layers parallel to the surface. The polymer concentration at an interface can be two extreme situations. In one case polymer segments accumulate at the interface, resulting in adsorption. Also, polymer segments can be excluded from the interface, resulting in depletion. These effects are determined by a balance of the polymer-solution parameter χ, the segmental adsorption energy parameter χ_s and the unfavorable entropic forces due to the loss of conformations a polymer chain can assume upon adsorption (contained in the critical adsorption energy, χ_{sc}). Adsorption of a segment onto a surface includes first breaking contacts of the segment with solvent molecules followed by displacing solvent from the surface, and then adsorbing the segment onto the surface. Adsorption occurs only when the total free energy change in the whole process is negative, i.e., energetically favored.[39] The concept of χ is schematically depicted in Figure 3.20.[52] χ is defined as follows:[52]

$$\chi = [\varepsilon_{12} - 0.5\,(\varepsilon_{11} + \varepsilon_{22})]\, z / kT \qquad \text{Eq. 3.2}$$

where, ε represents the interaction free energies between solvent molecules (1) and polymer segments (2); z is the coordination number. The χ value is inverse to the solvent power, i.e., χ is smaller in a better solvent. As mentioned previously, the viscosity

measurements indicated that the polymer chains are more expanded in THF and thus have a stronger polymer-solvent interaction with THF than with toluene. Roovers et al. also found that THF is a good solvent for poly(ether ether ketimine), while toluene at 35°C is close to a θ-solvent for poly(ether ether ketimine).[60] Thus, the χ parameter of the stabilizer precursor in THF should be smaller than in toluene, and the χ parameter-associated process, desolvation, is more energetically unfavored for THF than for toluene. Therefore, strong polymer-solvent interaction in THF may be one of the reasons that no adsorption was observed from a good solvent, THF, while good adsorption was observed from a poor solvent, toluene.

Another reason for the observed solvent effect might be directly related to the adsorption energy, $\chi_s kT$, which, as defined by Silberberg,[39] is the free energy change associated with the transfer of a polymer segment from a bulk site to a surface site, minus the corresponding energy of a solvent molecule in pure solvent. This process is described in Figure 3.21.[52] By this definition, χ_s is a function of three types of binary interactions acting among the adsorbent surface (s); solvent molecules (1) and polymer molecule (2). χ_s can be expressed as follows:[52]

$$\chi_s = [\varepsilon_{2s} - \varepsilon_{1s} + 0.5\,(\varepsilon_{11} - \varepsilon_{22})] / kT \qquad \text{Eq. 3.3}$$

If $\chi_s > \chi_{sc}$ (the critical adsorption energy, usually estimated as a few tenths of kT),[52] adsorption will occur. If $\chi_s < \chi_{sc}$, polymer segments will be depleted at the interface with respect to the bulk solution. In practice, it seems that χ_s values are usually > 1 so that segments are very likely to crowd on an interface.[52,61] Using S-F mean field theory, the volume fraction of segments in each layer as one moves outward from a surface for a

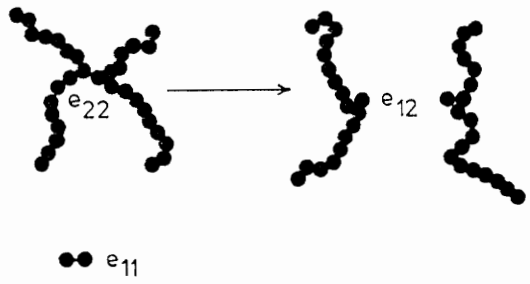

Figure 3.20 χ is the net energy change between the situation in the right-hand diagram and that in the left-hand one[52]

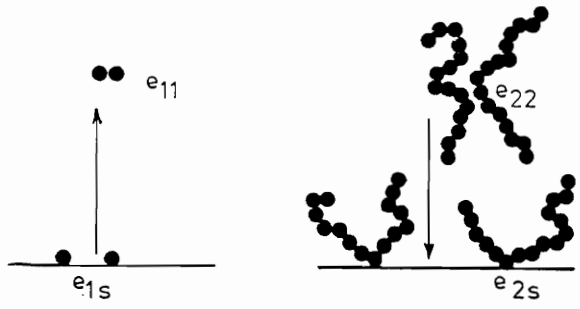

Figure 3.21 χ_s is the net energy difference between the process in the right-hand diagram and that in the left-hand one[52]

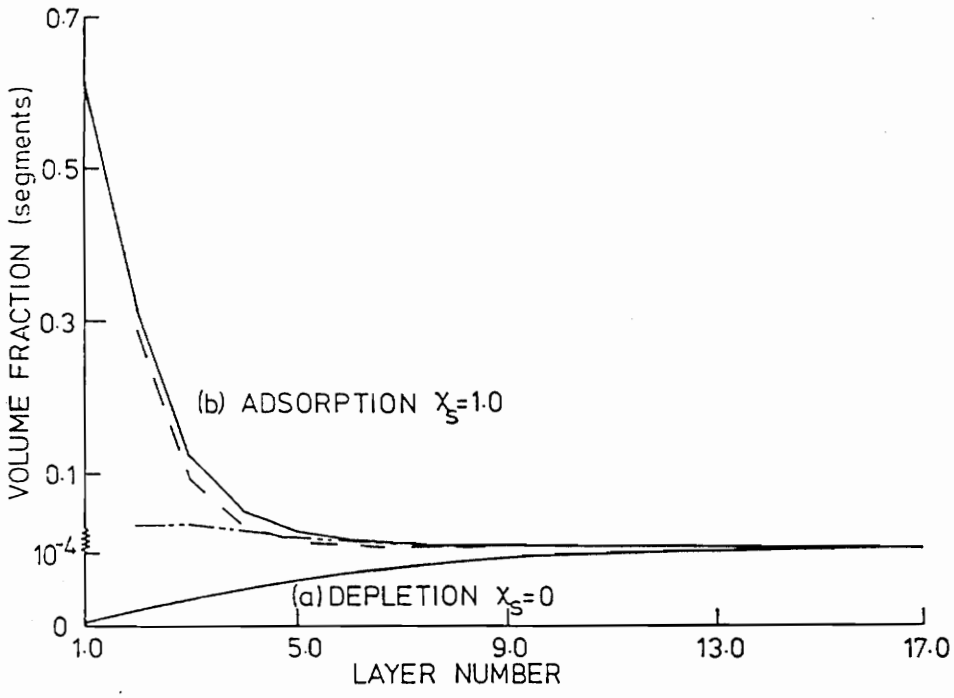

Figure 3.22 Volume-fraction profiles for depletion and adsorption; $\chi = 0.5$, $r = 100$, c_{eq} = 100 ppm; ----- loops; ····· tails[52]

chain of 100 segments in a theta solvent ($\chi = 0.5$) and for $\chi_s = 0$ (depletion: a) and $\chi_s = 1$ (adsorption: b) are predicted (Figure 3.22).[52] The polymer solution concentration was 1000 ppm for this case. It should be pointed out that the scale in the depletion case has been enlarged in order to show the detail of the profile. Therefore, one can see from Figure 3.22 that the χ_s is an important parameter in determining either polymer adsorption onto, or depletion from, the interface. The segmental adsorption parameters (χ_s) for adsorption of the stabilizer precursor from THF and toluene are different since the interactions between the solvents and adsorbent surface (PEEK particles) are different, i.e., ε_{1s}'s are different (Equation 3.3). Interactions (solubility) between organic solvents and PEEK (both amorphous and crystalline PEEK) were investigated using absorption experiments.[62-70] The percentage weight increase in PEEK observed on exposing amorphous PEEK to THF is 40% at 22°C after reaching the equilibrium state, and the diffusion coefficient is 0.81×10^{-12} m^2/s.[63] The percentage weight increase observed on exposing amorphous PEEK to toluene is 19.8% at 35°C after reaching equilibrium state, and the diffusion coefficient was 0.35×10^{-12} m^2/s.[64,66] It was also found that solvents containing an activated hydrogen atom and an electronegative atom attached to the same carbon atom cause greater bulk swelling.[63] All of these experiments demonstrate that THF is a better solvent than toluene for PEEK. The solubility parameters of THF, toluene, PEEK and poly(ether ether ketimine) (PEEKt) were calculated by utilizing the group additivity calculation method developed by Hoftyzer and Van Krevelen[71] as 15.80, 17.40, 15.92 and 15.35 $J^{1/2}cm^{-3/2}$, respectively. These calculated solubility parameters also predict that THF should be a better solvent for PEEK. The experimental solubility parameter values are 19.5 for THF and 18.2 ~ 18.3 for toluene.[71] This is inconsistent with the calculated values. However, THF still seems to be a better solvent for PEEK than toluene. Lewis acid-base interactions between PEEK and the solvent are the likely

explanation for the enhanced solvent compatibility of THF for PEEK.[62] Therefore, THF has a stronger interaction with the PEEK surface; hence, a larger ε_{1s} value (Equation 3.3) than toluene. According to Equation 3.3, χ_S in toluene would be greater than in THF for adsorption of the stabilizer precursor onto the PEEK particle surface, i.e., $\chi_{S,tol.} > \chi_{S,THF}$. This difference in χ_S values leads to adsorption in toluene ($\chi_{S,tol.} > \chi_{SC}$) and depletion ($\chi_{S,THF} < \chi_{SC}$) in THF. The following isothermal adsorption experiments were then conducted in toluene rather than in THF.

3.2.5 Isothermal Adsorption of the Stabilizer Precursor onto 12 micron PEEK particles

Isothermal adsorption of the stabilizer precursor onto the 12 micron PEEK particles was studied by stirring 0.6 g particles with stabilizer precursor solutions of known concentrations in toluene at room temperature. The stabilizer precursor, poly(pyridine ether-co-ether ether ketimine) has a number-average molecular weight of 25,000 g/mole with 30 mole% pyridine. The particle concentration in solution was 12% (g/mL). The mixtures were stirred for 70 hours until adsorption equilibrium was reached. Then the particles were separated from the solution by centrifugation. The concentration of stabilizer remaining in the supernatant was measured by UV spectroscopy. The amount of adsorbed polymer was calculated by comparing the polymer concentrations of the original solution with the supernatant using equation 3.1.

Particles Size Analysis leads to values for the specific surface area of the particles assuming the particles are spherical. The adsorbed amount per surface area was calculated using this specific surface area value (Equation 3.4):

$$\Gamma_a = W_{a.s} / (A_s \times W_p) \qquad \text{Eq. 3.4}$$

In which, Γ_a (mg/m^2) = adsorbed amount of stabilizer precursor per unit surface area;

$W_{a.s}$ (mg) = adsorbed amount of stabilizer precursor;

A_s (m^2/g) = specific surface area of the particles;

W_p (g) = weight of the particles.

The adsorbed amount of stabilizer precursor (mg/m^2) was plotted as a function of stabilizer equilibrium concentration (Figure 3.23a). For convenience, the weight percentage of adsorbed stabilizer precursor relative to particles was plotted as a function of weight percentage of stabilizer originally used relative to particles (Figure 3.23b). Most discussions are based on Figure 3.23a. However some straightforward results can be obtained from Figure 3.23b.

As it is known, three concentration regimes can be distinguished for a typical polymer adsorption isotherms.[72] In extremely dilute solutions the molecules on the surface adsorb as isolated chains and assume relatively flat configurations (the Henry region). In this region the adsorbed amount depends greatly on molecular weight, however the adsorbed amount is still very small. In a very wide concentration range from dilute to moderate concentrations (volume fraction ≤ 0.1), the solid surface is crowded with polymer molecules and the adsorbed amount depends only weakly on concentration (the pseudoplateau region). The adsorbed amount in the pseudoplateau region increases linearly with the logarithm of chain length in a poor solvent, while in a good solvent the molecular weight dependency is smaller. In concentrated solution, the adsorbed molecules

extend far into the solution because of polymer chain entanglements, obeying Gaussian statistics. The adsorbed amount is proportional to the square root of chain length, regardless of solvent power.

If one plots the adsorbed amounts as a function of the polymer concentrations, an adsorption isotherm is obtained. As shown in Figure 3.23a, the concentration of stabilizer precursor ranged from 0.5 mg/mL to 10.8 mg/mL in the pseudoplateau region, and an adsorption pseudoplateau was obtained. The amount of adsorption in the pseudoplateau region was 73.6 mg/m^2. This value is considered large compared to most experimental adsorption values. For physically adsorbing homopolymers or random copolymers, the pseudoplateau region is typically of the order of 1 mg/m^2.[52] An important reason is that apparently the specific surface area measured by the Particle Size Analyzer is lower than the actual value. The shape of the 12 micron PEEK particles is irregular and far from spherical, and the surface of these particles is rather porous (Figure 3.19). Thus, the actual particle surface area would be much larger than the measured value in which it was assumed that the particles were spherical. Therefore, the actual pseudoplateau adsorption would be much smaller than 73.6 mg/m^2.

Many theories have been developed to study the isotherms of polymer adsorption.[36,39,73-78] All theories predict polymer adsorption isotherms with an initial steep rise, followed by a nearly horizontal pseudoplateau. Such a curve is called a high-affinity isotherm (a sharp isotherm). However, experimental isotherms usually show a rounded shape (rounded isotherm), i.e., the adsorbed amount increases gradually with the equilibrium concentration as shown in Figure 3.23a. Also, a well-defined plateau is not always observed experimentally. A very important reason is that these theories apply only

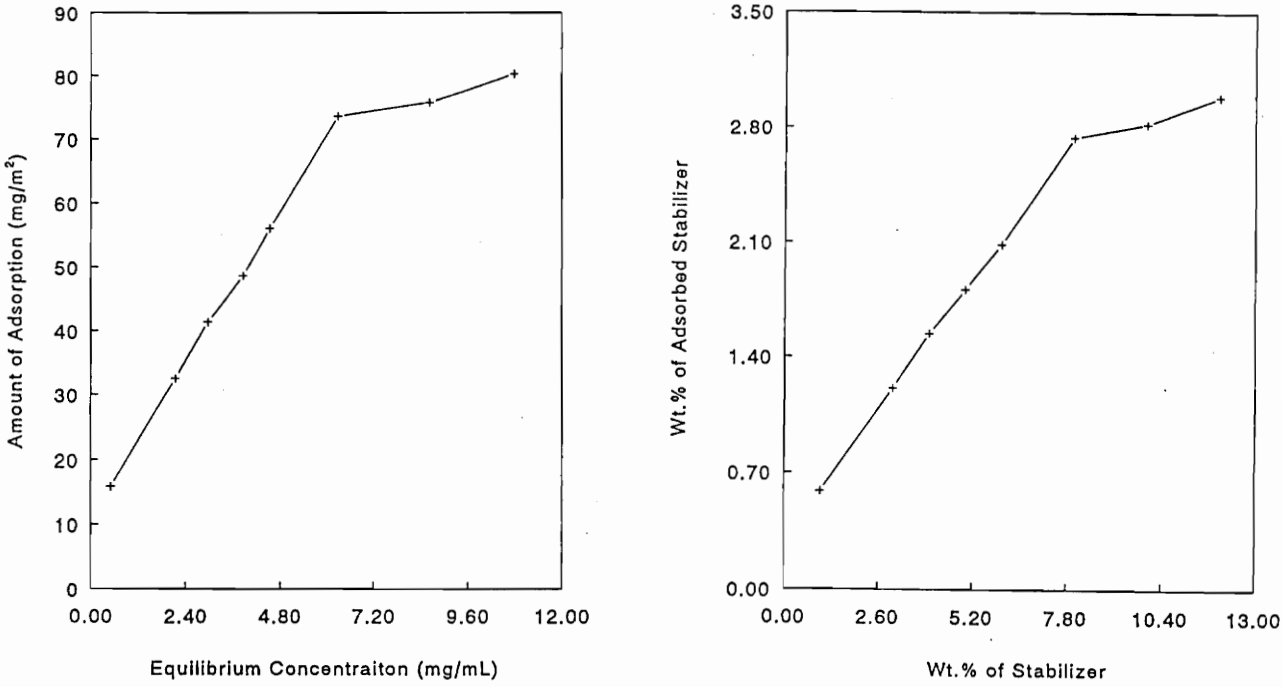

Figure 3.23 Isothermal adsorption of stabilizer onto 12 micron particles; a. adsorbed amount of stabilizer (mg/m2) versus equilibrium concentration of the stabilizer in the supernatant; b. wt.% of adsorbed stabilizer relative to particles versus wt.% of stabilizer relative to particles

to monodisperse polymers, while most experiments were carried out with polydisperse samples. For adsorption of poly(pyridine ether-co-ether ether ketimine) onto PEEK particles, the molecular weight distribution of the polymer is rather dispersed, a result of the condensation mechanism by which it was synthesized. For a polydisperse system, smaller molecules adsorb initially since they diffuse faster than larger molecules, and later on the larger molecules can replace the smaller molecules since they have more adsorption sites, thus higher adsorption energy. This phenomenon is called competitive adsorption. Competitive adsorption in a polydisperse system leads to a rounded isotherm, as well as the rather long time required to reach adsorption equilibrium as was discussed in section 3.2.3.

According to Cohen Stuart,[61] in adsorption from a dilution solution, polymer molecules arrive at the adsorbent surface one by one. The molecules arriving first would have enough time and space to unfold and assume a very flat conformation, forming tightly bound molecules, which cannot easily be exchanged by other molecules. Therefore, competitive adsorption is less important for adsorption from a dilute polymer solution. At higher concentration, molecules arrive at the surface at a faster pace. Unfolding toward a flat conformation is restricted by the time and space available. Adsorption takes place in a much "looser" conformation with relatively few anchor points. These loosely bound molecules would be replaced much easier. Therefore, competitive adsorption is more important when polymer concentration is higher. It is also important to realize that the adsorbed amount is mainly determined by the amount of loops and tails presented. The loosely bound molecules lead to a higher adsorbed amount while the tightly bound molecules less. Two conclusions can be drawn from the picture given by Cohen Stuart. The first, for isothermal adsorption of a polydisperse system, competitive

adsorption leads to an increment of adsorption amount with increasing concentration, resulting in a round-shaped isotherm. The second, a sharper isotherm would be obtained from a more diluted polymer solution since competitive adsorption is less likely to occur. The experimental results herein, as well as other experiments,[61,79,80] seem to support these conclusions. Compared with theoretical predictions (e.g., Figure 3.22), the adsorption of poly(pyridine ether-co-ether ether ketimine) onto PEEK particles showed a rounded isotherm (Figure 3.23a and b).

Some direct and useful data are shown in Figure 3.23b. The amount of stabilizer adsorbed started to plateau at 8 wt.% stabilizer relative to particles in the solution indicating that at the particle concentration used, maximum adsorption was achieved at that stabilizer level. The maximum adsorption is 3 wt.% adsorbed stabilizer relative to particles. Subsequent acid hydrolysis of the poly(pyridine ether-co-ether ether ketimine) particle coating, wherein the ketimine functionalities were converted to ketones with simultaneous protonation of the pyridine groups (Figure 3.24), yielded electrostatically stabilized PEEK particles. These coated particles were rinsed to wash away the organic solvents and by-products resulting from hydrolysis, then were resuspended in deionized water. These aqueous suspensions of electrostatically stabilized 12 micron PEEK particles were then analyzed for stability, as discussed in following section.

3.2.6 Stability Study of the Aqueous 12 micron Particle Suspensions

The stability study of 12 micron particle suspensions was conducted using sedimentation experiments since the particles had relatively large sizes. The density of

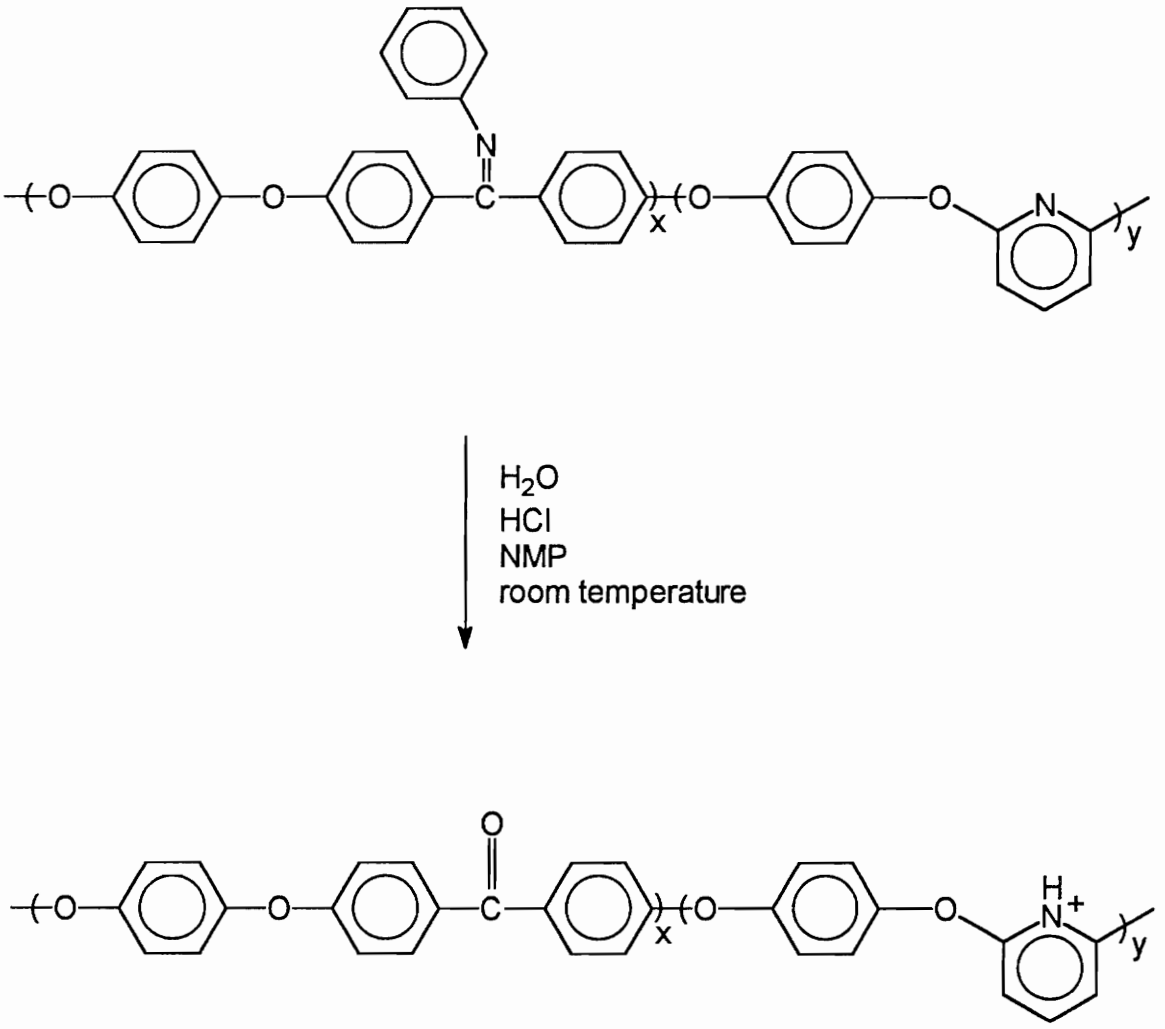

Figure 3.24 Acid hydrolysis of poly(pyridine ether-co-ether ether ketimine) (stabilizer precursor) to protonated poly(pyridine ether-co-ether ether ketone) (electrostatic stabilizer)

semi-crystalline PEEK is ~ 1.3 g/mL. The particles will settle in a aqueous suspension because of the gravitational force. Protonation of pyridine is an equilibrium process, and the pKa value of protonated pyridine is 5, as follows:

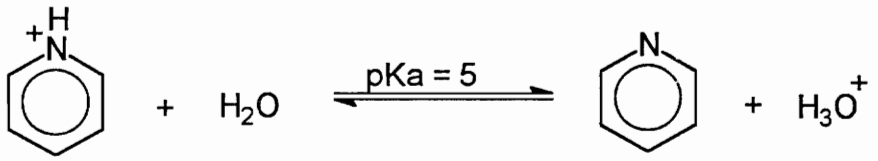

Eq. 3.5

Given:

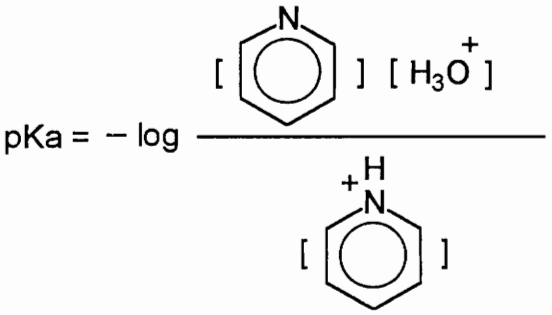

Eq. 3.6

and

Eq. 3.7

Then:

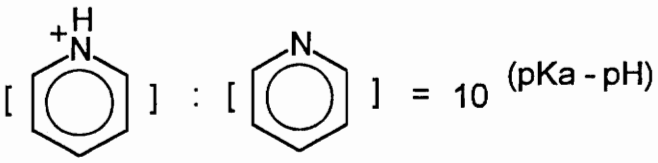

Eq. 3.8

Based on definitions of pKa and pH (Eq. 3.6 and Eq. 3.7), the ratio of protonated pyridine over unprotonated pyridine can be predicted at known pH values (Eq. 3.8). These ratios are 1000, 100, 10 and 1 at pH values of 2, 3, 4 and 5, respectively. To ensure that significant percentages of pyridine moieties in the stabilizer particle coatings were

protonated, the stabilities of the suspensions were investigated under mildly acidic conditions, i.e., at pH values of 2 and 4.

0.6 g 12 micron particles coated with various amounts of the electrostatic stabilizer, poly(pyridine ether-co-ether ether ketone) were resuspended in 12 mL water at pH values of 2 and 4 adjusted using hydrochloric acid. The suspensions were transferred into graduated cylinders, were well-dispersed, then allowed to settle (Figure 3.25). The sediment volumes, which indicate the stabilities of the suspensions, were measured after one hour. When a stabilized suspension settles, the repulsion forces necessary to ensure stability enable the particles to move past each other and form closely packed sediments. On the other hand, less stable suspensions tend to flocculate and form network structures. The settling of these structures forms loosely packed sediment.[51] Therefore, the higher sediment volume indicates less stability. These volumes are plotted as a function of the wt.% of adsorbed stabilizer relative to PEEK particles (Figure 3.26). As expected, the suspension stability increases with increasing amount of adsorbed stabilizer. More adsorbed stabilizer provides more positive charges on the particle surface, resulting in a thicker double-layer and a stronger electrostatic repulsion force. As shown in Figure 3.27, the electrostatic repulsion force (dashed line) increases with increasing adsorbed amount of stabilizer. As a result, the total interaction energy between two particles (solid line) is increased, resulting in a more shallow secondary minimum and a higher primary maximum. Thus, the particles are less likely to fall into the secondary minimum state (forming flocculates), or overcome the primary maximum (forming coagulates). A more stable suspension is obtained. Also, as expected, the suspension stability is better at lower pH values, since more pyridine moieties are protonated at lower pH values. Relatively stable

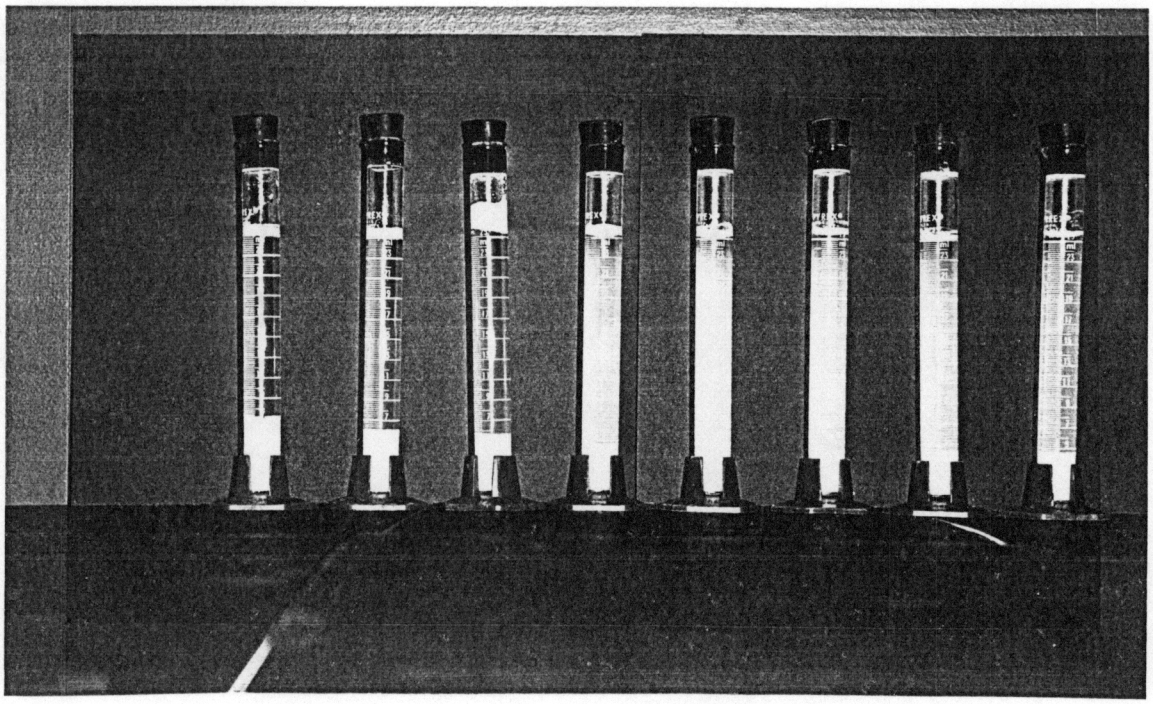

Figure 3.25 Sedimentation test for analyzing the stability of 12 micron PEEK particle suspensions

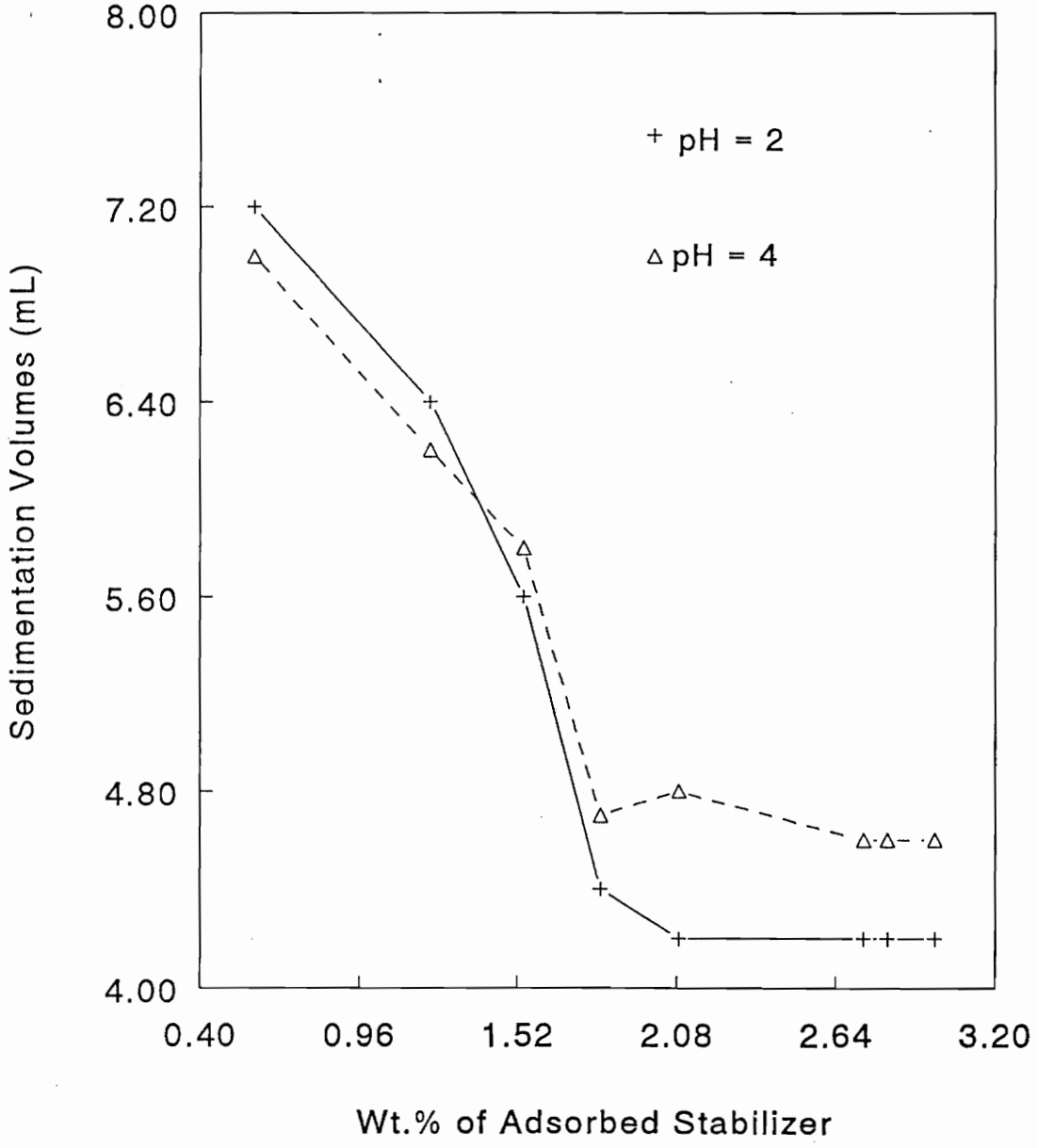

Figure 3.26 Sediment volumes at different pH values versus wt.% of adsorbed stabilizer relative to particles (12 micron PEEK particles)

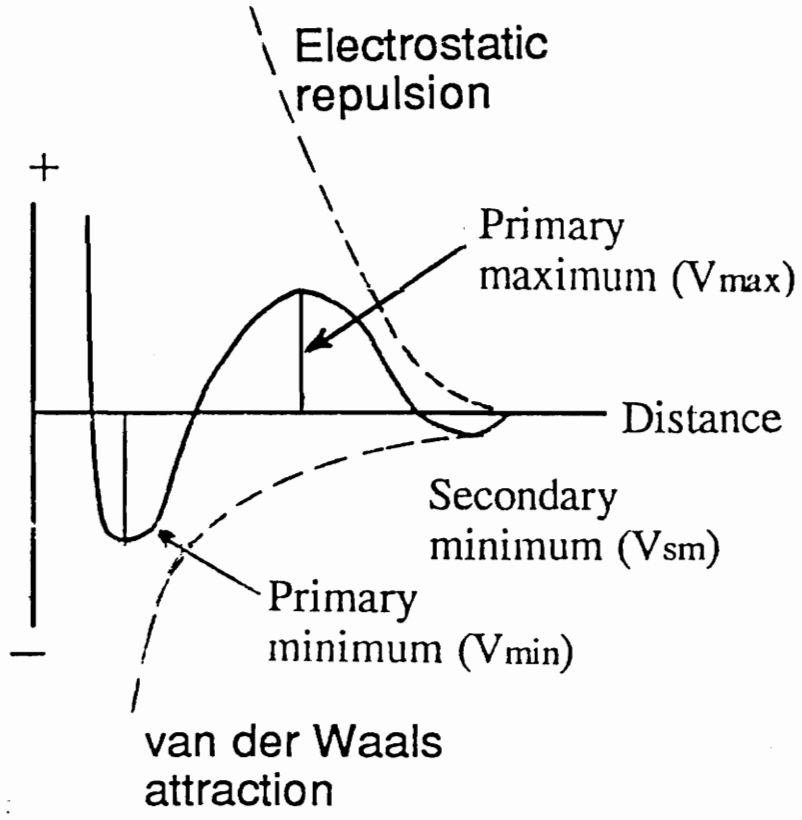

Figure 3.27 Particles interaction energy as a function of distance for electrostatically stabilized suspensions

suspensions are obtained while the adsorbed stabilizer is only 2 wt.% relative to PEEK particles (Figure 3.26).

3.2.7 Isothermal Adsorption of the Stabilizer Precursor onto the Submicron PEEK Particles

Isothermal adsorption of the stabilizer precursor onto the submicron PEEK particles was studied in a similar manner as the 12 micron PEEK particles. Toluene was used as solvent for the stabilizer precursor, poly(pyridine ether-co-ether ether ketimine), which has a number-average molecular weight of 25,000 g/mole with 30 mole% pyridine. The particles and the stabilizer precursor solution was stirred for 70 hours to ensure that adsorption equilibrium was reached. However, the particle concentration in solution used for the adsorption of submicron particles was 0.88% (e.g., 0.07 g submicron particles stirred in 8 mL solution), while it was 12% for the 12 micron PEEK particles (e.g., 0.6 g particles stirred in 5 mL solution). This was designed because of practical reasons. If the concentrations of the submicron particles were made higher, the mixture would become too viscous and "slurry-like". As a result, each individual particle couldn't be sufficiently separated, and the particle surfaces aren't sufficiently exposed to the stabilizer solution for adsorption. The amount of adsorbed stabilizer precursor was measured using UV spectroscopy and calculated according to Equation 3.4. The adsorbed amount per unit surface area (mg/m^2) is plotted as a function of stabilizer equilibrium concentration (Figure 3.28a). Also for convenience, the weight percentages of adsorbed stabilizer precursor relative to particles were plotted as a function of weight percentages of stabilizer originally used relative to particles (Figure 3.28b).

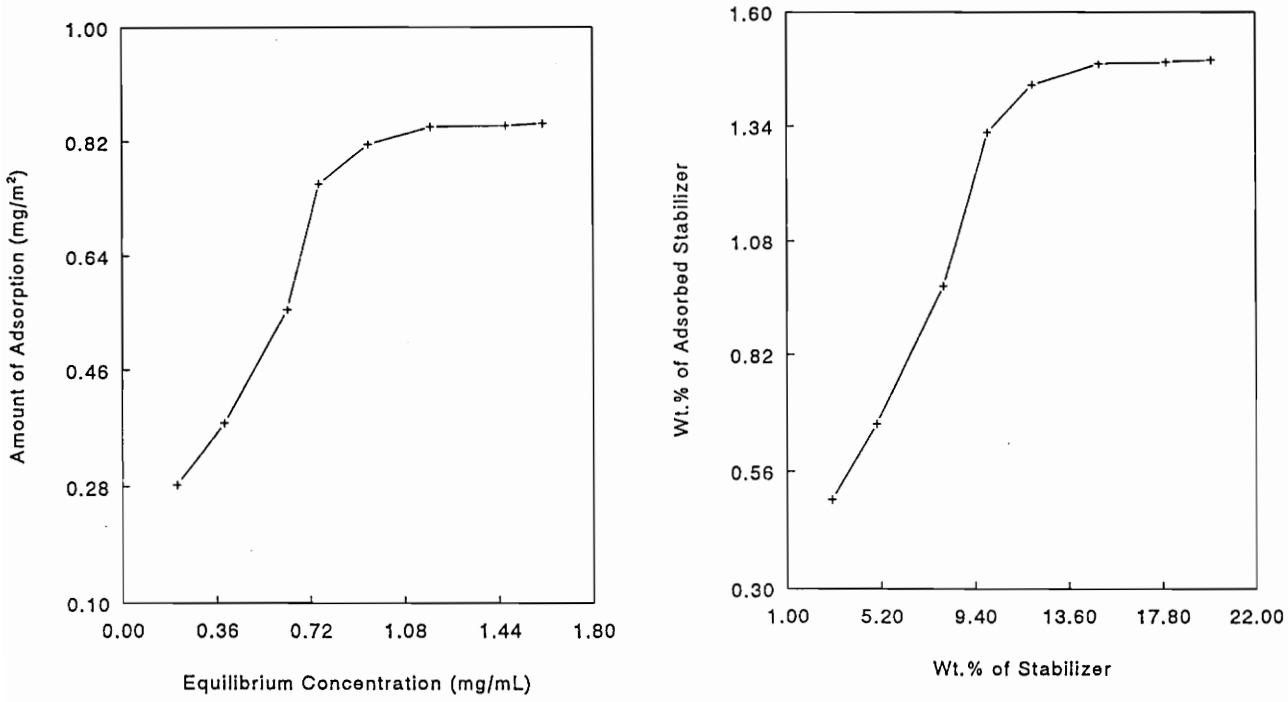

Figure 3.28 Isothermal adsorption of stabilizer onto submicron particles; a. adsorbed amount of stabilizer (mg/m^2) versus equilibrium concentration of the stabilizer in the supernatant; b. wt.% of adsorbed stabilizer relative to particles versus wt.% of stabilizer relative to particles

As shown in Figure 3.28a, the concentration of stabilizer precursor covered a reasonable range in the pseudoplateau region from 0.2 mg/mL to 1.6 mg/mL. A pseudoplateau adsorption was obtained at which the adsorbed amount per unit surface area was 0.84 g/m^2 while the equilibrium concentration of the solution was ~ 1 mg/mL. This value is reasonable compared to most experimental values since for physically adsorbing homopolymers or random copolymers, the pseudoplateau region is typically of the order of 1 mg/m^2.[52] It is important to recognize that a large portion of the adsorbed stabilizer molecules were presented as loops and tails in the adsorption interface. If the polymer adsorbed in a flat conformation, covering the surface completely with a monolayer, not more than 0.3 mg/m^2 would be obtained for the adsorption, provided 25 A^2 for the area of a segment.[81] The isotherm (Figure 3.28a) is round-shaped as a result of the polydispersity of the stabilizer precursor. As mentioned in section 3.2.5, polymer concentration also affects the shape of the isotherms. A more dilute polymer solution leads to a sharper isotherm. It seems that the isotherm of the submicron particles (Figure 3.28a & b) is sharper than that of the 12 micron particles (Figure 3.23a & b). It is not intended to make a precision comparison since the concentration scales are different. Also, the surface area of the 12 micron particles is not well defined. The adsorbed amount (g/m^2) (Figure 3.23a) should be corrected by a constant for the 12 micron case.

As shown in Figure 3.28b, 15 weight percent of stabilizer precursor relative to particles was required to reach the pseudoplateau adsorption at the particle concentration used (0.88% g/mL) and the stabilizer concentration range investigated (0.2 - 1.6 mg/mL). The weight of adsorbed stabilizer precursor relative to the particles at the pseudoplateau region is about 1.5%. Subsequent acid hydrolysis of the poly(pyridine ether-co-ether ether ketimine) coating, wherein the ketimine functionalities were converted to ketones with

simultaneous protonation of the pyridine groups (Figure 3.24), yielded electrostatically stabilized PEEK particles. These coated particles were rinsed to wash away the organic solvents and by-products resulting from hydrolysis, followed by resuspension into deionized water. These aqueous suspensions of electrostatically stabilized submicron particles were then analyzed for stability.

3.2.8 Stability Study of the Aqueous submicron PEEK Particle Suspensions

Because of the size difference between the 12 micron PEEK particles and the submicron particles, the techniques used for analyzing the suspensions of these two sizes were different. To analyze the stability of the 12 micron particle suspensions, sedimentation experiments were used. In the case of submicron particle suspensions, the gravitational force, which causes the particles to settle, is counterbalanced by the Brownian motion of the particles. The particles never completely settle. Therefore, the sedimentation technique can't be used to analyze the stability of submicron particle suspensions. Instead, the stabilities of submicron PEEK particle suspensions were analyzed using a turbidimeter, a light scattering apparatus, at ambient temperature. The stabilities of the suspensions are also measured at different pH values. A turbidimeter measures the turbidity change of an initially well-dispersed suspension with time as the particles flocculate and settle. 0.1 g "wet" (~7 mg after drying) of the coated submicron particles were dispersed into 15 mL deionized water (adjusted to pH = 2 or 4 using hydrochloric acid) in a sample tube by sonication. The turbidities of the suspension were then measured at ambient temperature as a function of time. The concentrations of the particles were limited to fairly dilute since at higher concentrations, the intensity of transmitted light is too low for the detector to make an accurate measurement.

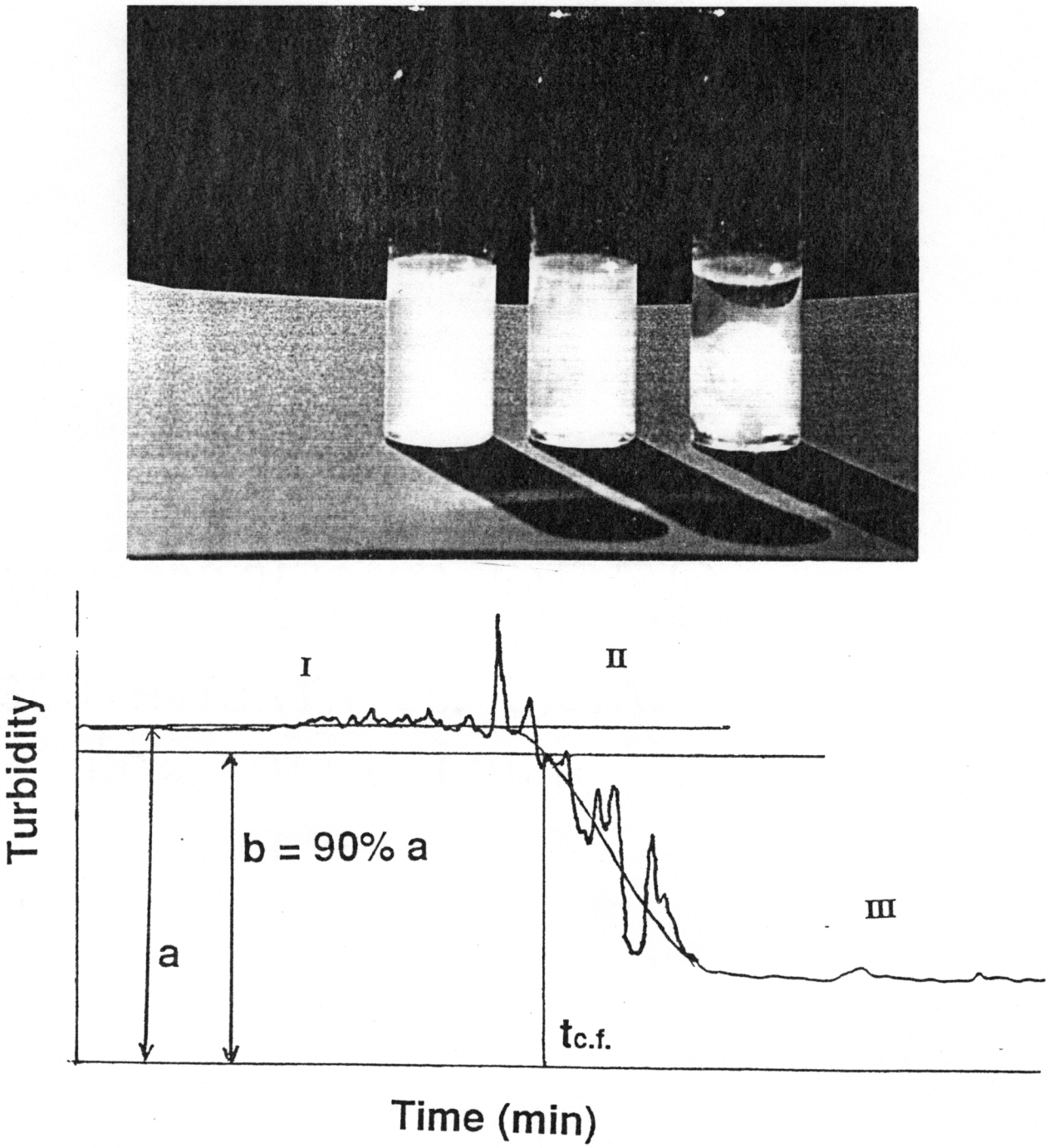

Figure 3.29 Analyzing the stability of the submicron particles suspensions by flocculation rate using turbidimeter

Figure 3.29 shows a typical spectrum for the turbidimeter in measuring the turbidity change of the suspensions. At the initial stage, A, the suspension was well-dispersed by sonication. It was stable and homogeneous. During this period, the turbidity of the suspension maintained a relatively constant value. As the experiment progressed, particles started to flocculate and formed small clusters, as indicated by the sample at stage B. These clusters fall at a relatively higher velocity than individual particles[82] (note that in the case of very small particles, $\leq$ 1 micron, the individual particles actually didn't settle). When the clusters settle, they were followed by relatively clearer water solutions, i.e., low particle concentration domain. Thus, the turbidity values showed some sudden rises and falls. At the final stage C, most of the clusters have already settled, and a layer of constant turbidity was formed. The rate of flocculation indicates relative stability of suspension,[46,54,55] with slower flocculation rates indicating higher stability. Therefore, the time required for the particles to form flocculates could serve as a criterion for stability. In the spectrum, a smooth curve was drawn along the Stage B in order to give an average turbidity value. The time it takes for the turbidity to decrease to 90% of the original value is defined as the Critical Flocculation Time ($t_{c.f.}$). Larger $t_{c.f.}$ values indicate more stable suspensions.

The critical flocculation times were plotted as a function of the weight percentages of the adsorbed stabilizer relative to particles (Figure 3.30). Similar to the results obtained from the 12 micron particle suspensions, the stabilities of the submicron particle suspensions increased with increasing percentages of the electrostatic coating and decreasing pH values. When the adsorbed stabilizer was about 1.5 wt.% relative to particles (the maximum coating obtained for the submicron particles at the experimental conditions used), the suspensions reached the highest stability. A well defined stability

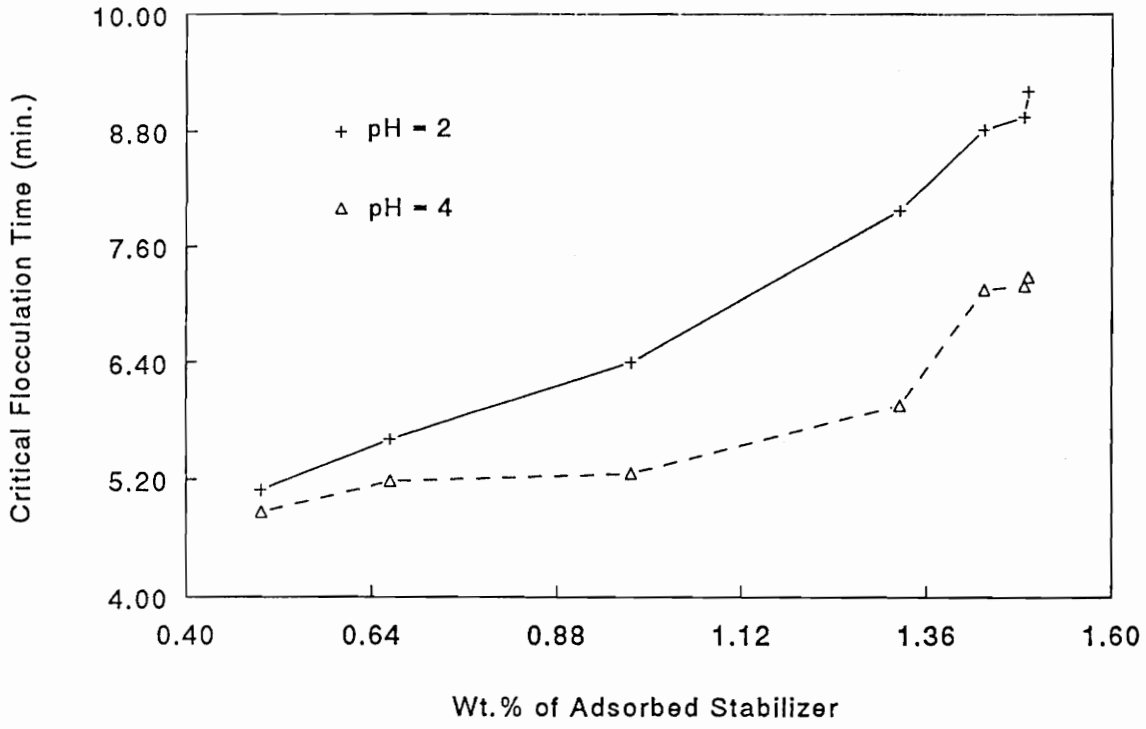

Figure 3.30 The critical flocculation times versus the wt.% of adsorbed stabilizer relative to particles

plateau, such as the one obtained for the 12 micron particles was not obvious. One reason might be that the smaller particles are more difficult to stabilize. According to the modified DLVO theory, the stability of colloidal suspensions is determined by the repulsive electrostatic interaction energy, van der Waals attraction energy, and steric repulsion energy (zero in this case) (Figure 3.27). The van der Waals attraction energy decays approximately with the sixth power of the distance between particles. Small particles have smaller interparticle distance, and thus, the attraction force is more significant for smaller particles.[45] However, relatively stable submicron PEEK particle suspensions were obtained with only ~ 1.5 wt.% of adsorbed stabilizer relative to particles.

Chapter 4. Conclusions

An amorphous, soluble PEEK precursor, poly(ether ether ketimine) was developed within our research group.[56] Acid hydrolysis of this precursor proceeds very rapidly, resulting in poly(ether ether ketone), to crystallizing from solution in the form of fine particles. The particle size can be controlled by the temperature, acid concentration, water concentration and solvent concentration. The particle size can be as small as ~ 0.1 micron in diameter. These PEEK particles have essentially the same thermal properties as commercial PEEK. Amorphous, soluble stabilizer precursors, poly(pyridine ether-co-ether ether ketimine)s were also developed by our group.[56] This thesis investigated the adsorption of the stabilizer precursor onto PEEK particles, including the ball-milled 12 micron diameter particles and the submicron particles. The adsorbed stabilizer precursors were transformed into insoluble, semi-crystalline, high performance poly(pyridine ether-co-ether ether ketone) by acid hydrolysis. Upon hydrolysis, the stabilizer precursor crystallizes from solution and lies rather tightly against the PEEK particle surfaces. Simultaneously, hydrolysis resulted in protonation of the pyridine moieties, which enabled the polymer to function as an electrostatic stabilizer. Procedures for adsorbing the stabilizer precursors onto PEEK particles and preparing aqueous PEEK suspensions by utilizing the electrostatic stabilizers have been developed. Adsorption studies of the stabilizer precursor onto both the 12 micron particles and the submicron particles have been conducted. The adsorbed stabilizer precursors were hydrolyzed, and the coated particles were resuspended into water. Different techniques were developed to analyze the stabilities of the prepared suspensions. The stabilities of both the 12 micron particles and the submicron particles were characterized.

It is found that relatively poor solvents such as toluene improve adsorption while no adsorption was obtained from good solvents such as THF because the good solvent, THF, decreased the adsorption energy parameter, χ_s, to a lower value than the critical adsorption energy parameter, χ_{sc}. An experimental procedure to measure the adsorption isotherms was developed, in which the stabilizer precursor was first adsorbed from toluene solution, then samples of the original solution and the supernatant after adsorption were dried and converted to HPLC grade THF for UV measurements. The adsorbed amounts were calculated by the concentration difference of stabilizer precursor in solution before and after adsorption. This procedure was demonstrated effective. The time required to reach adsorption equilibrium was determined as 70 hours by conducting time-dependent studies on the 12 micron particles. This rather long time was caused mainly by the stabilizer precursors' polydispersity of 2.0 which results from the condensation mechanism by which they were prepared, and also by the porous nature of the particles. A general phenomenon is that long chains are able to displace segments initially adsorbed, so-called competitive adsorption. This phenomenon is responsible for many differences between experimental results and theoretical predictions for adsorption isotherms. Isothermal adsorption of a stabilizer precursor (25,000 g/mole with 30 mole% pyridine) onto the 12 micron PEEK particles resulted in a pseudoplateau adsorption amount of 73.6 mg/m^2 at an equilibrium concentration of 6.3 mg/mL (8 wt.% of stabilizer precursor relative to particles in the original solution). This value was considerably larger than most of the experimental values, which is of the order of 1 mg/m^2. It was concluded that the surface area on these particles had probably not been measured accurately by the light scattering method used due to high porosity and irregular shapes. It is recommended that gas/solid adsorption/desorption techniques be explored to probe this aspect. After hydrolyzing the adsorbed stabilizer precursor, aqueous suspensions of the 12 micron particles were

analyzed by sedimentation experiments. Relatively stable suspensions were obtained with those samples which adsorbed from a solution with a stabilizer precursor concentration > 2 wt.% relative to particles. Isothermal adsorption of the same stabilizer precursor onto the submicron PEEK particles resulted in a pseudoplateau adsorption amount of 0.84 mg/m^2 at equilibrium concentrations of ~1 mg/mL (15 wt.% of stabilizer precursor relative to particles in the original solution). Aqueous suspensions of the hydrolyzed samples were analyzed by flocculation rate since the submicron particles never settle completely and thus sedimentation experiments can't be applied. Stability studies showed that relatively stable suspensions were obtained with those samples which adsorbed from a solution with a concentration of stabilizer precursor relative to particles > 15 wt.% at a solid concentration of 0.88% (g/mL). However, a much lower stabilizer concentration might be used for adsorption at a higher solid concentration provided sufficient stirring. For aqueous suspensions of both the 12 micron particles and submicron particles, relatively higher stabilities were obtained at lower pH values, indicating that poly(pyridine ether-co-ether ether ketone)s were indeed functioning as a semi-crystalline, high performance electrostatic aqueous suspension stabilizer.

Chapter 5. Future Work

Future work will focus on developing more efficient aqueous suspension stabilizers, conducting further adsorption/stabilization studies and using the relatively stable aqueous suspensions for preparing prepregs utilizing the aqueous dispersion prepregging technology. The following is recommended for extending the current research:

1. To synthesize an electrostatic stabilizer precursor, poly(pyridine ether-co-ether ether ketimine) with higher mole % of pyridine moieties. This copolymer might provide more positive charges upon hydrolysis. Therefore, a more stable aqueous suspension could be obtained.

2. As found in the solvent effect studies (section 3.2.4), there was no adsorption of poly(pyridine ether-co-ether ether ketimine) onto PEEK particles from THF. In this case, THF seemed to act as a displacer. A displacer is a organic molecule which has a stronger interaction with particle surface than polymer segment. It was found that low molecular weight displacers with a sufficiently strong affinity for a surface may completely desorb polymer segments at a critical displacer volume fraction due to the competitive phenomenon. Measurements of the critical displacer volume fraction for a series of displacers with different strengths allows to calculate the adsorption energy parameter of the polymer, χ_s.[48,61] This procedure involves two type of measurements. One of them is to study the dependence of adsorbed polymer amount on displacer concentration, i.e., the so-called displacement isotherm. It measures the amount of adsorbed polymer in the existence of displacer in certain kind of solvent. Another type of measurement is

adsorption isotherms of displacer alone in that solvent. Both of these measurements are necessary for calculating the adsorption energy parameter of the stabilizer precursor.

3. Specific surface area of the 12 micron particles was not well-defined in this research. It is recommended that gas/solid adsorption/desorption techniques be explored to probe this aspect.

4. In the adsorption studies of poly(pyridine ether-co-ether ether ketimine) (stabilizer precursor) onto the submicron particles, light scattering techniques could be used to measure the adsorbed layer thickness. By this method, pseudoplateau adsorption region could be defined as well as the adsorption kinetics, i.e., the time period required for reaching adsorption equilibrium. After hydrolysis of the particle coating, the electrostatically stabilized particles could be studied by an electrophoresis at different pH values. Some data, such as Zeta Potential (mV) or magnitude of positive charge on the particles, could be obtained to determine the stabilities of these suspensions.

5. To investigate the sediment structure of both 12 micron and submicron particles by microscopy. For the 12 micron particle suspensions, they could be let settle by themselves. However, the submicron particles will never completely settle since the force of gravity which causes the particles to settle is counterbalanced by the Brownian motion of the particles. The submicron particles suspensions could be centrifuged at relatively low speed to make the particles to settle. Sediments from both the 12 micron and submicron suspensions could be freeze-dried and then observed by microscopy. It is expected that sediment from a relatively stable suspension will have a close-packed

structure, while sediment from a relatively unstable suspension will have a loosely packed structure.

6. Practically, adsorption of stabilizer precursor onto PEEK particles could be conducted at more concentrated suspensions (i.e., higher solid concentration) provided sufficient stirring. Therefore, the concentration of stabilizer precursor solution could be lowered and still obtain the same amount of adsorption. The relatively stable suspensions are going to be used for prepregging both continuous carbon fiber tow and pre-woven graphite fabric utilizing the aqueous dispersion prepregging technology.

References:

1. M. J. Jurek and J. E. McGrath, Polymer, *1989*, 30, 1552.
2. P. M. Hergenrother, B. J. Jensen and S. J. Havens, Polymer, *1988*, 30, 358.
3. T. E. Attwood, P. C. Dawson, J. L. Freeman, L. R. J. Hoy, J. B. Rose and P. A. Staniland, Polymer, *1981*, 22, 1096.
4. F. A. Carey and R. J. Sundberg, Advanced Organic Chemistry Part A: Structure and Mechanisms, Plenum Press, NY, *1990*.
5. R. N. Johnson, A. G. Farnham, R. A. Clendinning, W. F. Hale and C. N. Merriam, J. Polymer Sci. A-1, *1967*, 5, 2375.
6. W. F. Hale, A. G. Farnham, R. N. Johnson and R. A. Clendinning, J. Polymer Sci. A-1, *1967*, 5, 2399.
7. R. N. Johnson and A.G. Farnham, J. Polymer Sci., A-1, *1967*, 5, 2415.
8. P. A. Staniland in "Comprehensive Polymer Science", G. Allen and J. C. Bevington, series eds., Pergamon Press, New York, *1989*, 5, 483-497.
9. T. E. Attwood, P.C. Dawson, J. L. Freeman, L. R. Hoy, J. B. Rose and P. A. Staniland, Polymer, *1981*, 22, 1096.
10. D. R. Kelsey, L. M. Robeson and R. A. Clendinning, Macromol. *1987*, 20, 1204.
11. D. K. Mohanty, T. S. Lin, T. C. Ward and J. E. McGrath, SAMPE Symp. Exp., *1986*, 31, 945.
12. D. K. Mohanty, R. C. Lowery, G. D. Lyle and J. E. McGrath, Int. SAMPE Tech. Conf., *1987*, 32, 408.
13. D. K. Mohanty, J. S. Senger, C. D. Smith and J. E. McGrath, Int. SAMPE Tech. Conf., *1988*, 33, 970.
14. K. R. Lyon, D. K. Mohanty, G. D. Lyle, T. Glass, H. Marand, A. Prasad and J. E.

McGrath, Int. SAMPE Tech. Conf., *1991*, 36, 417.

15. W. H. Bonner, (Du Pont Ltd), US Pat. 3,065,205, *1962*.
16. I. Godman, J. E. McIntyre and W. Russell (ICI plc), Br. Pat. 971227, *1964*.
17. T. E. Attwood, P. C. Dawson, J. L. Freeman, L. R. J. Hoy, J. B. Rose and P. A. Staniland, Am. Chem. Soc. Polym. Prepr., *1979*, 20(1), 191.
18. B. M. Marks (Du Pont Ltd.), US Pat. 3,441,538, *1969*.
19. M. Ueda and F. Ichikawa, Macromol., *1990*, 26, 2535.
20. I. Colon and D. R. Kelsey, J. Org. Chem., *1986*, 51, 2627.
21. M. Ueda, Y. Seino, Y. Haneda, M. Yoneda and J. I. Sugiyama, J. Polymer Sci., A, *1994*, 32, 675.
22. Y. Lee and R. S. Porter, Macromol., *1988*, 21, 9, 2770.
23. P. Zoller and T. A. Kehl, J. Polymer Sci., B, *1989*, 27, 993.
24. Y. Lee, R. S. Porter and J. S. Lin, Macromol., *1989*, 22, 1756.
25. J. Devaux, D. Delimoy, D. Daust, R. Legras, J. Mercier, C. Strazielle and E. Nield, Polymer, *1985*, 26, 1994.
26. J. I. Kroschwitz, editor, High Performance Polymers and Composites, John Wiley & Sons, Inc., *1991*.
27. C. A. Arnold, P. M. Hergenrother and J. E. McGrath, Composite Applications: The Role of Matrix, Fiber and Interface, T. L. Vigo and B. J. Kinzig, eds., VCH Publishers, NY, *1993*.
28. D. W. Holty, Chemtech, *1993*, June, 40.
29. D. Hirt, J. Marchello and R. Baucom, Int. SAMPE Tech. conf., *1990*, 22, 360.
30. T. Towell, D. Hirt and N. Johnston, Int. SAMPE Tech. Conf., *1990*, 22, 1156.
31. R. Conchran and R. Pipes, Int. SAMPE Tech. Conf., *1991*, 23, 1169.
32. R. M. Davis, A. Texier, T. H. Yu, K. Lyon, A. Gungor, J. E. McGrath and J. S.

Riffle, Am. Chem. Soc. Polym. Prepr., *1992*, 33, 416.

33. A. Texier, R. M. Davis, K. R. Lyon, A. Gungor, J. E. McGrath, H. Marand and J. S. Riffle, Polymer, *1993*, 34, 896.

34. T. Lin, K. W. Stickney, M. Rogers, J. S. Riffle, H. Marand, J. E. McGrath, T. H. Yu, R. M. Davis, Polymer, *1993*, 34, 772.

35. J. Lyklema, Flocculation, Sedimentation and Consolidation, Proceedings of the Engineering Foundation Conference, *1986*, 3-21.

36. J. M. H. M. Scheutjens and G. J. Fleer, The Journal of Physical Chemistry, *1979*, 83, 1619.

37. J. M. H. M. Scheutjens and G. J. Fleer, The Journal of Physical Chemistry, *1980*, 84, 2, 178.

38. P. G. De Gennes, Journal De Physique, *1976*, 37, 1445.

39. A. J. Silberberg, J. Chem. Phys. *1968*, 48, 2835.

40. P. Flory, Principles of Polymer Chemistry, New York, *1953*.

41. G. V. Schulz, Angew. Chem., *1952*, 64, 553.

42. G. V. Schulz and U. Kantow, J. Polymer Sci., *1953*, 10, 79.

43. G. J. Howard and P. McConnell, J. Phys. Chem. *1967*, 71, 2974.

44. M. A. Cohen Stuart, G. J. Fleer and B. H. Bijsterbosch, J. Colloid Interface Sci., *1982*, 90, 310.

45. D. H. Napper, Polymeric Stabilization of Colloidal Dispersions, Academic Press, NY, *1983*.

46. D. J. Shaw, Introduction to Colloid and Surface Chemistry, 4th edi., Butterworths-Heinemann Ltd, Oxford, *1992*.

47. R. Buscall, T. Corner and J. F. Stageman, Polymer Colloids, Elsevier Applied Science Publishers, NY, *1985*.

48. C. Chen, Studies of Adsorption and Stabilization of Silica Suspensions Using Well-Defined Polymeric Dispersants, Ph.D. dissertation, Virginia Tech, *1994*.

49. H. C. Hamaker, Physica, *1937*, 4, 1058.

50. J. T. G. Overbeek, Advances in Colloid and Interface Science, *1982*, 16, 17.

51. P. J. Flory, Principles of Polymer Chemistry, Cornell University Press, Ithaca, *1953*.

52. Th. F. Tadros, Solid/Liquid Dispersions, Academic Press, *1987*.

53. M. W. J. van den Esker and J. H. A. Pieper, Surfactants, Academic Press, *1984*, 219-228.

54. J. T. G. Overbeek, Colloid Science, *1952*, 1, 278-301.

55. R. H. Ottewill and J. N. Shaw, Discuss. Faraday Soc., *1966*, 42, 154.

56. A. E. Brink, The Synthesis, Stabilization and Sintering of High Performance Semicrystalline Polymeric Powders, Ph.D dissertation, Virginia Tech, *1994*.

57. M. Nardin, E. M. Asloun, J. Schultz, Surf. Interface Anal., *1991*, 17, 485.

58. Yu. S. Lipatov and L. M. Sergeeva, Adsorption of Polymers, John Wiley & Sons, New York-Toronto, *1974*.

59. G. J. Howard, in Interfacial Phenomena in Apolar Media, Chapter 7, H. F. Eicke; G. D. Parfitt (Ed.), Marcel Deker Inc., New Hork, *1987*.

60. J. Roovers, J. D. Cooney, P. M. Toporowski, Macromolecules, *1990*, 23, 1611.

61. M. A. Cohen Stuart, F. Cosgrove and B. Vincent, Advances in Colloid and Interface Science, *1986*, 24, 143.

62. B. H. Stuart and D. R. Williams, Polymer, *1994*, 35, 6, 1326.

63. J. N. Hay and D. J. Kemmish, Polymer, *1988*, 29, 613.

64. C. J. Wolf, J. A. Bornmann and M. A. Grayson, Journal of Polymer Science, Part B: Polymer Physics, *1991*, 29, 1533.

65. E. J. Stober and J. C. Seferis, Polymer Engineering and Science, *1988*, 28, 9, 634.

66. C. J. Wolf, J. A. Bornmann, M. A. Grayson and D. P. Anderson, Journal of Polymer Science, Part B: Polymer Physics, *1992*, 30, 251.

67. A. Michele and V. Vittoria, Polymer Communications, *1991*, 32, 8, 232.

68. G. Mensitieri, A. Apicella, J. M. Kenny and L. Nicolais, Journal of Applied Polymer Science, *1989*, 37, 381.

69. A. Arzak, J. I. Eguiazabal and J. Nazabal, Journal of Polymer Science, Part B: Polymer Physics, *1994*, 32, 325.

70. M. A. Grayson and C. J. Wolf, Journal of Polymer Science, Part B: Polymer Physics, *1988*, 26, 2145.

71. D. W. Van Krevelen, Properties of Polymers, 3rd edi., Elsevier Science Publishing company Inc., New York, *1990*.

72. G. J. Fleer and J. M. H. M. Scheutjens, Advances in Colloid and Interface Science, *1982*, 16, 341.

73. A. J. Silberberg, J. Colloid Interface Sci., *1982*, 38, 217.

74. A. J. Silberberg, J. Chem. Soc., Faraday Discuss., *1975*, 59, 203.

75. A. J. Silberberg, J. Chem. Phys., *1967*, 46, 1105.

76. C. A. J. Hoeve, J. Chem. Phys., *1965*, 43, 3007.

77. C. A. J. Hoeve, J. Polym. Sci., Part C, *1971*, 34, 1.

78. R. J. Roe, J. Chem. Phys., *1974*, 60, 4192.

79. M. A. Cohen Stuart, J. M. H. M. Scheutjens and J. Fleer, Journal of Polymer Science: Polymer Physics Edition, *1980*, 18, 559.

80. L. K. Koopal, Meded. Landbouwhogesch. Wageningen, *1978*, 78, 12, 70.

81. J. M. G. Lankveld and J. Lyklema, J. Colloid Interface Science. acc., *1972*.

82. W. C. Thacker and J. W. Lavelle, Phys. Fluids, *1978*, 21, 2, 291.

Vita

The author was born in Hunan, P. R. China on September 17, 1966. In 1985 she graduated from the First High School of Changde City and enrolled in Beijing University of Aeronautics and Astronautics. She graduated in 1989 with Academic Excellence with a major in Polymeric Materials Science and Engineering. After that, she entered the M.S. program in the Materials Research Institute, Southern China University of Technology, in the area of Polymer Engineering. In 1991, she came to the U.S. and in 1992 she enrolled in graduate school at Virginia Polytechnic Institute and State University under the direction of Professor Judy S. Riffle. She obtained her M.S. degree in the area of Organic Chemistry of Polymers in 1995. She joined Moore Business Forms, Inc. as a Polymer Chemist in December 1994.